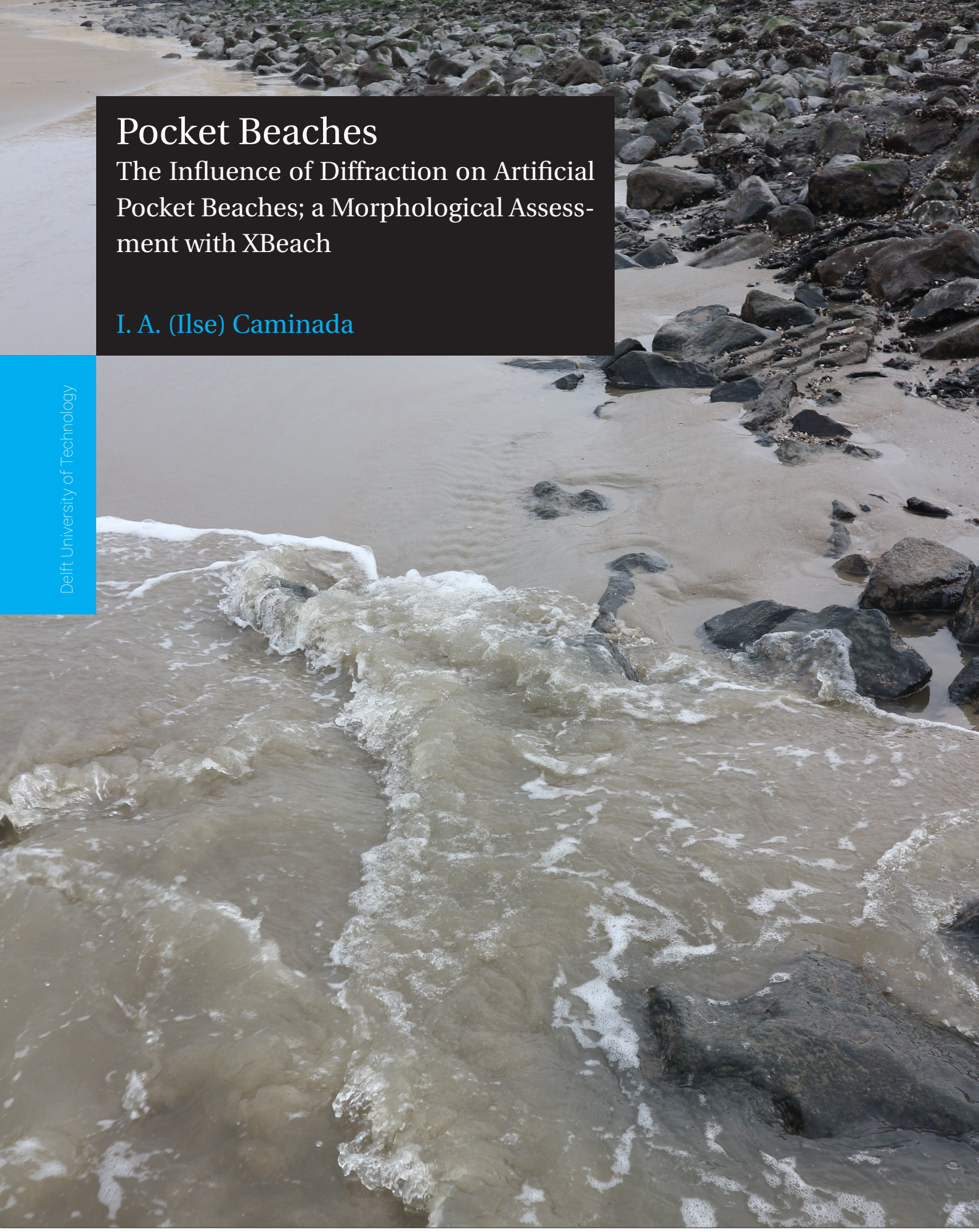

Pocket Beaches

The Influence of Diffraction on Artificial Pocket Beaches; a Morphological Assessment with XBeach

I. A. (Ilse) Caminada

Delft University of Technology

TU Delft Delft University of Technology

Van Oord Marine ingenuity

Challenge the future

Pocket Beaches

The Influence of Diffraction on Artificial Pocket Beaches; a Morphological Assessment with XBeach

by

I. A. (Ilse) Caminada

to obtain the degree of Master of Science in Civil Engineering
at the Delft University of Technology,
to be defended publicly on 23 April 2018 at 03:00 PM.

Student number:	4093348	
Project duration:	June 6, 2017 – April 23, 2018	
Thesis committee:	Prof. dr. ir. S. G. J. Aarninkhof,	TU Delft, chair
	Dr. ir. M. A. de Schipper,	TU Delft
	Dr. ir. R. T. McCall,	Deltares
	Ir. P. G. F. Brandenburg,	van Oord

This thesis is confidential and cannot be made public until April 23, 2019.

TU Delft Delft University of Technology

Van Oord
Marine ingenuity

Preface

This report is the result of my final work to obtain the master degree in Civil Engineering at Delft University of Technology. This research has been conducted on the influences of diffraction on artificial pocket beaches and therewith completes the master track Hydraulic Engineering and a specialisation in Coastal Engineering.

This master thesis has been carried out at Van Oord, a maritime contractor. I am really thankful for the opportunity to fulfil my final research at this company. The subject of research has been very interesting and the environment has been motivational and inspiring.

Furthermore, I would like to thank my committee, consisting of Stefan Aarninkhof, Matthieu de Schipper, Robert McCall and Peter Brandenburg, for their contribution to this work. Your guidance and valuable feedback during our meetings helped me to improve my work time after time. Stefan Aarninkhof, I would like to thank you for the constructive guidance of the committee meetings and your enthusiasm. Besides, I would like to express my gratitude to Robert McCall, for your advice and ideas on the variations initiated by XBeach and how to deal with these. In addition, I would like to thank Matthieu de Schipper, for the critical look at my report and the feedback to improve the value of my research. Peter Brandenburg, special thanks to you for being my daily supervisor. I really appreciated our weekly meetings, to verify my findings and thank you for being the sparring partner I sometimes really needed.

Next to my committee, I would like to express my gratitude to my fellow students. To start, my fellow interns at Van Oord, I really value your support and the good times during our breaks the past few months. Furthermore, my fellow students of the master Hydraulic Engineering. You have been a good help during my final research but also before, with your support I made it to this point in my master studies. Especially, I owe my buddies of Flood Proof Myanmar thanks.

Finally, I would like to thank my friends and family for always supporting me during my study time in Delft. I could always count on you, during fun and during hard times. I am very grateful to my friends, who made my student years unforgettable and pleasant. In Delft, Rotterdam and around the rest of the world, at home, at the faculty, on the hockey field or at the bar, it has been great! Finally, my warmest thanks go to my parents who always believed in me and encouraged me to achieve my full potential.

I. A. (Ilse) Caminada
Rotterdam, April 2018

Abstract

Information about the hydrodynamic, sediment transport and morphodynamics is limited in pocket beaches (Dehouck et al., 2009). However, a good understanding is necessary for effective management of coastal areas (Scholar et al., 1998). A small artificial pocket beach has relatively large shadow zones, therefore, diffraction might be an important process. Designs of pocket beaches are now based on equilibrium beaches and morphological changes and sediment losses during storm conditions. The numerical model XBeach is used to predict the beach development and losses. However, so far diffraction has not been included in these simulations. Therefore, the main objective of this research is to gain better insight on the effect of including short wave diffraction in the simulations on the morphological development in pocket beaches. Various modes of XBeach give the opportunity to variate including short wave diffraction or not.

First, simulations of simplified pocket beaches with perpendicular groynes has been used to research the influence of short wave diffraction on the morphological development and the underlying hydrodynamic and sediment transport processes. The simplified beach used, had a length of 500 metres and the shadow zone covered about 30% of the embayment area. The effect of short wave diffraction appeared to be a wider circulation cell than without diffraction. This resulted in a circulation cell and therewith sediment transport pattern of 90% of the embayment length with diffraction and 35% without diffraction. Furthermore the outflow velocities along the groyne are 33% lower in case diffraction is incorporated in the simulations. The sediment transport patterns show a gradual development from the exposed into the shadow zone with diffraction, whereas an abrupt decrease of 95% without diffraction can be found at the boundary. Erosion and sedimentation patterns are dispersed gradually over the embayment in case diffraction is included in the simulations. In case diffraction is neglected the transitions of erosion and sedimentation are very abrupt. Especially the exposed areas show large variations; at the shoreline erosion is less severe with diffraction and in the embayment sedimentation is larger. A pattern of gradual transitions with diffraction and abrupt transitions without diffraction could be noticed.

The influence of short wave diffraction, within a storm condition, on the beach development has also been researched for a stable designed, real, curved pocket beach. A case study beach in Constanta, Romania with a similar surface area as the simplified beach but a total shadow area of 40%, has been used. The circulation cell with diffraction again is longer than without diffraction, 95% and 80% of the embayment. Furthermore, the outflow velocity along the groyne is 25% lower with diffraction than without diffraction. The sediment transport patterns looks like the circulation patterns, although, the magnitudes are different. With diffraction a more gradual decrease and increase can be seen, whereas without diffraction an abrupt decrease of 95% could be seen just inside the shadow zone. The results of the morphological development look more reliable than the simplified pocket beach results. Both cases show erosion, however, with diffraction the total loss of sediment is 10% less relative to without diffraction. With diffraction, the exposed shoreline shows less erosion (10%), the shadow shoreline shows more erosion (90%), the shadow embayment shows less sedimentation (30%) and the exposed embayment shows more sedimentation (350%). The transitions from exposed to shadow zone are more gradual with diffraction. Without diffraction abrupt vertical changes of about one metre exist at the boundary of shadow to exposed zones. The results with diffraction look promising however, a real validation of the results was not possible with the available data.

In conclusion, diffraction appears to be an important phenomenon in relatively small pocket beaches. The sedimentation and erosion pattern is much more gradually dispersed over the area. The main alongshore velocities and sediment transport direction in the exposed zone and the gradual development of sediment transport into the shadow zones cause these gradual transitions. The abrupt transitions in the sediment transport patterns without diffraction result in very abrupt changes in the bed level alterations.

Contents

List of Figures

List of Tables

Nomenclature

Symbols

k	wave number	rad/m
λ/L	wave length	m
θ	wave direction	$^\circ$
f	frequency	s^{-1}
f_p	peak frequency	s^{-1}
s	spreading parameter	rad^{-2}
ϕ	angle of incidence	$^\circ$
c	wave propagation speed	m/s
σ_θ	directional width	rad
H_{m0}	significant wave height	m
H_s	significant wave height	m
H_{rms}	root mean square wave height	m
T_p	peak period	s
T_{rep}	representative period	s
m_0	variance	m^2
d	depth	m
g	acceleration of gravity	m/s^2

Abbreviations

stat	stationary mode
surf	surfbeat mode
non h	non hydrostatic mode
mono	monochromatic waves
spec	spectrum of waves
MWL	mean water level

1 Introduction

1.1. Context

Coastal areas are and have always been very popular with humans to settle. Due to the transport opportunities, fishing and fertile grounds, these areas have developed into densely populated and economically important locations. However, coastal areas are also very vulnerable to flooding. Flooding in these areas can have major consequences. Therefore, coastal areas are of great interest to researchers and there is a demand for engineering solutions to protect these important areas against flooding.

The coast is a general term indicating the transition of water (oceans and seas) to land (continents). Part of the coastal area consist of beaches. A beach consist of materials like sand, cobbles and or shells. Beaches are (natural) barriers that dampen de waves and therewith decrease the energy impact and flooding on the hinterland. Beaches exist in several types, the main ones are long mainland beaches, barrier island beaches and pocket beaches. This last one will be subject of this research. Another common name for pocket beaches is (headland) embayed beaches.

Pocket beaches are usually small beaches located between two headlands (Figure 1.1). This type of beach is common worldwide (Dehouck et al., 2009). About half of the world's coastline is characterized by headland embayed beaches (Short and Masselink, 1999). When the alongshore drift is intercepted by a headland or groyne, the wave action will be the main cause of redistribution of the beach material (Reeve et al., 2015). Due to the adjustment of incoming wave fronts, these beaches have a characteristic curved coastline (Silva et al., 2010). Due to changing wave conditions, these beaches do not remain static, they respond to climatic changes, storms and calms. These beaches react very different from long mainland beaches because of the more or less closed beach system. The influence of the boundaries are significant on hydrodynamic and sediment transport processes.

Pocket beaches can originate from a natural or an artificial cause. The natural pocket beaches are often an erodible beach between to less erodible (often rocky) headlands, an example of a natural pocket beach can be seen in figure 1.1a. The artificial pocket beaches (for an example see figure 1.1b) are created by the construction of groynes. Groynes are structures built perpendicular to the shore and usually extend through the surfzone, these structures can be straight or curved. The purpose of the construction of groynes may be to prevent the existing shoreline from erosion or to build up a sandy beach at a place where before a beach hardly existed (Dunham, 1965). The main effect of these groynes is trapping sediment that is transported along the coast (Dunham, 1965) or retaining artificially placed sand.

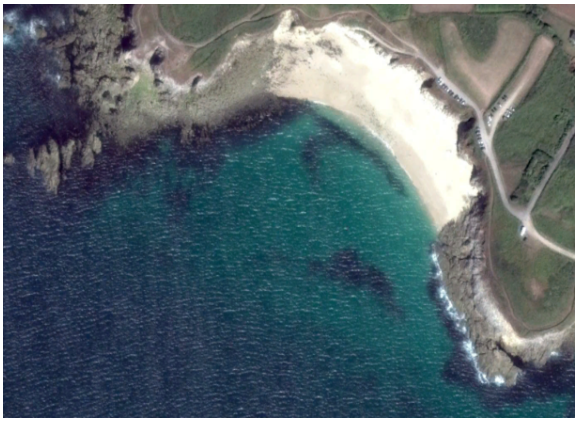

(a) Natural Pocket Beach in Plouarzel, France (Google Earth Pro V7.1.8.3036, 2016d)

(b) Artificial Pocket Beach in Constanta, Romania (Google Earth Pro V7.1.8.3036, 2016c)

Figure 1.1: Example of a natural and an artificial pocket beach

In the case the main objective is to restore or create a beach, often groynes are constructed relatively close to each other and a nourishment is performed to extend the sandy beach. A nourishment is the artificial placement of sand at locations with a loss or lack of sand. The construction of groynes and the nourishment of beaches is performed by dredging companies. For execution of projects whereby beaches are created or retained, it is important to know how to design, construct and maintain these beaches. Beaches have to withstand wave conditions for years without eroding too much, therefore, long term predictions of the morphodynamics within an artificial pocket beach are necessary to make a robust project.

Several methods have been thought of to predict the shoreline behaviour. Various empirical models, based on the concept of stable bay beach (Silvester, 1960), have been developed. One of the most successful was the Parabolic Bay Shape Equation. However, due to the limitation of not taking into account wave conditions and near shore processes in this empirical model it is not ideal for engineering solutions (Bemmelen, 2017). Furthermore, also a statistical method has been developed, this method is called the Principal Component Analysis. This method has been shown capable of explaining various coastal processes on site specific cases (Harley et al., 2011; Turki et al., 2013). However, for this method large amounts of high quality site specific data are necessary and often it is not suitable for beaches with human interventions, which makes it not suitable to use for the design of engineering solutions (Bemmelen, 2017).

Another way to predict the behaviour of pocket beaches is with numerical coastal models. The past few years these models have been used for coastal predictions extensively but not that often in pocket beaches yet. Daly et al. (2011) showed it is possible to predict long term morphological responses of pocket beaches with the process based model Delft3D. Bemmelen (2017) used XBeach, another process based model, to research the applicablity for the long term simulation of pocket beaches. Daly et al. (2011) as well as Bemmelen (2017) performed their research on a schematization of a pocket beach.

Numerical models can be a good help with long term predictions of morphodynamics, but computational time is an important restriction. At the moment, long term predictions for the desing of pocket beaches are therefore made in two parts. An equilibrium coastline based on yearly averaged wave energy flux and short storm response simulations to compute the sediment losses. The equilibrium coastline is modelled by the assumption that each beach segment is oriented perpendicular to the direction of the wave energy flux. During normal conditions no sediment is lost out of the pocket beach system. The losses occur during storm events and therefore, several storm events from an 1 year return to a 100 year return period are modelled more precise. The weighted sediment losses per event per year are counted up to a total yearly sediment loss, including the probability of occurrence, which is used in the design. For reliable long term predictions it is therefore necessary to simulate the storm events as accurate as possible. From literature it can be concluded that high energy events (storms) with high wave heights and long wave periods increase the flow velocities in the circulation cells and the outflow along groynes within pocket beaches (Pattiaratchi et al., 2009; Dehouck et al., 2009; Daly et al., 2011; Loureiro et al., 2012; Castelle et al., 2016).

1.2. Problem Definition

In the field of coastal engineering a lot of research has been done on wide and open beaches in contrast to pocket beaches (Dehouck et al., 2009). According to Dehouck et al. (2009), information about the hydrodynamic, sediment transport and morphodynamics is limited. Some research has been done, but to give a more comprehensive review more observations are needed (Dehouck et al., 2009). Scholar et al. (1998) stated: 'An understanding of the basic sediment transport processes on pocket beaches and along their coastlines is necessary for sound and effective management of these coastal areas'. A better understanding of the processes that influence the erosion and sedimentation patterns in pocket beaches can make more sustainable beaches possible. Since approximately 70% of the world's sandy coastlines have encountered erosion over the past few decades (Bird, 1985), it is getting more important to be able to design, construct and maintain stable beaches. To be able to design dynamic stable pocket beaches it is essential to understand the importance of processes in artificial pocket beaches, initiated by the structures that form the boundaries of these beaches.

It has been found that complex circulation patterns and flow motions play an important role in the hydrodynamic and sediment transport processes of pocket beaches (Dehouck et al., 2009; Daly et al., 2011; de Santiago González, 2014; Turki et al., 2015; Bowman et al., 2014; Lasagna et al., 2011; Kim and Lee, 2009; Ab Razak et al., 2014). Often, rip currents are mentioned as significant phenomena in these researches.Silva et al. (2010) and Ab Razak et al. (2014) show that wave angle and wave height variations are important in the formation of circulation patterns. Therefore, processes that have an influence on the wave angle and wave height variation could be pointed out as important processes for the currents in pocket beaches. According to Silva et al. (2010); Bowman et al. (2014); Kim and Lee (2009); Ab Razak et al. (2014); Castelle et al. (2016) it can be concluded that diffraction, refraction, reflection and set-up play important roles in the formation of circulation patterns. However, most research on pocket beaches is about beach transformations and not on the underlying wave processes that cause these beach transformations. The processes are sometimes mentioned but the individual effects have been rarely researched in small artificial pocket beach environments. The location of the structures in combination with the incoming wave angle create relatively large shadow zones. Therefore, it is expected that diffraction could play an important role.

Furthermore, research on numerical simulations of pocket beaches has been done, however, to a very limited extent. Yamashita and Tsuchiya (1993) constructed a numerical model to do some research on the integration of wave theory, nearshore dynamics, sediment transport and shorline change models. Reniers et al. (2004); Daly et al. (2014, 2011) examined embayed beaches using the numerical model Delft3D. Furthermore,Bemmelen (2017); Ab Razak et al. (2014); de Santiago González (2014); Castelle and Coco (2013); Ab Razak et al. (2013) examined embayed beaches with the numerical model XBeach. All these researches differ on main interest, beach size scale and simulation time. Besides these researches from literature, designs are now made based on XBeach simulations of storm conditions. For designs of these beaches, storm events are assumed to determine the losses and are therefore an important factor. So far, diffraction is not included in the simulations with XBeach, although, it is assumed it could have a large influence.

1.3. Research Question

The objective of this research is to gain better insight in the influence of diffraction on the hydrodynamic, sediment transport and morphodynamics in artificial pocket beaches. These insights give a better understanding of how and why beach behaviour is different with diffraction. The main research question is formulated as:

How does the morphological behaviour of artificial pocket beaches change when diffraction is included in simulations and why does it change?

To answer this main research question several sub questions are formulated focussing on the several processes taken place in an artificial pocket beach.

What is the effect of diffraction on general circulation patterns within an artificial pocket beach?

What is the effect of diffraction on general sediment transport patterns within an artificial pocket beach?

What is the effect of diffraction on the general sedimentation and erosion within an artificial pocket beach?

2

Approach

The main objective of this research is to gain better insight in the dynamics in artificial pocket beaches initiated by diffraction. The dynamics which is focused on in this research are the sediment and erosion patterns but also the underlying circulation and sediment transport patterns. To achieve this, several steps have been taken. An overview can be seen in figure 2.1. As can be seen in this figure, this research has been approached by different phases. First a theoretical part, then a part based on a case study. First of all, in the theoretical part, literature on different aspects has been examined. Later on this literature knowledge has been applied on some simplified pocket beach layouts. Thereafter, the case study has been introduced and measurements and model results of a real beach have been studied. For the simplified pocket beach simulations and the case study beach simulations the numerical model XBeach has been used. XBeach has 3 modes with a different level of wave resolving. Due to these difference the different modes can be used to research the influence of diffraction. Below, all different parts are explained in more detail.

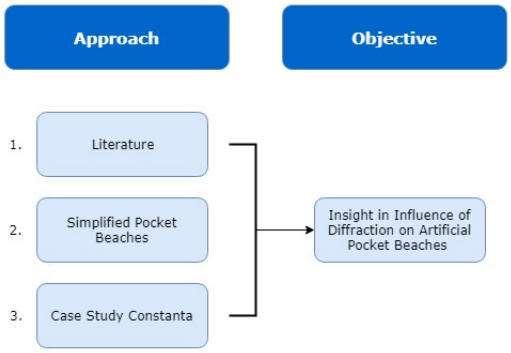

Figure 2.1: Scheme of the general approach of the research

2.1. Literature

This phase of literature study is subdivided into two parts. First, a process part, examining all kind of wave characteristics, hydrodynamic and sediment transport processes. Furthermore, a literature review on the processes that are important for the beach dynamics in pocket beaches has been given. The main focus is on diffraction, circulation patterns, rip currents and long waves, since, these are important processes and phenomean in this reasearch. The other information is provided to give a more complete picture of processes and it supports the explanation of the processes of main interest. The second part is about the predictive methods that can best be used for the simulation of pocket beaches. The used model in this research, XBeach, is explained in more detail. A schematic view on this phase can be seen in figure 2.2.

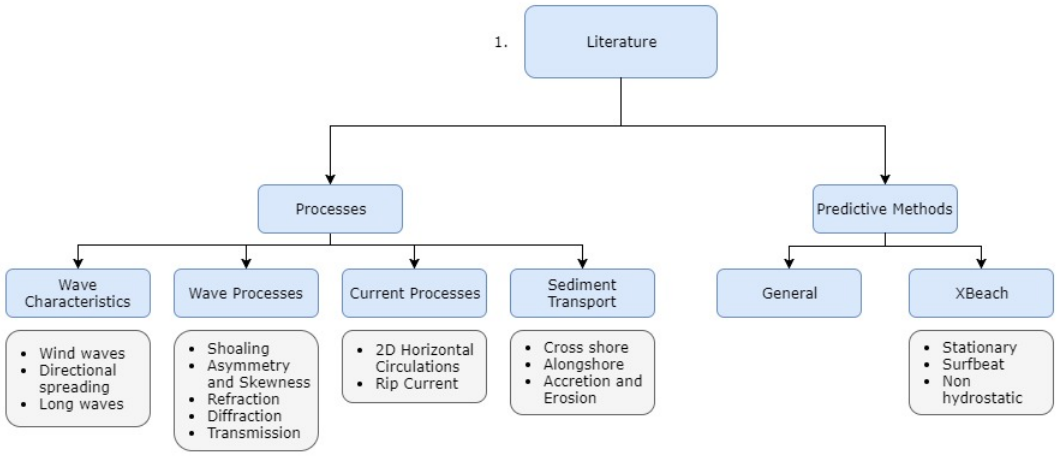

Figure 2.2: Scheme of the literature study

2.2. Simplified Pocket Beach

The knowledge gained by the literature study has been applied on simplifications of pocket beaches. These pocket beaches have a simplified layout and can therefore be easily compared. A schematic overview of phase 2 is given in figure 2.3.

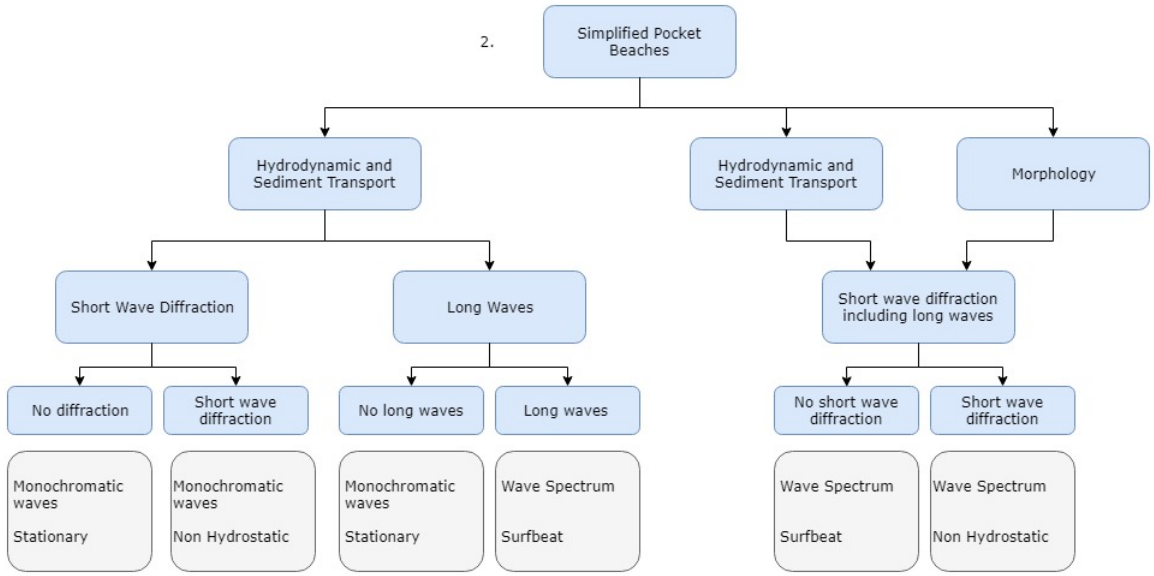

Figure 2.3: Scheme of the simplified pocket beach research

Artificial pocket beaches where diffraction could play an important role in the dynamics are relatively small. The simplified pocket beaches in this research have a beach length of about 500 metres. The schematized pocket beaches in the research of Daly et al. (2011) and van Bemmelen (2017) have both more or less the same layout and sizes. Comparing with the research of Daly et al. (2011) and van Bemmelen (2017) the pocket beaches in this present research do not have the same headlands but have extending groynes. A sketch of the used simplified pocket beach can be found in figure 2.4.

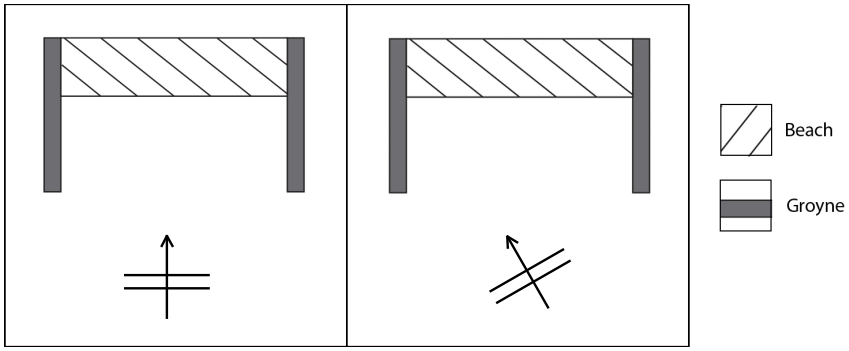

Figure 2.4: Simplified pocket beach layout with variation in wave direction

Based on the gained knowledge of the literature research and some simulations of different variations of pocket beaches, hypotheses are formulated on the influence of diffraction and long waves on the dynamics in artificial pocket beaches. To be able to simulate pocket beaches including diffraction and long waves first the processes are examined separately. First, the influence of short wave diffraction on the hydrodynamic and sediment transport patterns has first been researched with monochromatic waves in the stationary and the non hydrostatic mode of XBeach. Second, the influences of long waves (including long wave diffraction) have been investigated by comparing the results of the stationary mode with monochromatic waves with results of the surfbeat mode with a wave spectrum with a very small directional spreading. Thereafter, the findings are combined in more realistic circumstances. The surfbeat mode and the non hydrostatic mode both with a wave spectrum are used to examine the influence of short wave diffraction in case long waves are taken into account. The research on these two simulations has been extended with the morphological development within these beaches. After this phase, some findings are given on the significance of diffraction on the dynamics within an artificial pocket beach.

2.3. Case Study Constanta

In this section a case study has been be assessed. Several pocket beaches that are constructed in 2015 in Constanta, Romania, have been examined. In figure 2.5 an overview of the approach of the case research is shown.

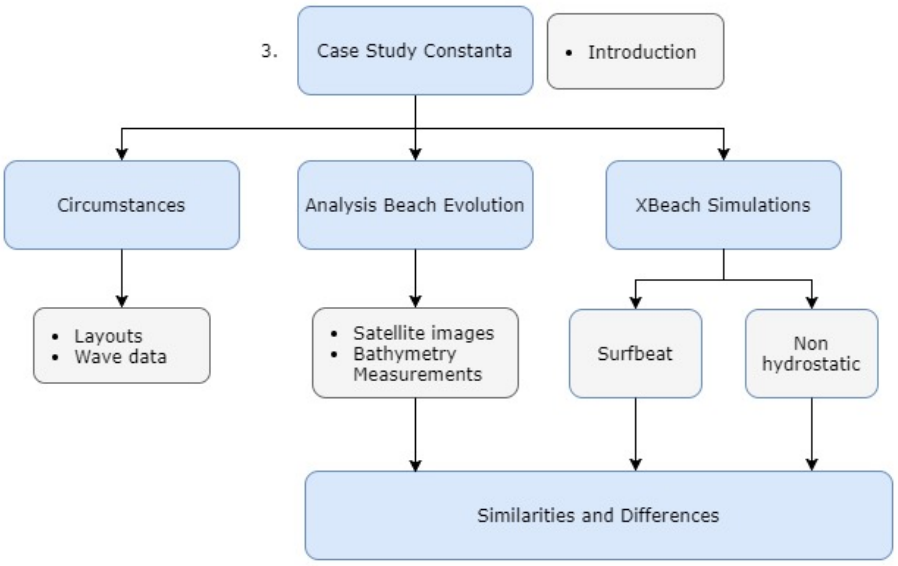

Figure 2.5: Scheme of the case study research

The in 2014 and 2015 constructed pocket beaches along the coast of Constanta are used to verify the findings of simplified XBeach simulations on simulations of real pocket beaches. First, the case study circumstances

are discussed. Thereafter, the beach evolution is analysed in two ways. A general idea of the coastline evolution is obtained by analysing satellite images of 2015, 2016 and 2017. A more detailed idea of the evolution of the entire beach is obtained by bathymetry measurements.

Thereafter, one of the beaches is simulated with XBeach. Two modes of XBeach will be used to test the findings of the simplified pocket beach research on a real pocket beach. The results of the simulations in surfbeat and non hydrostatic mode are compared to see the influence of short wave diffraction on the dynamics in a real pocket beach. Finally, also a general comparison has been attempted to make between the model results and the real beach evolution to be able to assess the general sedimentation and erosion patterns.

3

Literature

3.1. Introduction

Several processes play an important role in shaping the coasts. Due to waves and currents in several kind of appearances, the coast is shaped in a certain way and is changing continuously. The most important parameters and processes that play a role in shaping the coast are discussed in this chapter. An overview of the most important wave characteristics and hydrodynamic and sediment transport processes is provided. Especially the characteristics and processes that are important in pocket beaches are discussed. For a good understanding of the processes that drive the dynamics of in an artificial pocket beach, some background information is given. Furthermore, the findings from literature about the importance and effects of several processes and phenomena and predictive methods for pocket beaches have been discussed.

To start, different kind of waves are explained in section 3.2: Wave Characteristics. Subsequently, wave processes are discussed in section 3.3. One of these processes is diffraction. The main wave process in this research. Section 3.4 will elaborate on currents, since currents are mentioned as significant phenomena in pocket beaches. The effects of the hydrodynamic processes on the beach material will be discussed in the sediment transport processes in section 3.5 because beach stability is influenced by the transport of sediment which causes erosion or sedimentation. In conclusion the predictive methods for pocket beaches are described in section 3.6.

3.2. Wave Characteristics

Waves can be classified based on various characteristics: disturbing force, restoring force and length of the wave. The relative amount of energy as a function of the wave period in the ocean can be seen in figure 3.1. Ordinary wind waves contain less energy than storm surges and tsunamis but occur more frequent. Therefore, the relative energy in the wind wave range is higher (Bosboom and Stive, 2015a).

Wind-generated gravity waves are thereby the major supplier of energy to the coastal system (Bosboom and Stive, 2015a). Waves do not transfer matter, only energy. Sea waves and swell waves are both wind-generated gravity waves. Especially swell waves can move large distances through the ocean.

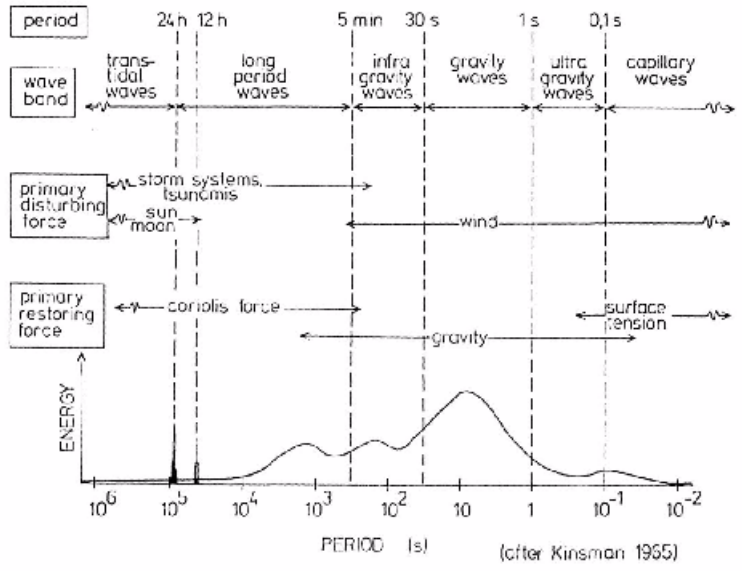

Figure 3.1: Ocean waves classifications (Bosboom and Stive, 2015a)

3.2.1. Wind Waves

Wind waves originate from random and irregular oscillations of the water surface generated by local wind fields. Close to a wind field all kind of waves occur from 1 to 25 seconds. Due to different frequencies the travel speed of the waves is different. One wave will travel faster than another one therefore, the wave field disperses. This is called frequency dispersion. Longer waves travel faster than shorter waves. At some distance from the wind field the longer, fast travelling waves arrive first followed by the waves with shorter wave periods. Far away from the storm centre the short waves are filtered out due to dissipation processes which affect the short waves more strongly than the longer waves and only the longer waves still exist. At a large distance from the storm only swell waves remain, which are long and fairly regular waves. These waves have typical periods of 10 to 30 seconds. Furthermore, the swell is uni-directional due to direction dispersion. This phenomena is explained below in section 3.2.2. The characteristics of the wind field, the distance to the storm and local water depth determine the characteristics of the waves. Swell and sea waves are both generated by the wind and are restored by gravity. Since gravity is the restoring force of the wind wave motion, these waves are also called gravity waves.

Waves are mostly indicated by their height and period. Also the wave length (λ) and wave number (k) are important characteristics of waves. Wave length is the distance over which a wave's shape repeats. The wave number is the number of radians per unit distance. So, the wave number can be calculated by formula 3.1. This value is often used in relation with the depth to give information of the ratio between the waves and the water depth.

$$k = \frac{2\pi}{\lambda} \tag{3.1}$$

3.2.2. Directional Spreading

At oceans and seas, harmonic wave components travel across the surface in all kind of periods, directions, amplitudes and phases. Random waves moving around are the sum of a number of these different harmonic wave components. Wave fields are created by storms and spread out across the ocean. Many directions are generated within these storms. In a two-dimensional spectrum, the wave energy density over directions and frequency is shown (see figure 3.2a). In figure 3.2b the normalised distribution of the wave energy density over directions at one frequency can be seen. The width of this distribution is a measure for the directional spreading. A very wide and low distribution indicates a large variety in wave directions. A very small and high distribution indicates all wave energy is concentrated on a small variety in wave directions, a narrow spectrum indicates a regular wave field.

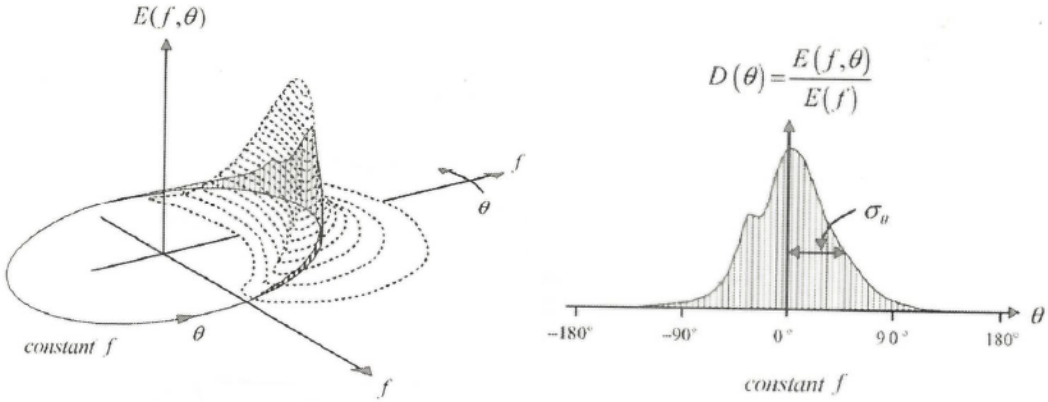

(a) Directional energy distribution over frequency and direction

(b) Normalised directional energy distribution at given frequency

Figure 3.2: Directional energy distribution (Holthuijsen, 2010)

As mentioned above, in a storm many wave directions are generated. Further away from the storm only waves with a certain direction arrive which causes the waves to be more long-crested. The wave field becomes more regular with an increasing distance from the storm (Holthuijsen, 2010). This spreading due to variation in the directions of propagation is called directional dispersion. Due to this phenomena the directional spreading changes from large, close to a storm, to small far away from a storm. Swell is the result of frequency and direction dispersion. It has therefore a narrow spectrum in frequency and direction (Bosboom and Stive, 2015a). Directional spreading of wave energy in a wave field influences waves processes of refraction and diffraction (Goda, 2010). These processes have different effects in case of a narrow spectrum or a broad spectrum. More about this effects can be read in the section about diffraction (section 3.3.4).

3.2.3. Long Waves

Waves with a lower frequency than swell waves are called infra-gravity waves or long waves. These waves are longer than gravity waves and have periods of 25 to 250 seconds. Long waves are mainly a shallow water phenomena. Infra-gravity waves are caused by groups of wind waves. The interference between waves of different wave lengths cause groupiness. In figure 3.3 it can be seen how two sinusoidal waves interact with each other. The interference of the waves causes differences in wave heights, a wave group is formed.

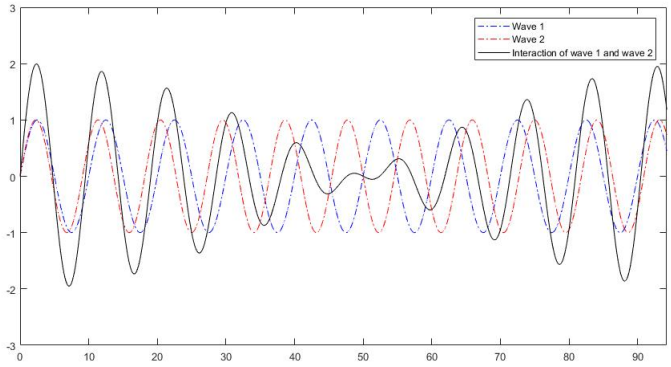

Figure 3.3: Wave interaction of two sinusoidal waves

Due to the variations in wave height in wave groups the radiation stresses vary as well. The highest stresses can be found under the highest waves and the lowest stresses under the lowest waves. A time-varying set-down in the shoaling zone is the result. Under the highest waves the largest depression can be found. This results in a long wave motion on the wave group scale. This long wave has the length and frequency of the group and it travels with the wave group speed. Since it is associated with the group this kind of wave is called

a bound long wave. This is illustrated in figure 3.4. In the surfzone this wave will respond differently since the short waves, the originators of the wave group, will break and the bound long wave is released from the group and will become a free long wave. These bound and free long waves are important for the sediment transport. How this sediment transport works, is treated later this chapter in section 3.5.

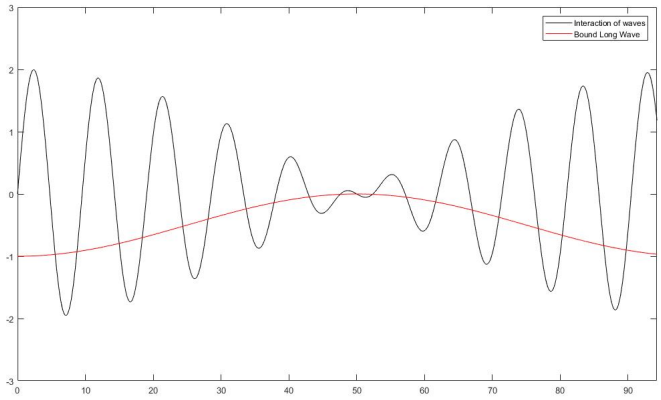

Figure 3.4: Wave group and the resulting bound long wave

The broader the spectrum is, the more irregular the waves are and the less clear the groups can be distinguished. Because of the narrow spectrum, grouping is prominent in swell and more pronounced if the swell is dispersed more (Bosboom and Stive, 2015a). Even more explicit, it can be said that infra-gravity waves are driven by swell, this can be indicated by a strong correlation between the energy levels of infra-gravity waves and swell (Wunk, 1949; Tucker, 1950).

3.3. Wave Processes

Sea and swell waves originate from wind blowing over the water surface and long waves originate from the groupiness of wind waves. When these waves approach the shore, several processes can take place, which transform the waves. This happens when the waves start to feel the bottom or run into structures. In general it can be said that waves start to feel the bottom when the depth is half the wavelength. These processes will now be explained one by one.

3.3.1. Shoaling

As waves propagate to shore, their celerity decreases, since the front of the wave is experiencing more deceleration than the back of the wave. Due to the differences in depth, the back of the wave will run in on the front of the wave or the wave behind will run in on the wave in front. A concentration of wave energy and an increase in wave height is the result. This increase in wave height is called shoaling. The process of shoaling does work the other way around as well. After increase in wave height the wave height can decrease if the depth increases again. This can happen in case of passing over a shoal, but only if no breaking has occurred (Bosboom and Stive, 2015a). The increase in wave height in the shoaling zone is limited by wave breaking.

The energy flux per unit wave crest width, the rate at which energy is transmitted in the direction of wave propagation, is constant. Therefore energy flux at one location can be set equal to the energy flux at another location. Due to the energy balance in which wave height is included, the wave heights at two arbitrary locations can be calculated.

The frequency of a shoaling harmonic wave does not change. However, the (mean) wave frequency of random waves will not remain constant when shoaling occurs. The lower frequencies of the spectrum are affected more than the higher frequencies. Therefore, shoaling is stronger for the lower frequencies. In approaching the shore, this results in a shift of the mean frequency slightly to lower values (Holthuijsen, 2010).

3.3.2. Asymmetry and Skewness

In reality waves are not sinusoidal as often drawn for simplicity. Waves become more and more asymmetric when propagating towards the shore. As mentioned above shoaling includes an increase in wave height, but the shoaling process also includes two non-linear effects: asymmetry and skewness. These non-linear effects are important for wave-induced transport. Both effects have to do with asymmetry, one on the horizontal axis and one on the vertical axis. The last one is just called asymmetry and it implies a pitched forward wave shape or relative steepening of the face of the wave. This is caused by the fact that the wave crest moves faster than the trough in shallow water. In figure 3.5a this effect of asymmetry can be seen. The asymmetry on the horizontal axis is called skewness. This implies peaking of the wave crest and flattening of the wave trough. In figure 3.5b a skewed wave in shallow water is shown.

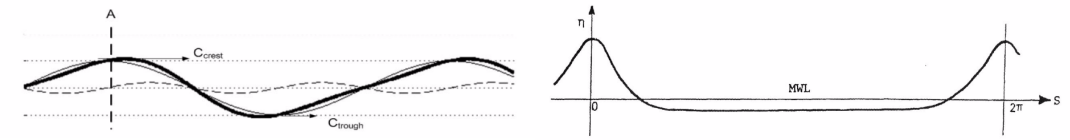

(a) Asymmetry (relative to vertical axis)

(b) Skewness (asymmetry relative to horizontal axis)

Figure 3.5: Non-linear effects: Asymmetry and skewness (Bosboom and Stive, 2015a)

3.3.3. Refraction

Refraction is the phenomena that waves bend towards the shore. When the depth contours are parallel and a long-crested obliquely incident linear wave approaches the shore, it will turn due to differences in speed along the wave crest. In the deeper parts the wave crest travels faster than in the shallower parts, which causes the wave crest to turn towards the depth contour. At the same moment in time, one side of the wave crest has travelled further towards the shore than the other side. In case of parallel depth contours, the direction of the waves changes proportionally to the wave propagation speed according to Snell's law (equation 3.2)(Bosboom and Stive, 2015a).

$$\frac{sin\phi_2}{c_2} = \frac{sin\phi_1}{c_1} \tag{3.2}$$

In figure 3.6a the idea of refraction can be seen in a sketch. If depth contours are not parallel, like a lot of cases in reality, waves will converge or diverge. This means an accumulation or dissipation of energy respectively, with high wave heights and reduced wave heights as a result. This often happens in bays with headlands (figure 3.6b). The waves bend towards the headlands and most energy is concentrated there (Bosboom and Stive, 2015a).

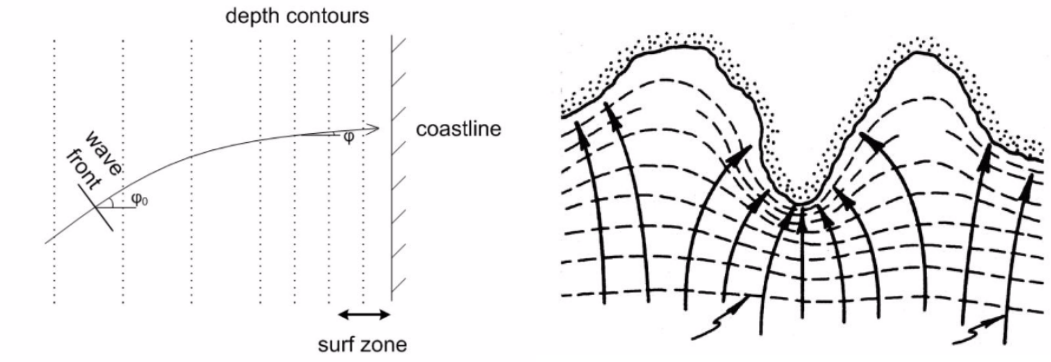

(a) Refraction on parallel depth contours

(b) Refraction on non parallel depth contours

Figure 3.6: Refraction (Bosboom and Stive, 2015a)

3.3.4. Diffraction

Wave propagation can be obstructed by a structure or a headland. The wave will be partly blocked by this structure. Due to these obstruction a large (initial) variation of wave energy along the wave crest arise. This leads to energy transfer along the wave crests. Behind the structure the wave crest will bend around the obstacle. This phenomena is called diffraction and can be explained by the Huygens-Fresnel principle (Bosboom and Stive, 2015b). This principle implies that every point on the wave crest can be seen as a source for the wave. The wave moves away from this point in circles, all circles together show the wave crest. In case of an obstruction, no waves are generated and the point in the end will cause the wave crest to bend. The wave energy is transferred along the wave crest into the shadow zone of the structure. This phenomena results in a gradual decrease of wave energy and therewith wave height into the shadow zone. In figure 3.7a this principle is illustrated.

The wave height gradually decreases from 100% of the incoming wave height in the totally undisturbed area towards zero a distance into the shadow zone. In case of harmonic, long-crested waves and a constant water depth, the wave height is about 50% of it's original height at the boundary of the shadow zone (see figure 3.7b) (Bosboom and Stive, 2015a).

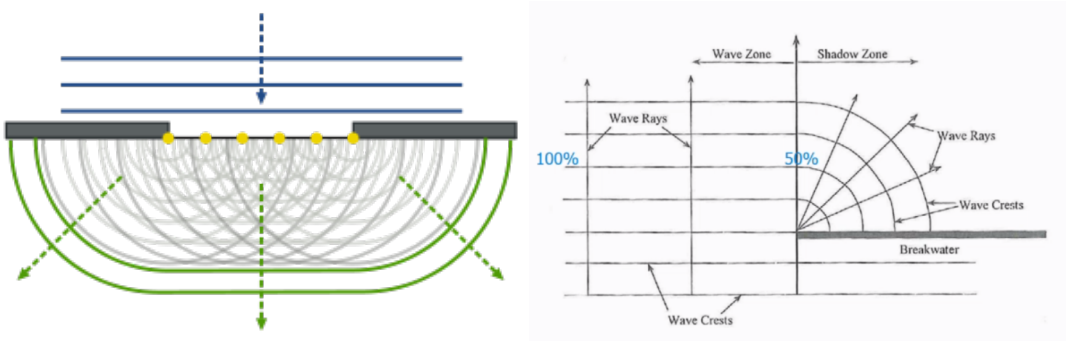

(a) Diffraction points

(b) Diffraction pattern

Figure 3.7: Diffraction patterns (Bosboom and Stive, 2015b)

However, harmonic long crested waves give a different diffraction diagram than random short crested waves. In case of irregular, random, short-crested waves and a constant water depth, the wave height at the boundary is about 70% of the incoming wave height (Goda, 2010). The diffraction patterns of random waves penetrate therefore further into the shadow zone. This causes an underestimation of the wave height in shadow zones in case diagrams for regular waves are employed on a case with random waves (Goda, 2010). Furthermore, the incident wave height is reached closer to the boundary of the shadow zone in case of regular waves. This causes a decreased wave height in a more wide area in case of random waves. In figure 3.8 this is illustrated.

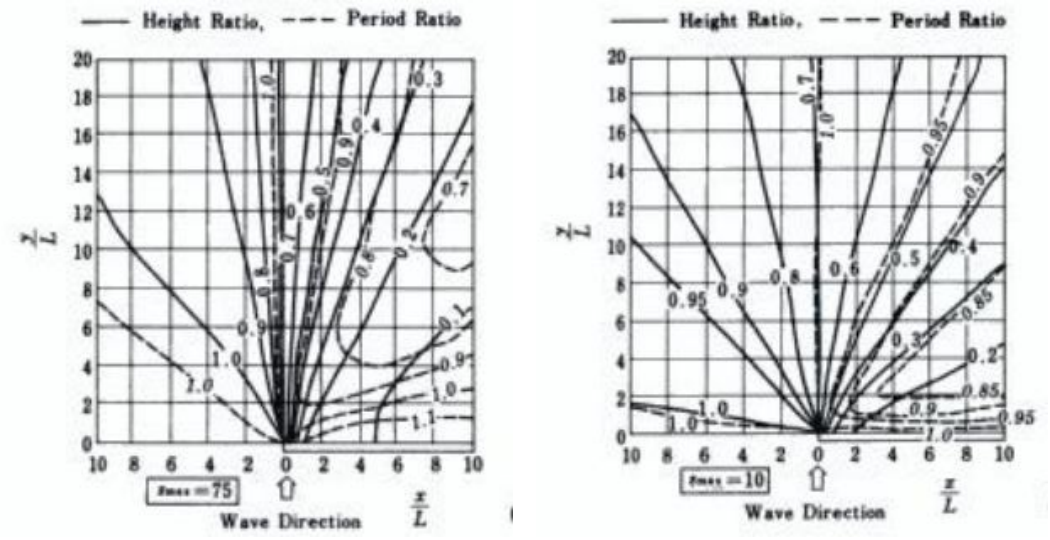

(a) Diffraction Diagram for random waves with a small spreading

(b) Diffraction Diagram for random waves with a large spreading

Figure 3.8: Diffraction diagrams with various spreading factors (Goda, 2010)

In a changing water depth the ratios between local and incident wave height are different than stated above. Other processes like refraction, shoaling and wave breaking will play an important role in the wave propagation as well. Often this is the case because structures are often found close or adjacent to the coast. Therefore, the diagrams can not be used exactly on diffraction situations close to the coast.

3.3.5. Transmission

In case an obstacle is located in the sea, waves are obstructed in their propagation direction. What exactly happens depends on the obstacle. Obstacles like breakwaters can be very open or very closed, they can be submerged or emerged and they can be shore attached or detached. Wave energy can be reflected, it can be absorbed and it can travel over and through the structure. Wave transmission is the part of the wave energy which can continue. Due to the reflection and absorption of energy the waves behind the breakwater will be different from the incident waves. As mentioned before, the exact effects depend very much on the kind of structure and its dimensions.

3.4. Current Processes

Due to wave breaking, refraction, diffraction and other wave processes, wave conditions can vary along a stretch of coast. These variations give rise to variations in wave forces and therewith the wave set-up shows variations along the coast. Set-up is defined as: 'a wave-induced increase in the mean water level near the shore' by Pattiaratchi et al. (2009). These variations result in current patterns. Below, several wave induced current processes are described.

3.4.1. 2D Horizontal Circulation

Some areas are sheltered from waves due to structures like groynes and detached breakwaters, this side of structures is called the leeward side. In these areas special current patterns develop due to the sheltering effect. These current patterns are caused by set-up differences. The set-up in the exposed areas is larger than the set-up in the adjacent sheltered areas which generates a gradient in the water-level towards the sheltered areas (Mangor, 2004). This difference causes current flows from the areas with a higher set-up to areas with a lower set-up. Eventually, the water has to leave the area so, a return flow is present in deeper water. This flow patterns are called eddies. In figure 3.9 two sketches of eddy formation can be seen, one situation with a groyne and one with a detached breakwater.

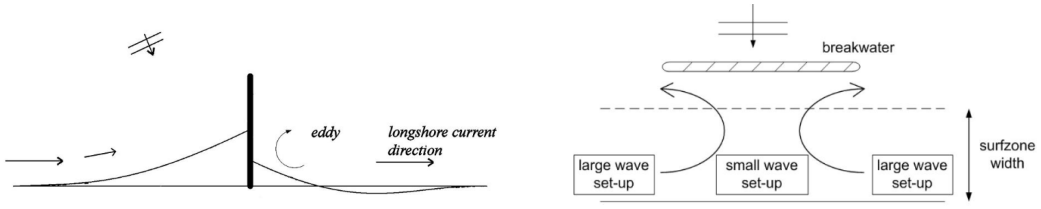

(a) Eddy formation next to a groyne

(b) Eddy formation behind a breakwater

Figure 3.9: Eddy formation in shadow zones (Bosboom and Stive, 2015a)

In pocket beaches the headlands influence the processes in the bay sufficiently. Due to headlands, shadow areas come into existence. The wave angle and geometry of the headlands determine the size of the shadow zone and with that the amount of wave dissipation driving the boundary circulation (Pattiaratchi et al., 2009). In the research of Pattiaratchi et al. (2009) a constant re-circulation cell, driven by set-up differences, was present in the lee of the groyne. An example of the circulation pattern measured can be seen in figure 3.10. All other measurements and model runs of Pattiaratchi et al. (2009) show similar circulation patterns. Pattiaratchi et al. (2009) showed in all model runs, similar to the observations of the field measurements, that around the wave shadow zones an eddy was formed.

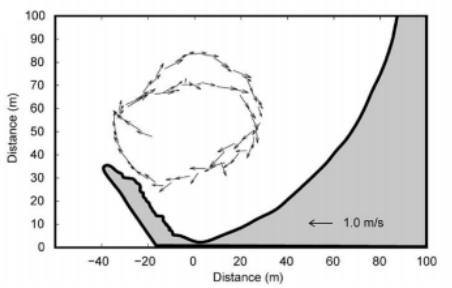

Figure 3.10: Drifter speeds recorded at Cottesloe Beach on 29 June 2004 period of 1500-2000 s by Pattiaratchi et al. (2009)

Indicated by sensitivity studies, it is apparent that the circulations are controlled by incident wave angle, wave period, and especially by the wave height (Pattiaratchi et al., 2009). An increase in the wave energy flux increased the strength of the eddy circulation (Pattiaratchi et al., 2009). The vorticity of the eddy increased with higher wave heights and also with higher wave periods but, in the latter case, less. When the vorticity increased, the eddy tended to move offshore, however, the alongshore location hardly ever changed (Pattiaratchi et al., 2009). Furthermore, Pattiaratchi et al. (2009) concluded that the outflow along the groyne was strongest with large wave height and wave period and an angle of incidence close to 45 degrees.

3.4.2. Rip Current

According to Castelle et al. (2016) rip currents are defined as: 'narrow and concentrated seaward-directed flows that extend from close to the shoreline, through the surf zone, and varying distances beyond'. Alongshore directed currents in the surf zone turn seaward on several places; rip currents are formed. This can be recognized in the above circulation patterns close to structures. However, rip currents are not only present close to structures. The alongshore currents can be driven by gradients in radiation, shear stress or by set-up differences (Bosboom and Stive, 2015a).

The angle of incidence of waves on the beach play a role in the formation of rip currents (Silva et al., 2010). Ab Razak et al. (2014) found that wave breaking conditions were important in the development of a large scale rip current. Furthermore, alongshore variations in wave heigth result in rip currents (Bowen, 1969). Baquerizo Azofra et al. (2002) found a relation between the gradient of the wave height and the velocity of the circulations. Even in a macro tidal environment, the mean flow in the pocket is exclusively wave-driven in the intertidal zone since, the headlands or groynes isolate the shoreface from the active tidal circulation (Dehouck et al., 2009). However, the tidal level does have an influence on the section where erosion could take place (de Santiago González, 2014).

Rip currents occur in all different types, Castelle et al. (2016) categorized these types by their dominant controlling forcing mechanism. These types are subdivided in two types by their different physical driving mechanisms. The three main rip current types are hydrodynamically-controlled, bathymetrically-controlled and boundary-controlled rips. Hydrodynamically-controlled rips are subdivided into shear instability rips and flashrips. Bathymetrically-controlled rips consist of channel rips and focused rips. Boundary-controlled rips are subdivided into deflection rips and shadow rips. The shadow rips originate from the eddies shown above in section 3.4.1. Deflection rips occur when a strong alongshore current, generated by oblique waves, is deflected seaward when encountering a groyne or headland (Castelle et al., 2016). Apart from these six types of rips a lot of combinations of driving mechanisms occur in the rip current formation and therefore, many more forms of rip currents occur on beaches which are a mixture of above mentioned types. Examples of mixed rip current types are channel-flash rips, focus-channel rips, boundary-channel rips and embayed cellular rips. More information on all kind of rip currents can be found in the research of Castelle et al. (2016).

Since this research is about small artificial pocket beaches, the embayed-cellular rips will be treated in more detail. These rips particularly occur if the embayment width is narrow compared to the surfzone width. The boundary, the headland or groyne, dominates the circulation within the entire embayment. A cellular rip can flow offshore in the middle, at one end or at both ends (see figure 3.11). However, in most research mostly rips at the boundary are described (Ab Razak et al., 2014; Short and Masselink, 1999). The location of the rip current depends on the shape and cross-shore extent of the boundary, wave conditions and beach curvature (Castelle and Coco, 2012).

Also, Ab Razak et al. (2014) showed that the development of rip currents is influenced by headland structures and the embayment length. These structures cause, due to the shadow zone creation, processes like diffraction. The scale of the pocket beach also has an influence on the effects of wave angle and wave height on circulation patterns (Ab Razak et al., 2014). The entire beach circulation may eventually become impacted by the effects of boundaries when wave heights increase or headlands are closer together or a combination (Short and Masselink, 1999). The non-dimensional embayment scaling parameter is used to express the influence of the headlands to the circulation patterns on a beach (Short and Masselink, 1999). In an embayment dominated by the end effects one or at most two 'natural' rips occur at the boundaries, this is called cellular circulation (Short and Masselink, 1999). From Ab Razak et al. (2014) the embayment scaling parameter is, for a beach length of 500 metres and wave heights between 0.5 and 5 metres, always below 8 and thus of cellular type. In the research of Ab Razak et al. (2014) the middle rip current hardly occured in this short embayment length of 500 metres but some small developing rip could be found. The headland rips could be found in all cases of Ab Razak et al. (2014).

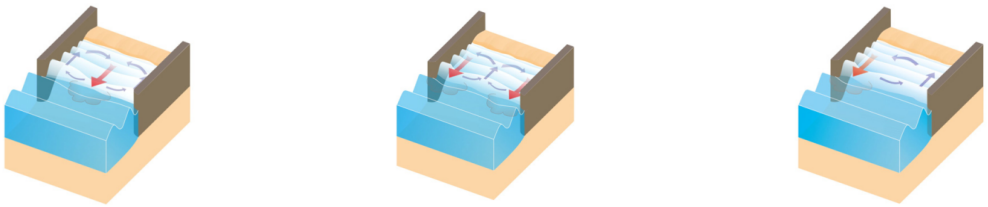

(a) ripcurrent at the centre of an embayment

(b) Ripcurrent at both ends of the embayment

(c) Ripcurrent at one end of the embayment

Figure 3.11: Schematics of cellular rip currents in embayed beaches (Castelle et al., 2016)

Higher energetic conditions increase the current speeds in the cellular rips. With increasing wave height or decreasing water depth, the rip flow velocity increases (Castelle et al., 2016). Also Daly et al. (2011) mentioned that increased wave heights cause stronger currents, which will cause an accelerated morphological development. These findings are also observed by Dehouck et al. (2009), who found that mean flow motions are active during energetic wind and wave events. Other studies also have found dat storm wave conditions strenghten the cellular currents. Among others, Loureiro et al. (2012) found that cellular rips are specifically common during storm wave conditions.

3.5. Sediment Transport

The interaction of hydrodynamics and sediment transport is very complex. Sediment transport can be defined as the movement of sediment particles in a well-defined area over a certain time (Bosboom and Stive, 2015a). This movement depends on the characteristics of the transported material, the initiation of motion and the transport regimes.

The total transport rate consist of the the sum of the bed load transport rate and the suspended transport rate. This are two different transport modes that can be distinguished. Bed load transport is sediment transport close to the bed, particles are more or less continuously in contact with the bed. The particles roll or slide over the bed, with an increased bed shear stress they make small jumps. In case the jumps become too large, the particles loose contact with the bed and become suspended load. Suspended load transport means the transport of sediment particles suspended in the water column, without contact with the bed. Sediment particles in a certain vertical plane can move horizontally across it with the water particles and thus with the same speed as the water particles.

The sediment transport is dependent on the sediment concentration and the horizontal velocity of the water. In the area close to the coast, waves are important in the water motion. As a result, the water velocity and the sediment concentration vary in time, correlated to the wave period. Often wave-averaged velocities and concentrations are used. Wave motions stir up the sediment and turbulent forces transport the sediment upwards. Stronger waves generate a higher sediment concentration.

Sediment transport can be distinguished in two main directions, cross-shore transport and alongshore transport. The sediment transport in pocket beaches is in both directions. This could cause beach rotation and accretion or erosion of the beach. This sediment transport is driven by waves and currents. Below, these transport directions and the corresponding processes will be elaborated.

3.5.1. Cross-shore Transport

Cross-shore sediment transport is very complex and consist of several processes. Under normal, mild conditions undertow, bound and free long waves and short wave skewness are important. In this case onshore transport by short wave skewness is dominant. Under more extreme conditions undertow and long waves are dominant (Bosboom and Stive, 2015a). Furthermore, the wave induced currents like the above described rip currents play an important role in the cross-shore sediment transport.

Undertow

Undertow is a return current in the surf zone as a result of breaking waves. Due to wave breaking the mass transport between wave through and wave crest is quite large, this is compensated by a large seaward directed flow below wave through level (Bosboom and Stive, 2015a). Due to this high offshore-directed velocities in the lower part of the water column, where the sediment concentrations are high, undertow plays an important role in seaward sediment transport. Especially during heavy storm conditions this could cause severe beach erosion.

Long Waves

As long as long waves and their originating wave group are in their original phase, so it is a bound long wave, the sediment transport of long waves is offshore directed. The short waves in the wave group stir up the sediment and the long wave determines the direction of the transport. Since the sediment concentration is higher under the higher waves in the wave group and the transport direction is offshore at this location in the wave group, the offshore directed sediment transport is larger than the onshore directed sediment transport. An illustration of this process is given in figure 3.12. When the waves in the wave group break, the long wave becomes a free long wave and the combination of concentration and transport direction is not the same anymore. Therefore, the main direction of transport under free long waves could be different.

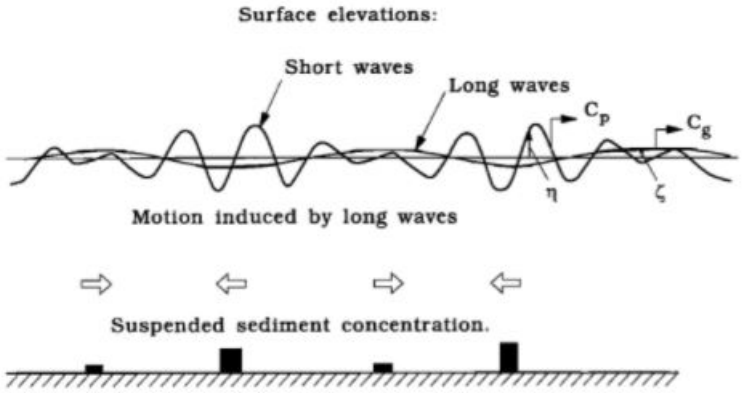

Figure 3.12: The mechanism of sediment tranport under bound long waves (Deigaard et al., 1999)

Rip Currents
The rip currents that are common in pocket beaches influence the sediment transport as well. The local sediment transport rates can be affected by circulation patterns in the shadow areas of groynes (Pattiaratchi et al., 2009). Also Mangor (2004) mentioned the outward-directed current along the lee side of groynes which cause offsore sand loss and local seabed erosion. Velocities and penetration length into the sea are important factors for the sediment transport. In case of high velocities, the rip current can transport more material and the further it is transported the longer it takes to return to shore (Short and Masselink, 1999). Sometimes it may even be lost from the system (Roy et al., 1994).

3.5.2. Alongshore Transport

Oblique waves approaching a coast at an uniform angel cause a constant, uniform transport of sand along this coast if no other driving forces are present. This wave induced alongshore transport can be interrupted by structures or openings. These obstructions will change the sediment balance and therewith sedimentation and/or erosion.

Next to the direct wave induced alongshore transport, the alongshore transport can also be induced by wave induced currents. The eddies, discussed in section 3.4.1 cause a sediment transport opposite to the wave induced alongshore transport. The alongshore sediment transport direction is dependent on the distance between the groynes, the wave energy and direction and the strength of the current.

3.5.3. Accretion and Erosion

A structure can block the alongshore sediment transport. The consequence is sand accumulation on the updrift side and erosion on the downdrift side. However, due to variations in wave attack due to sheltering effects, the erosion will not be right next to the groyne. A sketch of this phenomena can be seen in figure 3.13. Sheltered areas are sedimentation areas (Mangor, 2004; Ab Razak et al., 2013). Also, Fredsoe and Deigaard (1992) mentions that sediment will accumulate around groynes in the shadow zones by the sheltering effect.

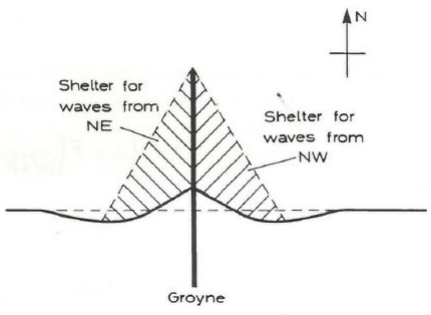

Figure 3.13: Sketch of erosion and sedimentation at both sides of a groyne with oblique incident waves with the shelter zones (Fredsoe and Deigaard, 1992)

The wave height is also important in sediment transport. Turki et al. (2015) stated that the beach evolution is faster in case of a higher wave heights. Furthermore, Martins et al. (2010) found that morphological changes in the coastline are shown by waves mainly above 2 metres. So, it can be concluded that high energy events play an important role in beach evolution in pocket beaches. However, what the physical processes exactly are that cause the beach transformation and are affected by the different parameters is not analysed in detail (de Santiago González, 2014).

Since the circulation pattern, induced by the variation in set-up, causes the sedimentation in the shelter zone and the rip currents cause erosion, the variations in wave height, wave period and embayment size are important parameters for the sediment transport and therefore the amount of erosion and accumulation. Variations in these processes are created by diffraction and storm conditions increase the effect of these processes.

3.6. Predictive Methods for Pocket Beaches

Ab Razak et al. (2014) mentioned that embayed beach morphodynamic modelling has not yet been done extensively and if it was done, it was for low wave energy conditions only. In the research of Ab Razak et al. (2014) a start has been made with variations in wave height and beach scales. The findings and recommendations of that research go in a row with the other findings of important processes and phenomena described above. More research is needed to the underlying processes that cause circulation patterns and therewith beach dynamics in pocket beaches. Furthermore, the modelling of embayed beaches including storm conditions would be valuable. A lot of research already shows the importance of storm conditions for circulation patterns and beach dynamics. Ab Razak et al. (2014) also suggested to include storm wave grouping in the numerical models to research the effects of real storm waves to the development of current circulations in the surf zone of small scale embayed beaches. However, model results on storm conditions in pocket beaches are limited.

For the model to use, it is important that it can show the hydrodynamic, sediment transport and sedimentation and erosion patterns in pocket beaches. Furthermore, it should be able to model storm conditions. Beside that, it is important the variation including or excluding diffraction can be made to examine the effect of diffraction.

The first requirement of showing different patterns would militate for an area model. So, a Delft3D or XBeach model could be used to show what is happening with the waves and the currents in the pocket beaches. Furthermore, these models could show sediment transport and morphological changes in the pocket beach as well. The processes and the general movement of sediment are important, not the exact location of the shoreline. Therefore, a equilibrium bay shape model is not suitable for this research.

Additionally, morphodynamic changes during storm conditions will be researched. To include storm conditions and with that storm wave grouping, XBeach is a useful model. XBeach has originally been created to model hydrodynamic and morphodynamic processes and storm impact on sandy coasts (Roelvink et al., 2015). The model has been applied to more variations of coasts and purposes since then. Equilibrium bay shape models give a good approximation of the coastline under constant wave conditions. However, rapid impacts of short-term events are not taken along (Ojeda and Guillén, 2008). Other advantages of XBeach are the fact that it does not make use of an equilibrium, so losses out of the pocket beach system are possible. Besides, XBeach does not make use of an averaged wave condition.

XBeach has three hydrodynamic modes available to perform a calculation; stationary wave mode, surfbeat mode and non-hydrostatic mode. These modes differ on the time-scales resolved (Roelvink et al., 2015). This variation in wave resolving makes it possible to research the effect of diffraction. In the stationary wave mode, short waves are averaged and wave-group variations are neglected. This mode is often used to model morphological changes during moderate wave conditions, possibly in combination with tides (Roelvink et al., 2015). The surfbeat mode is an instationary hydrostatic mode in which the variation of the short-wave envelope is solved on the scale of wave groups. Short waves are still averaged but long waves and unsteady currents are included in this mode (Roelvink et al., 2015). The non-hydrostatic mode is a short-wave resolving model. A lot of processes are included however, this requires a high spatial resolution and associated smaller time

steps which makes this mode computationally much more expensive than the other modes (Roelvink et al., 2015). Furthermore, the simulation of the sandy morphology has not been extensively validated in this mode (Roelvink et al., 2015). A small overview of the abilities of the three modes is shown in table 3.1.

	Stationary wave mode	**Surfbeat mode**	**Non-hydrostatic mode**
Long waves	X	V	V
Diffraction	X	X *	V
Sediment Transport	V	V	X**
Short Computation Time	V	V	X

Table 3.1: Ability of different modes in XBeach (Roelvink et al., 2015) (* Only long wave diffraction, no short wave diffraction. ** Not extensively validated.)

XBeach has already been used in pocket beach simulations on a small scale (Bemmelen, 2017; Ab Razak et al., 2014; de Santiago González, 2014; Castelle and Coco, 2013; Ab Razak et al., 2013). Some storm events are modelled in large embayed beaches and a start has been made in the research of the applicability of XBeach on the long term modelling of pocket beaches (Bemmelen, 2017). So far, the surfbeat mode has been used for this pocket beach research. However, diffraction seems to be important and therefore it is interesting to look into the results of the non hydrostatic mode of XBeach. Therewith, more knowledge is gathered on the importance of diffraction and therewith the applicability of various XBeach modes on the design of artificial pocket beaches.

From this literature review, it becomes apparent that beach dynamics are mainly driven by high energy events. Long term pocket beach dynamics are therefore controlled by losses during storm conditions. Furthermore, it is supposed that diffraction plays an important role in shaping the circulation patterns. Therefore, diffraction could be important in the sediment transport processes and erosion and sedimentation patterns in relatively small artificial pocket beaches. The effect of diffraction on the dynamics within these pocket beaches can be researched by examinening different modes of XBeach. By using various modes of XBeach diffraction and long waves can be excluded or included and therewith the results can be compared.

4

Simplified Pocket Beaches

4.1. Introduction

In this chapter a simplified pocket beach has been simulated with various modes of XBeach to research the influence of diffraction on the hydrodynamic and sediment transport dynamics. This has been done on the basis of hypotheses based on the literature research and the simulation of different variations (appendix A). First, the influence of short wave diffraction is researched separately. Second, the influence of long waves is examined particularly. Third, these two phenomena are combined for more realistic circumstances; short wave diffraction is researched in case long waves are incorporated. This latter case is researched more extensively, also morphological developments are examined.

4.2. Model Set up

4.2.1. Layout

The layout is based on sandy beaches so the slope is chosen similar to examples of sandy beaches in the Netherlands, illustrated by Bosboom and Stive (2015a). For this simplified beaches a slope of 1:100 is chosen for the part below mean water level and a slope of 1:40 is chosen for the part above mean water level. So as usually, the upper shoreface is steeper than the lower shoreface. In figure 4.1 a 3D view of the pocket beach can be seen.

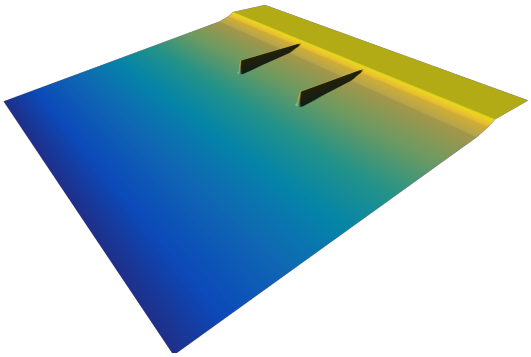

Figure 4.1: 3D view of the bathymetry of a simplified pocket beach (the colors indicate the bed level)

The pocket beach has a width of 500 metres at the shoreline because in chapter 3 it could be read that in beaches of 500 metres the influence of structures on circulation patterns is significant. The long groynes reach about 350 metres offshore seen from the 0 metre contour line. These dimensions are common for artificial pocket beaches and therefore interesting to research to achieve improved designs.

The model set up has been tested by a sensitivity analysis, which can be found in appendix B. In this sensitivity analysis the boundary effects and the effect of a non uniform offshore boundary are researched (appendix B.1). Boundary effects can be noticed, however, the beaches with groynes are less effected by boundary effects

than the plain beaches, the beaches without any groynes. Therefore, an area of 1000 by 1000 metres is enough to research the processes within the embayment. Though, the effects and processes outside the embayment area should not be looked at. Besides, the effect of the non uniform offshore boundary is small. The boundary effect caused by reflecting waves in case of waves initiated under an angle relative to the grid is much more. Therefore, it is chosen to work with rotated grids in this research. The two variations used in this research are shown in figure 4.2. In figure 4.2a the layout is shown for normal incident waves. For oblique incident waves figure 4.2b is used. The waves approach the coast under an angle of 30 degrees to normal incident waves. A shadow zone is present in this case. The normal incident wave cases function as a check for the oblique incident wave cases. The main interest to research diffraction effects can be achieved by the oblique incident wave cases. With this beach length, groyne length and wave direction the shadow zone captures about 30% of the embayment. The exposed zone takes up 70% of the embayment.

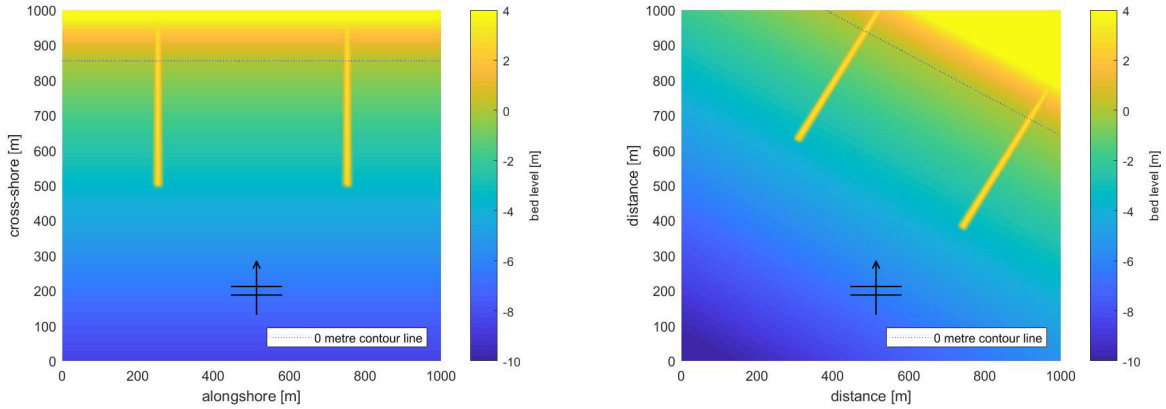

(a) Layout pocket beach for normal incident waves

(b) Layout pocket beach for oblique incident waves

Figure 4.2: Bed elevation of the pocket beach layouts used in this research

4.2.2. Wave Height

As mentioned in the introduction and literature review (chapters 1 and 3) storm conditions are important in the hydrodynamics and morphodynamics in pocket beaches. Martins et al. (2010) mentioned that morphological changes are especially shown as a result of wave heights above 2 metres. The wave height and wave period for the simulations in this chapter are chosen as shown in table 4.1. For the monochromatic cases a different input is required than for the cases with a wave spectrum. The wave spectrum is implemented as a JONSWAP spectrum with a H_{m0} and T_p value. Approximately, the input values can be converted into each other with formula 4.1.

$$H_{rms} = 0.5\sqrt{2}H_{m0} \tag{4.1}$$

	Monochromatic waves	Wave spectrum
Wave height	H_{rms} = 2 m	H_{m0} =2.84 m
Wave period	T_{rep} = 10 s	T_p = 14 s

Table 4.1: Wave height and wave period input for model simulations

4.2.3. Spreading

A JONSWAP spectrum requires a spreading parameter as well. The directional spreading can be expressed in the directional width σ_θ. The directional width can be converted to the width parameter of the JONSWAP spreading parameter, s. The relation between these two is shown in equation 4.2 (Roelvink et al., 2015). The monochromatic waves are regular, the directional with is very narrow. Therefore, the value of the directional width of the cases with a wave spectrum is chosen to be small as well to make the cases good comparable. The exact input value is chosen at s=800, since this value gives rise to the best match in wave height (see appendix B.3).

$$\sigma_\theta = \sqrt{\frac{2}{s+1}} \qquad s = \frac{2}{\sigma_\theta^2} - 1 \tag{4.2}$$

4.2.4. Grid Cell Size

In the sensitivity analysis also the numerical wave dissipation has been researched (appendix B.2). This has been done by checking the kd value and the grid cell size. From this examination it follows a grid cell size of 2.5 metres by 2.5 metres is necessary to limit the numerical wave dissipation in the non hydrostatic mode of XBeach. Therefore, the following simplified pocket beach simulations are all conducted with this grid cell size.

4.2.5. Simulation Results

The hydrodynamic and sediment transport simulations without morphological changes are simulations of 2400 seconds. The wave height, velocity and sediment transport results shown in this chapter are mean values over the last 300 seconds. The results are shown in top views, cross-shore and alongshore profiles. The cross-shore and alongshore profiles are given in the middle of the pocket beach in both directions. The exact locations can be seen in figure 4.3.

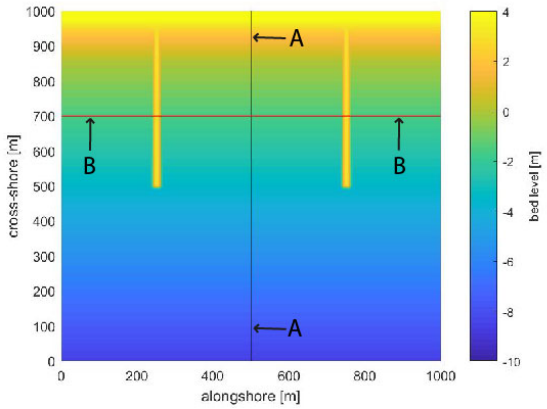

(a) Locations of the cross-shore AA (black) and alongshore BB (red) profiles in case of normal incident waves

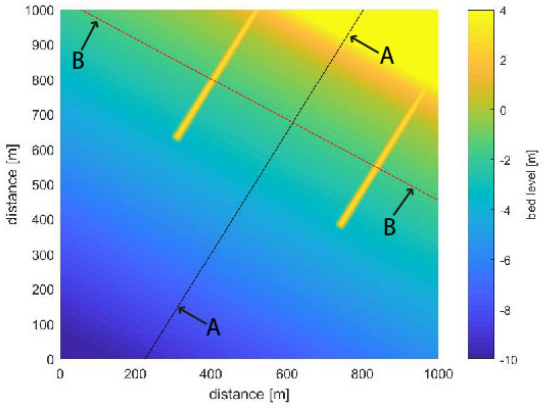

(b) Locations of the cross-shore AA (black) and alongshore BB (red) profiles in case of oblique incident waves

Figure 4.3: Locations of cross-shore and alongshore profiles in pocket beaches on the bathymetry of the pocket beach

The wave height, velocity and sediemnt transport results are all initials patterns. The bed level is not updated in these cases, therefore this figures are not representative for the hydrodynamic and sediment transport patterns over a long period. However, it gives some first insights.

The wave height output of the various modes is a bit different from each other. When the wave height is averaged the wave height (H_{rms}) is given as output, based on the instantaneous wave energy (Roelvink et al., 2015). However, in case the waves are resolved separately the wave height is not given as direct output. The variance (m0) of the water level is than given as an output variable. This value can be used for the calculation of the wave height by using equation 4.3. This equation is especially valid for deep water, therefore, it is not completely correct in this situation. However, it is the best method available to be able to compare results.

$$H_{m0} = 4\sqrt{m0} \qquad H_{rms} = \sqrt{8m0} \tag{4.3}$$

The stationary mode gives a direct output of the wave height, the non hydrostatic mode gives a value for the variance and the surfbeat mode gives both. In the surfbeat mode the wave height of the long waves is based on the variance and the short wave height is based on the output value H_{rms}. The shown mean wave height

is these two combined.

Another difference between the various modes are the sediment transport formulas implemented and the reliability of the sediment transport results. The formulas for sediment transport implemented in XBeach have been properly validated for the surfbeat and stationary mode, however, for the non hydrostatic mode it is not extensively validated yet (Deltares, 2017). Therefore, quantitative comparison of the magnitudes of the sediment transport of different modes of XBeach is not completely reliable. Though, a qualitative comparison of locations with high and low magnitudes of sediment transport within the pocket beaches is feasible. To be able to quantitatively compare the sedimentation and erosion results of two modes, in section 4.6 a factor has been used to bring the sediment transport to more comparable levels.

Next to the simplified pocket beach also simulations of plain beaches have been done. The plain beaches are the same as the pocket beaches except the groynes are absent in the plain beach cases. The results of these plain beaches can be found in appendix C. The plain beaches make clear what the differences are caused by the model. A plain beach with normal incident waves show the differences of wave breaking without any other differences. To research the differences with wave breaking and refraction included, a plain beach with oblique waves have been simulated. It should be kept in mind the plain beaches are more influenced by boundary conditions (appendix B.1). Therefore, the plain beach results are not completely reliable.

4.3. Short Wave Diffraction

In this section the influence of short wave diffraction is researched separately. Long waves are not taken into account in these first simulations. It is assumed short wave diffraction is of influence on the dynamics within relatively small artificial pocket beaches. This is based on the idea that circulation patterns are induced by set-up differences. Due to variations in wave height over the exposed and shadow zone a circulation pattern is created. Since, the wave height variation is very abrupt without diffraction and slow and gradually with diffraction, it is expected the circulation pattern with diffraction is wider. The following hypothesis is formulated:

Short wave diffraction in a relatively small pocket beach influences the circulation pattern and therewith the sediment transport pattern; it makes the circulation cell wider.

4.3.1. Model Set up

For this section the stationary and non hydrostatic mode, both imposed with monochromatic waves, are compared. The stationary mode does not include diffraction, but in the non hydrostatic mode diffraction is included. The monochromatic waves are used to exclude groupiness and long waves and make the two ways of modelling as similar as possible apart from the short wave diffraction.

4.3.2. Plain Beach

In appendix C.1 the results of plain beach simulations are shown. The results of both wave directions show that the wave height in the stationary mode decreases earlier than the wave height in the non hydrostatic mode. This could be explained by the different ways of calculating wave breaking. The velocities of the non hydrostatic simulation are a little bit higher than the velocities in the stationary mode, however, the differences are very small. With oblique incident waves the velocities have some more differences, however, the main direction along the coast towards the top left corner and the speed ranges are very similar.

4.3.3. Wave Height

In figure 4.4 the mean wave height in both simulations are shown. In figure 4.5 a cross-shore profile (AA) and an alongshore profile (BB) of the mean wave heights through the middle of the pocket beach can be seen. The wave height in the non hydrostatic mode is, in most part of the shore face, higher than in the stationary mode. This difference was also visible on the plain beaches and is therefore not related to the pocket beaches but probably to the different way of wave breaking in both modes.

Nevertheless, there are some differences in non hydrostatic simulation between the plain beach case and the pocket beach case. In figure 4.5 clearly a variation in the mean wave height of the non hydrostatic mode can be seen. This could also be seen in figure 4.4b, where colors are not uniform. These variations are caused by

reflection of the waves on the groynes. This is probably an overestimation since the groynes are schematised as impermeable and are thus much more reflective than in reality.

Furthermore, it is interesting to look at the wave height close to the groynes. This can be seen in figure 4.4, but it is more clearly seen in figure 4.5b. In the results of the stationary modes no variations in wave height are observed close to the groynes. The wave height only suddenly drops very close to the groynes. In contrary, in the results of the non hydrostatic mode the wave height close to the groynes is more gradually reduced to zero.

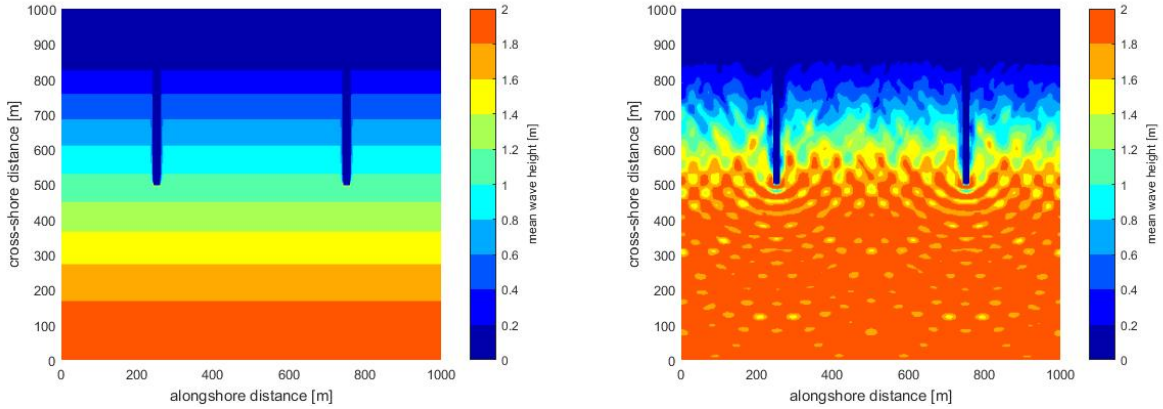

(a) Mean wave height in stationary mode

(b) Mean wave height in non hydrostatic mode

Figure 4.4: Mean wave height in pocket beach with normal incident monochromatic waves

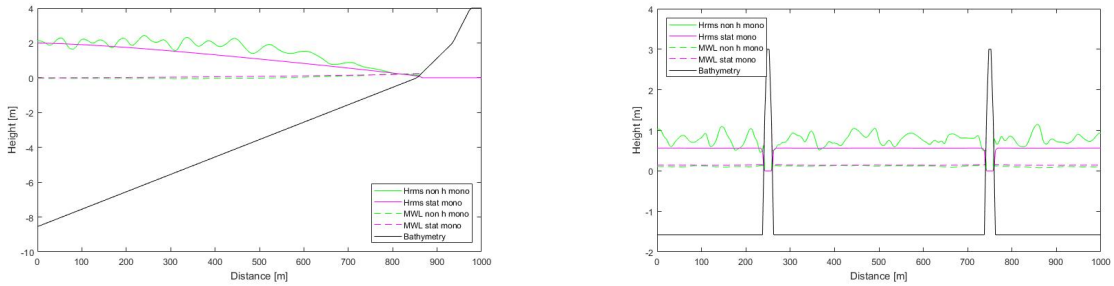

(a) Cross-shore profile AA of the mean wave height

(b) Alongshore profile BB of the mean wave height

Figure 4.5: Cross- and alongshore profiles of the mean wave height in pocket beach with normal incident monochromatic waves

In figure 4.6 and 4.7 the results for a pocket beach with oblique incident waves can be seen. Most outstanding are the complete shadow zones without any wave height in the results of the stationary mode (figures 4.6a and 4.7b). So, the decrease of wave height in the stationary mode is very abrupt at the shadow zone. In contrary, the results of the non hydrostatic mode show a wave height everywhere in the embayment. Even in the shadow zones a wave height still exists, even though, the wave height has been decreased in the shadow zones towards the groynes (figures 4.6b and 4.7b). The wave height at the shadow zone boundary is in fact already decreased in the non hydrostatic mode. In figure 4.7b it can be seen that the mean water level of the stationary mode is especially higher in the middle of the pocket beach. So, from these figures it can be seen clearly that the non hydrostatic mode includes diffraction and the stationary mode does not.

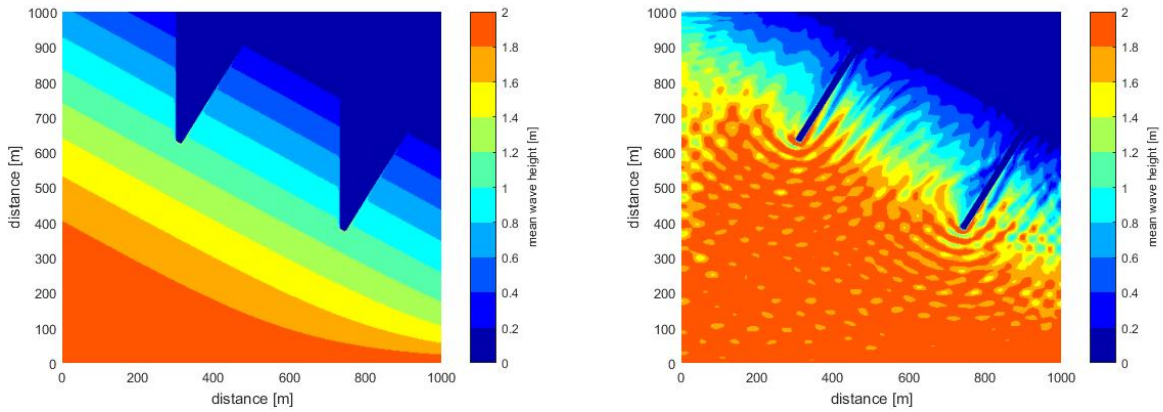

(a) Mean wave height in stationary mode

(b) Mean wave height waves in non hydrostatic mode

Figure 4.6: Mean wave height in pocket beach with oblique incident monochromatic waves

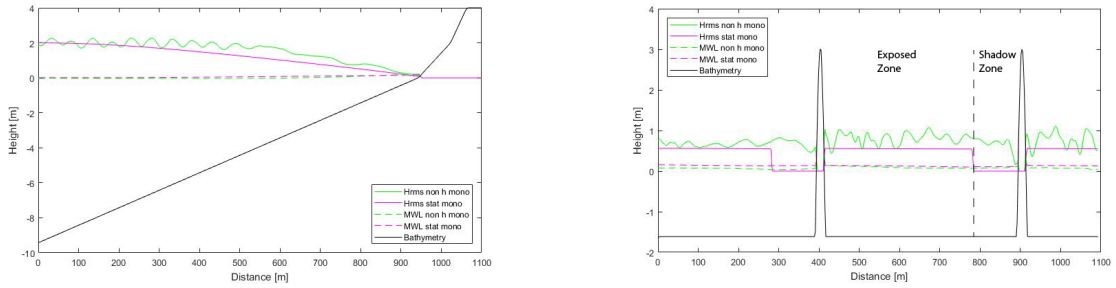

(a) Cross-shore profile AA of the mean wave height

(b) Alongshore profile BB of the mean wave height

Figure 4.7: Cross- and alongshore profiles of the mean wave height in pocket beach with oblique incident monochromatic waves

4.3.4. Circulation Patterns

The velocities resulting from normal incident waves are shown in figure 4.8. What stands out are the high velocities at both groynes. In these areas with high velocities the direction is in both cases towards the coast with a strong inflow along the groynes. The outflow is in both cases more spread out. This is contradictory to the cellular rip current patterns of (Castelle et al., 2016). This is probably caused by the processes very close to the groynes, like breaking of waves, which influence the currents.

The flow from the groynes towards the middle of the beach is located closer to the shoreline in the non hydrostatic simulation (figure 4.8b) than in the stationary simulation (figure 4.8a). Furthermore, the non hydrostatic mode has higher outflow velocities than the stationary mode. The higher wave heights and thus higher energy levels in the non hydrostatic mode are a possible explanation for these differences. The outflow in the non hydrostatic mode is not clearly directed offshore, the arrows are directed disorderly. This is caused by the fact that the short waves are resolved separately. So, some differences can be seen in the comparison of these two figures with velocities. However, the circulation patters of strong inflow close to the groynes and calm outflow over a broad area in the middle are quite similar.

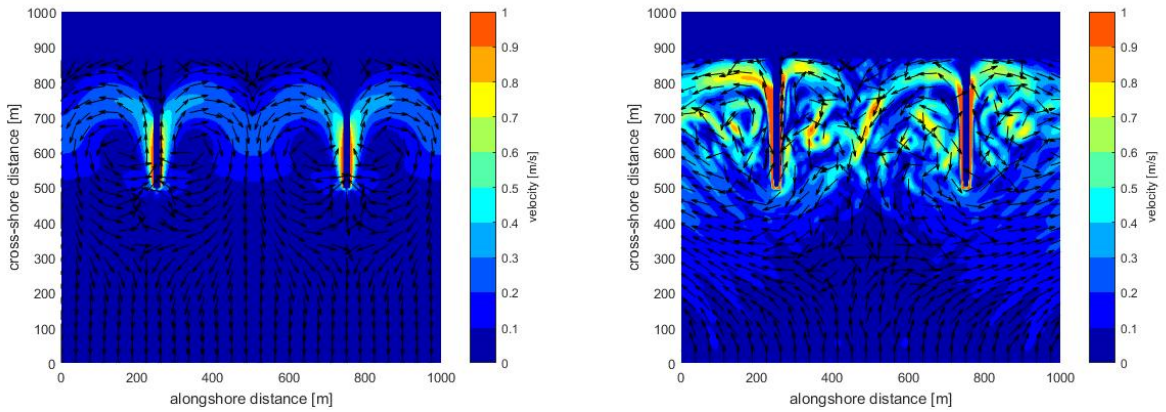

(a) Mean velocities in stationary mode

(b) Mean velocities in non hydrostatic mode

Figure 4.8: Mean velocities in pocket beach under normal incident monochromatic waves

For cases with shadow zones, a circulation is expected of inflow into the shadow zone close to the shore and of outflow along the groyne and back into the circulation more offshore (see section 3.4). The results of oblique incident waves on pocket beaches are shown in figure 4.9. In the wave height analysis shadow zones have been observed without any or with decreased wave height. In the velocity figures, these shadow zones are less clear, however, differences between the two modes could be seen.

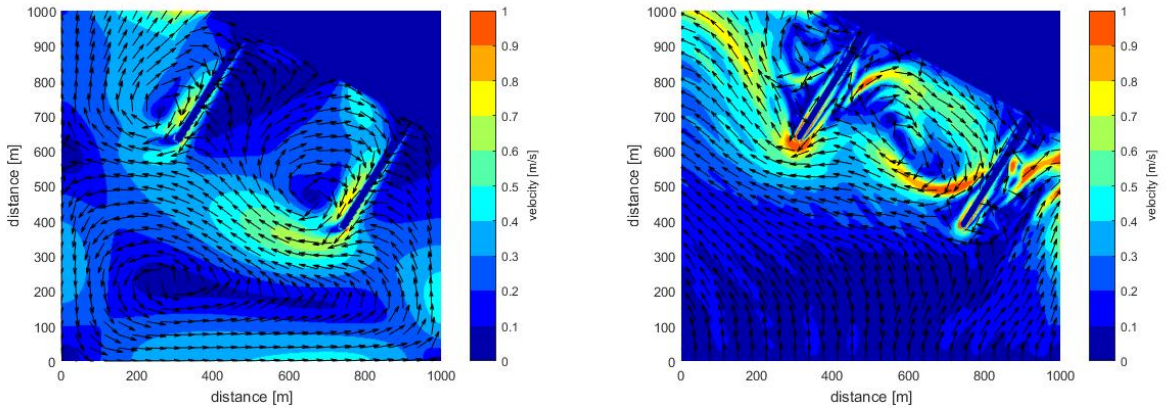

(a) Mean velocities in stationary mode

(b) Mean velocities in non hydrostatic mode

Figure 4.9: Mean velocities in pocket beach under oblique incident monochromatic waves

In both cases the expected directions of circulation can be found. However, the circulation patterns differ from each other. In the stationary case (figure 4.9a) a circulation pattern is present in and just outside the shadow zone. The circulation pattern covers about half the embayment. In contrary, the circulation pattern in the non hydrostatic case (figure 4.9b) covers a larger area of the embayment. This distinction can be made clear by the alongshore velocities. The direction of the alongshore velocity makes clear if the velocities are directed towards the shadow zone or away from the shadow zone. In figure 4.10a the alongshore velocities through the middle of the embayment are shown (profile BB). The change in direction (crossing the zero line) determines the length of the circulation cell for this research. In figure 4.11 the length of the circulation cells relative to the embayment length can be seen. The length of the non hydrostatic could even be longer since it has some metres around the zero line. The stationary mode covers about 55% of the embayment length and the non hydrostatic mode covers about 75% of the embayment length.

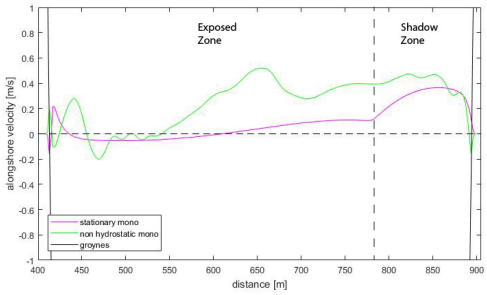

(a) Mean alongshore velocity components in stationary and non hydrostatic mode in profile BB

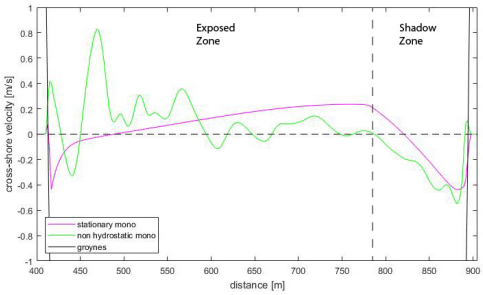

(b) Mean cross-shore velocity components in stationary and non hydrostatic mode in profile BB

Figure 4.10: Mean alongshore and cross-shore velocity components in stationary and non hydrostatic mode with monochromatic waves in alongshore profiles BB

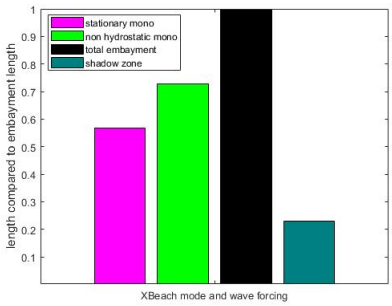

Figure 4.11: Relative cell length based on alongshore velocity components for monochromatic cases

In figure 4.10b the cross-shore velocities are shown. In the results of the non hydrostatic mode, an inflow (positive directed in figure) can be seen at the exposed groyne (left side figure). On the contrary, at this groyne an outflow can be seen in the stationary results. The velocities in the middle of the pocket beach are dominated by alongshore components in the non hydrostatic mode. The velocities are more dominated by cross-shore components in the stationary mode.

4.3.5. Initial Sediment Transport

According to literature, it is expected that the initial sediment transport has similar patterns as the velocity. Furthermore, differences in amount of sediment stirred up by wave motion might play a role in the magnitude. The initial sediment transport of the simulations are shown below in figures 4.12 and 4.13. The magnitudes of sediment transport within the embayment show some variations. In appendix C.1 in figure C.8 the initial sediment transport on plain beaches show some differences as well, especially in magnitude. This can be caused by the different energy levels. However, the sediment transport calculation in both modes is different. Therefore, differences could also be explained by these calculations and not only by the different processes playing a role.

The sediment transport patterns are indeed similar to the velocity circulation patterns. It can be seen that the initial sediment transport close to the groynes is very high. Just after construction the erosion will be large here, however, after some time this will stop due to increased depth. Furthermore, it is notable that the sediment transport within pocket beaches is very limited in simulations with the stationary mode. This appears to originate in the low velocities and low wave heights. Therefore, wave stir up seems to be not of significant influence. In the case with oblique incident waves slightly higher magnitudes can be found on the offshore outflow of the shadow zone. The outflow of the shadow zone is much higher in the non hydrostatic case, which can be explained by higher velocities in the non hydrostatic mode. Furthermore, also in the exposed corner of the pocket beach some higher magnitudes of sediment transport, directed towards the shoreline and middle of pocket beach, can be found.

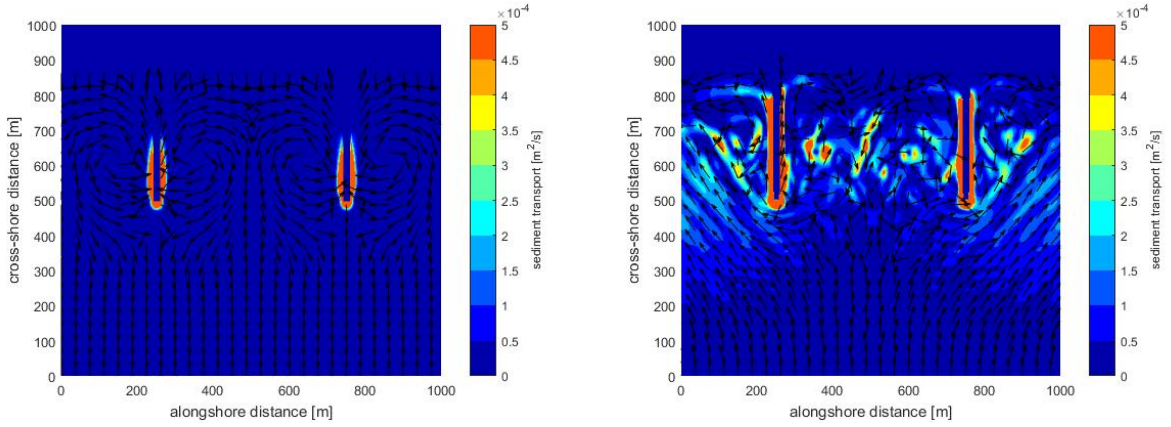

(a) Mean initial sediment transport in stationary mode (b) Mean initial sediment transport in non h mode

Figure 4.12: Mean initial sediment transport in pocket beach under normal incident monochromatic waves

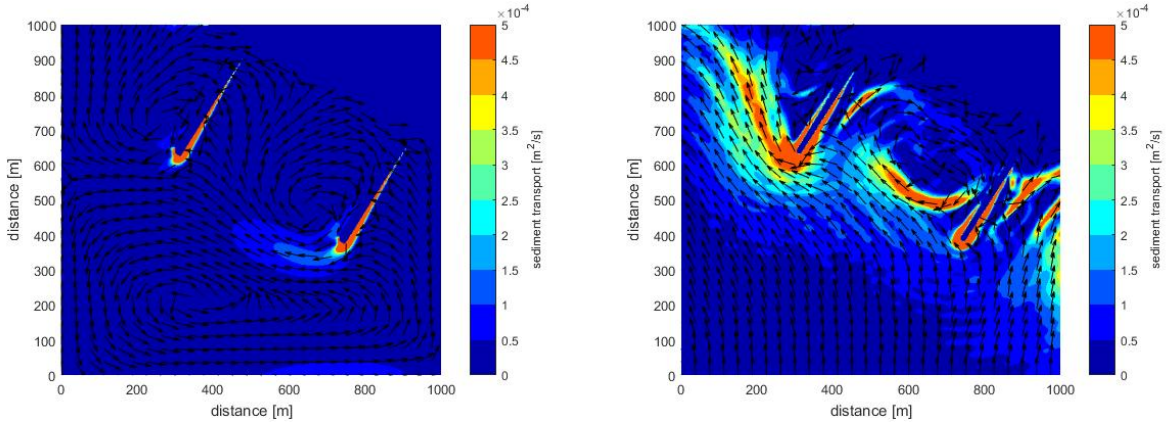

(a) Mean initial sediment transport in stationary mode (b) Mean initial sediment transport in non h mode

Figure 4.13: Mean initial sediment transport in pocket beach under oblique incident monochromatic waves

4.3.6. Results

In the beginning of this section a hypothesis was mentioned. With the above research on the simplified pocket beaches with monochromatic waves something can be said about this.

Short wave diffraction in a relatively small pocket beach influences the circulation pattern and therewith the sediment transport pattern; it makes the circulation cell wider.
In the above analysis it can be seen that the circulation patterns with and without diffraction are very different. Especially, it can be seen that in case diffraction is not incorporated the circulation pattern is more local, it covers about 55% of the embayment length. On the contrary, if the diffraction is incorporated the circulation pattern covers about 75% of the embayment length. The sediment transport patterns look like the circulation patterns. However, the magnitudes show more variation and are hard to compare. Therefore, no reliable conclusions concerning the magnitudes of sediment transport can be drawn based on these simulations. In conclusion this hypothesis can be confirmed.

4.4. Long Waves

In this section the influence of long waves on the wave height, circulation pattern and initial sediment transport is researched individually. The literature study (chapter 3) indicated the importance of higher waves and storm conditions. To be able to simulate real storm conditions, long waves are important and the effects on the dynamics and corresponding patterns should be known to be able to compare two cases both including long waves in a later stage. The influence of long wave diffraction on the circulation pattern is interesting as well. Therefore, the following hypothesis was formulated:

Long waves expose more energy on the coast and long wave diffraction does not influence the circulation cell significantly

4.4.1. Model Set up

In this section the stationary mode with monochromatic waves (section 4.3) is used again to show a case without long waves and wave groups. The other mode used here is the surfbeat mode with a wave spectrum. This mode is able to simulate long waves and wave groups. In both modes the short waves are averaged, so short wave diffraction is not included in both simulations. However, due to the incorporation of long waves long wave diffraction is included in the surfbeat mode. The results of these two modes can be compared to see the effect of wave groups and long waves. The differences in wave height, velocity and sediment transport are analysed to be able to find the influence of long waves and long wave diffraction on the hydrodynamic and sediment transport processes in pocket beaches.

4.4.2. Plain Beach

The plain beach simulations in the stationary and surfbeat mode can be found in appendix C.2. The plain beach comparisons show a difference in wave height from x=150 m towards the coast. The wave height of the stationary mode decreases much earlier than the wave height in the surfbeat mode. This could also be seen in the previous section and can be related to the different way of wave breaking in the models. Furthermore, the surfbeat mode shows a higher wave height around the coastline than the stationary mode. Also the velocity and sediment transport results show higher values around the shoreline, especially behind the shoreline. The oblique incident cases are too much influenced by boundary effects to give reliable results.

4.4.3. Wave Height

In the figures showing the mean wave height with normal incident waves (figures 4.14 and 4.15), it can be seen that the wave height in the surfbeat mode is higher. Half way into the pocket beach in profile BB (figure 4.15b) the mean wave height in the surfbeat mode has decreased less than in the stationary mode. The mean wave height is about 2 times higher. At the coastline, the mean water level and wave height of the surfbeat mode are much higher than in the stationary mode. Both findings are similar to the findings on the plain beaches. The higher wave height and set-up indicate long wave motion since the wave height reaches beyond the coastline.

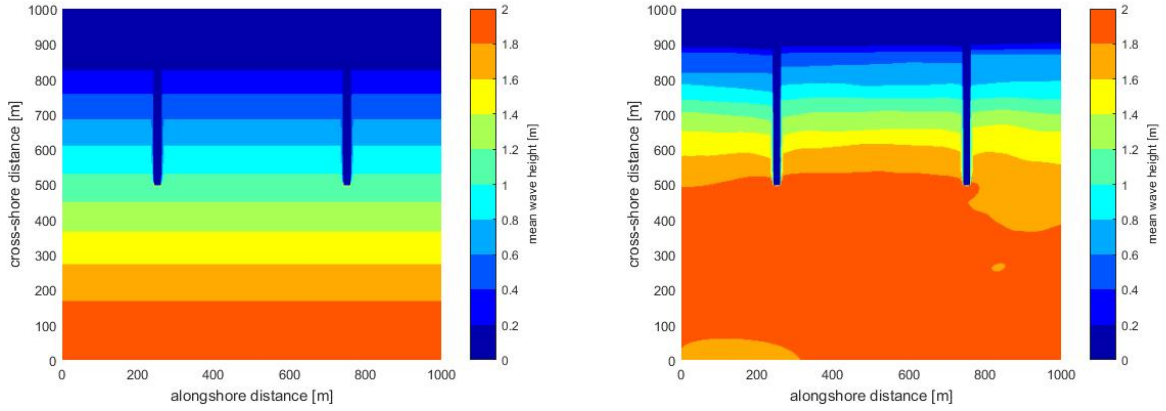

(a) Mean wave height in stationary mode

(b) Mean wave height in surfbeat mode

Figure 4.14: Mean wave height in pocket beach under normal incident waves

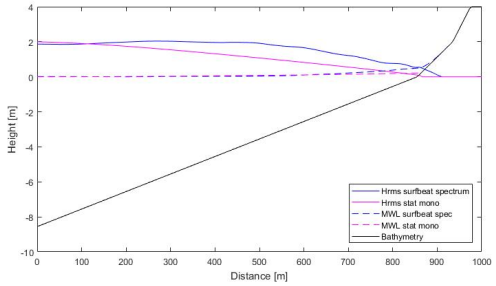

(a) Cross-shore profile AA of the mean wave height

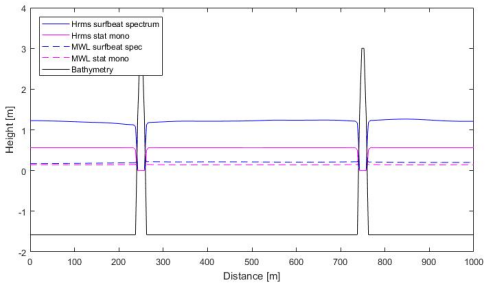

(b) Alongshore profile BB of the mean wave height

Figure 4.15: Cross- and alongshore profiles of the mean wave height in pocket beach with normal incident waves

In figures 4.16 and 4.17 a similar difference in wave height between the two modes can be seen. Within the pocket beach some variations can be seen. Within the shadows zones the wave height of the stationary mode has dropped to zero and the wave height of the surfbeat mode has dropped to about 40% of the incoming wave height (appendix D). The short wave height does not enter the shadow zone but the long waves do. Close to the exposed groyne the wave height is higher than in the rest of the embayment.

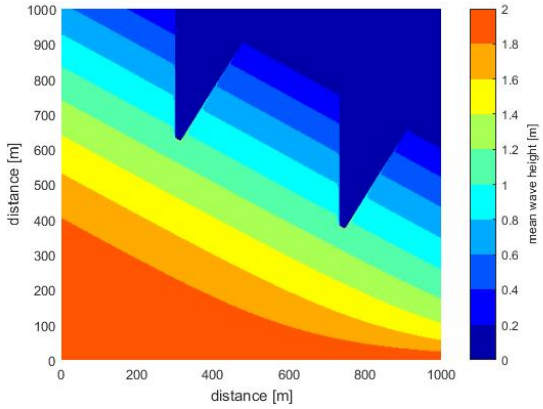

(a) Mean wave height in stationary mode

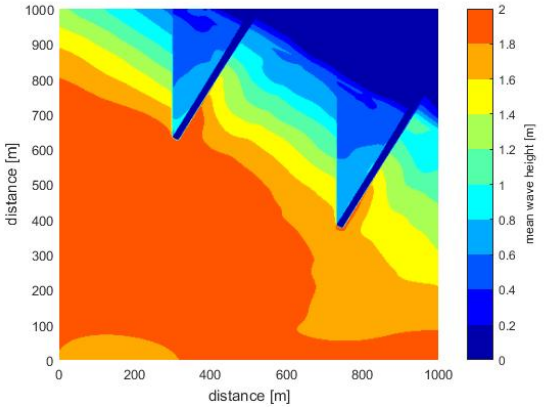

(b) Mean wave height in surfbeat mode

Figure 4.16: Mean wave height under oblique incident waves

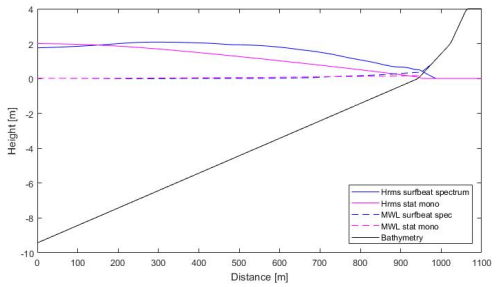

(a) Cross-shore profile AA of the mean wave height

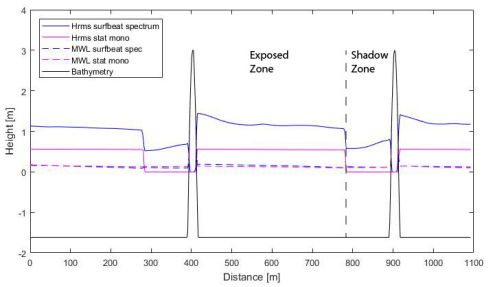

(b) Alongshore profile BB of the mean wave height

Figure 4.17: Cross- and alongshore profiles of the mean wave height in pocket beach with oblique incident waves

4.4.4. Circulation Patterns

In the below figures (4.18 and 4.19), the velocities as a result of the two simulations with normal incident waves can be seen. From x=725 m onwards the velocity of the surfbeat mode is a little bit higher than the stationary mode. What is striking are the higher velocities around the shoreline in the case with long waves (figure 4.18b). In figure 4.19 this difference can be seen clearly. In the middle of the pocket beach (profile AA) at the shoreline the velocity in the surfbeat mode is 10 times higher than in the stationary mode (0.01 m/s versus 0.1 m/s). The velocity increases even more in the surfbeat mode, which is possible due to the water level beyond the mean water level shoreline. It seems reasonable that this is an effect of the long waves, since the changing water level, the long waves, give the short waves a larger area of impact. The long waves make it possible water can reach beyond the shoreline. These findings also appeared on the plain beaches in the surfbeat mode.

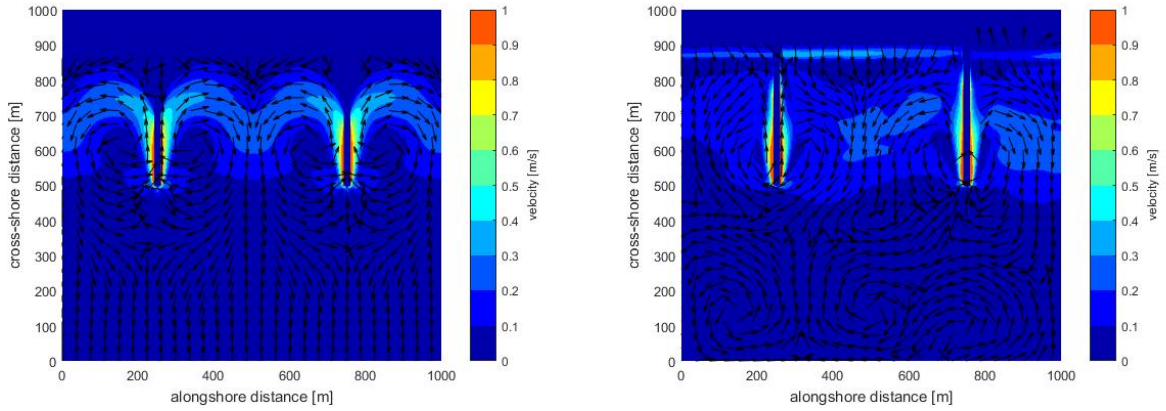

(a) Mean velocities in stationary mode

(b) Mean velocities in surfbeat mode

Figure 4.18: Mean velocities in pocket beach under normal incident waves

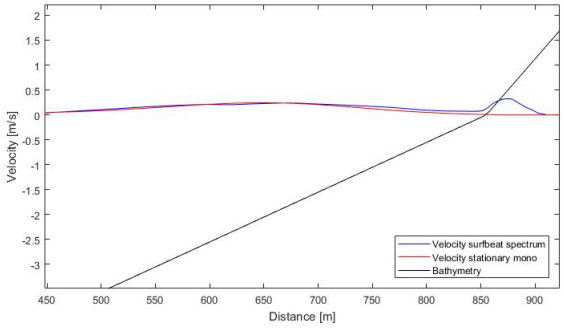

Figure 4.19: Mean velocities in the stationary mode with monochromatic waves and in the surfbeat mode with a wave spectrum

The circulation patterns of the cases with a shadow zone look very similar to each other. In the surfbeat and stationary mode the circulation patterns are local, mainly in and around the shadow zone. The direction of the circulation pattern is as expected, inflow more onshore and outflow more offshore (section 3.4).

The velocities around the coastline are higher in the surfbeat mode, especially in the exposed corner of the beach. In the shadow zone the velocities at the beach are low. However, more offshore in the shadow zone the outflow velocities of the surfbeat mode are high. In the stationary mode the velocities at the exposed shoreline are very low.

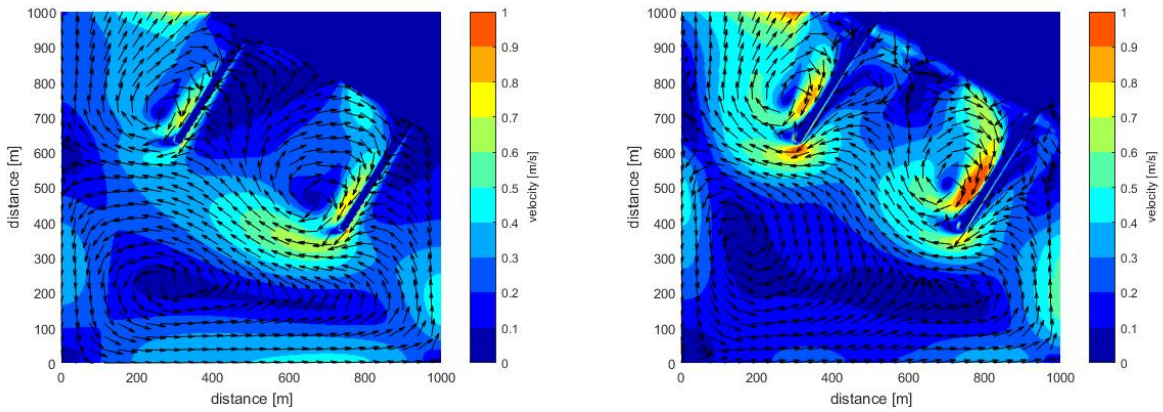

(a) Mean velocities in stationary mode

(b) Mean velocities in surfbeat mode

Figure 4.20: Mean velocities in pocket beach under oblique incident waves

In figure 4.21 the alongshore and cross-shore components of the velocities of both modes, within the pocket beach, are shown separately. It can be seen that the patterns are very similar, however the surfbeat values are higher and the cross-shore velocities in the exposed zone variate. Both circulation cells are located around the shadow zone. In the alongshore and cross-shore velocity results an abrupt change in the lines can be seen around the boundary of the shadow zone (x=780m). The circulation cell length based on the zero crossing of the alongshore velocities can be seen in figure 4.22. The circulation cell of the stationary mode contains about 55% of the embayment length (already shown above in section 4.3). The circulation cell of the surfbeat mode is even smaller and contains about 35% of the embayment length. The surfbeat mode shows more outflow velocities in the exposed zone.

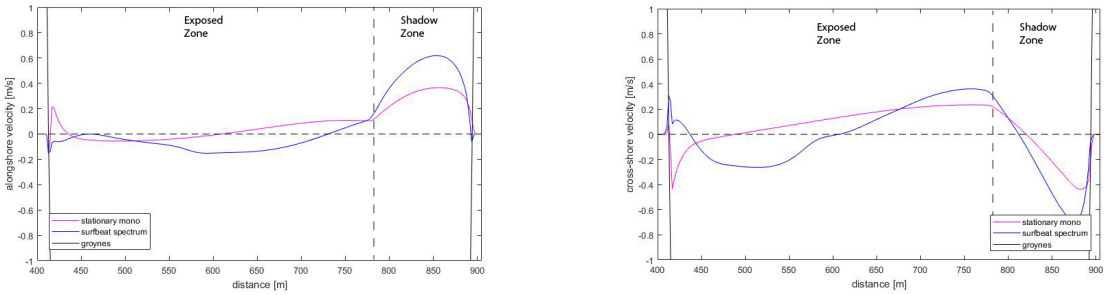

(a) Mean alongshore velocity components in stationary and surfbeat mode in profile BB

(b) Mean cross-shore velocity components in stationary and surfbeat mode in profile BB

Figure 4.21: Mean alongshore and cross-shore velocity components within the pocket beach in stationary and surfbeat mode in profile BB

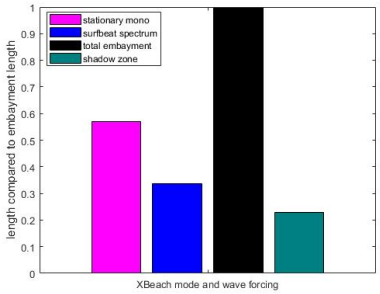

Figure 4.22: Relative cell length based on alongshore velocity components for stationary mode with monochromatic waves and surfbeat mode with wave spectrum

4.4.5. Initial Sediment Transport

In figure 4.23 and 4.24 the mean initial sediment transport is shown. Similar to the initial sediment transport in both simulations with monochromatic waves (section 4.3), the magnitudes of sediment transport in the surfbeat mode (figure 4.23b) are very large along the groynes. The direction of the initial sediment transport is again very similar to the circulation patterns, which are probably heavily influenced by these very high velocities along the groynes. Besides, higher magnitudes of sediment transport can be found at the shoreline in the case a wave spectrum is imposed (figure 4.23b) compared to the case without a wave spectrum (figure 4.23a). The magnitude of the surfbeat mode is $7.5*10^{-5}$ m^2/s at the shoreline (x=852). This sediment transport is higher than on the plain beach. So, the pocket beach seems to strengthen this effect.

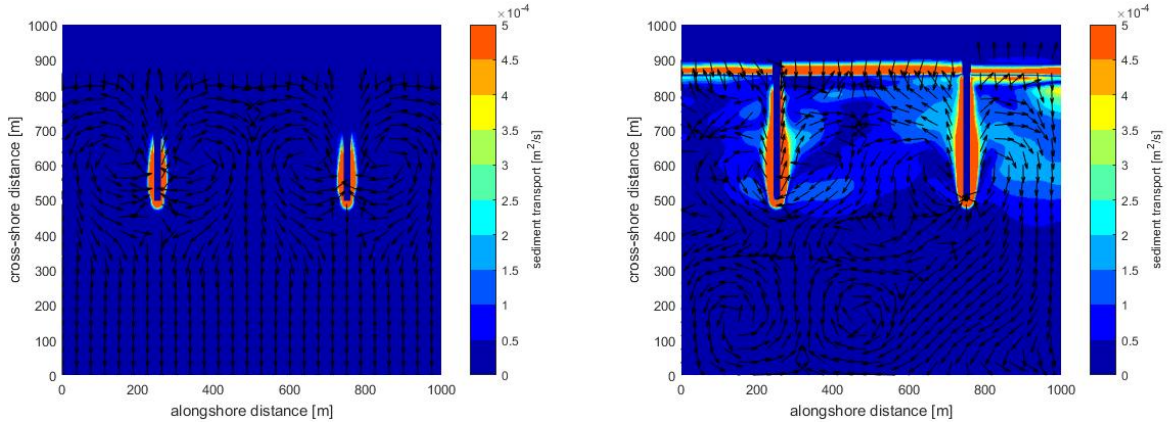

(a) Mean initial sediment transport in stationary mode (b) Mean initial sediment transport in surfbeat mode

Figure 4.23: Mean initial sediment transport in pocket beach under normal incident waves

In both simulations with a shadow zone the patterns of sediment transport look similar to each other. However, the magnitudes are different. The sediment transport patterns are very similar to the circulation patterns of the velocity. The magnitudes of the initial sediment transport are small within the shadow zone, except from the outflow at the offshore boundary. The magnitudes are higher just outside the shadow zone. In the stationary mode these differences are not visible in figure 4.24a. To make the differences in sediment transport in the stationary simulation visible the axis for sediment transport has been changed. In figure 4.25 it can be seen that the magnitudes are higher outside the surfzone, which is similar to the surfbeat mode. However, the magnitudes are dropped to zero within the bigger part of the shadow zone. This is a more extreme difference than in the surfbeat mode, which is probably caused by the long wave motion by long wave diffraction within the shadow zone.

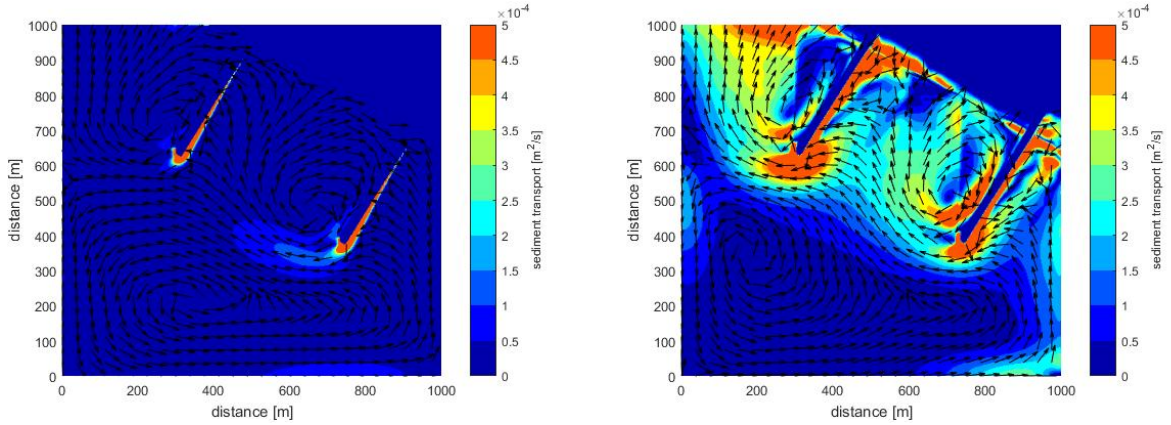

(a) Mean initial sediment transport in stationary mode (b) Mean initial sediment transport in surfbeat mode

Figure 4.24: Mean initial sediment transport in pocket beach under oblique incident waves

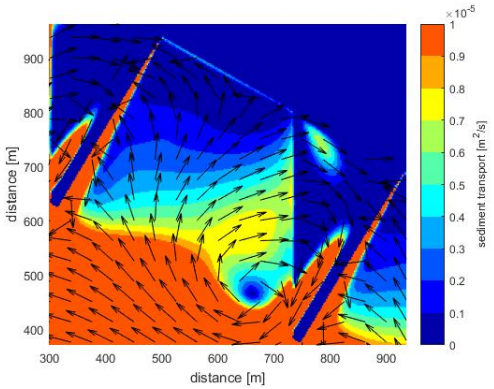

Figure 4.25: Mean initial sediment transport in pocket beach in stationary mode with monochromatic waves, zoomed in on shadow zone and with lower values of the magnitude of sediment transport (Colour axis changed!)

4.4.6. Results

At the beginning of this section the hypothesis was given about the effect of long waves on the dynamics in pocket beaches. With the above analysis on the simplified pocket beaches with a spectrum of waves and the comparison with simulations with monochromatic waves, something can be said about this hypothesis.

Long waves expose more energy on the coast and long wave diffraction does not influence the circulation cell significantly
The addition of groupiness and long waves to the simulations of the simplified pocket beaches give some variations compared to the cases with monochromatic waves. These differences can particularly be found in the velocities and the magnitudes of sediment transport around the shoreline. Much higher values can be found in case long waves are incorporated. Since the water level, velocities and sediment transport reaches beyond the mean shoreline with long waves, it can be concluded that more energy is exposed on the coast.

For the circulation patterns the long wave motion does not play a significant role. In the stationary mode and the surfbeat mode the patterns are very similar, both are concentrated around the shadow zone. The circulation pattern with long waves takes up about 35% of the embayment, without long waves the circulation pattern takes up 55%. The circulation cell length has been changed, however, it does not strengthen the effect of short wave diffraction. Therefore, long wave diffraction will not influence the short wave diffraction results significantly. The sediment transport patterns show similar results, although, a bit more transport in the shadow zone can be recognized. In conclusion, the hypothesis can be confirmed.

4.5. Short Wave Diffraction including Long Waves

In the previous sections (section 4.3 and 4.4) the effect of short wave diffraction and long waves and long wave diffraction are researched separately. In reality a wave spectrum is always imposed on a coast and in case of storm conditions, long waves play an important role (chapter3). Therefore, the combination of long waves and short waves influencing the processes within a pocket beach is interesting. From the first research it became clear that short wave diffraction is probably important for the circulation patterns and sediment transport pattern. In the second research it has been found long waves impose more energy on the coast, especially just behind the mean shoreline. Furthermore, the effect of long wave diffraction on the shape of circulation pattern is small. Therefore, long wave diffraction will not influence the results of the influence of short wave diffraction on the dynamics in pocket beaches too much. Short wave diffraction is the only variable in the comparison made in this section. The following hypothesis is set:

Short wave diffraction widens the circulation pattern compared to only long wave diffraction and including short wave diffraction lowers the impact on the exposed beach.

4.5.1. Model Set up

In this section two modes with the same wave spectrum are compared. The first is the surfbeat mode used in the previous section 4.4 and the other one is the non hydrostatic mode. In both modes a JONSWAP spectrum

is imposed with the same values as before. Both modes resolve waves on the wave group scale, long waves are included. This means both modes include long wave diffraction. The non hydrostatic mode resolves also the short waves separately, so in this mode short wave diffraction in incorporated.

4.5.2. Plain Beach

In appendix C.3 the results of the plain beach simulations can be seen. The wave height is very similar in both modes, however, the surfbeat mode decreases a bit later than the non hydrostatic mode which can be explained by the different ways of wave breaking in both modes. The velocity and sediment transport patterns are similar, however, there are some differences in magnitudes. The shoreline velocities and magnitudes of sediment transport are relatively higher in the surfbeat simulations. The sediment transport values are a bit lower in the non hydrostatic simulations over all. As explained earlier, the sediment transport within the non hydrostatic mode is not validated as properly as the surfbeat mode. Therefore, one should be careful with one on one comparisons.

4.5.3. Wave Height

In figures 4.26 and 4.27 the mean wave heights are shown. Like in the plain beach case the wave height in case of normal incident waves is very similar. The surfbeat mode has a higher mean wave height from a distance of 550 metres towards the coast, which is in the pocket beach area. This is probably caused by the different ways of wave breaking within the modes. Half way into the pocket beach, the surfbeat mode shows a value of about 1.2 metres and the non hydrostatic mode shows a wave height of about 1 metre, which is thus 17% lower (figure 4.26b).

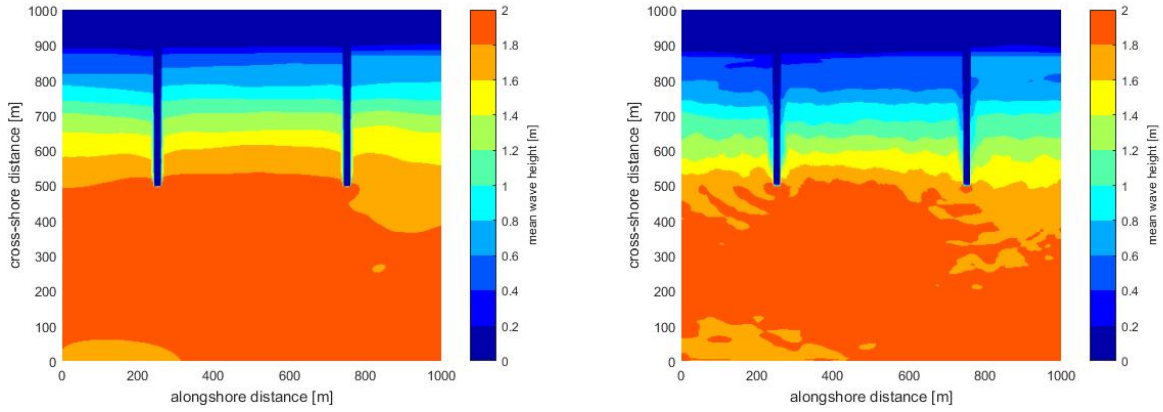

(a) Mean wave height in surfbeat mode

(b) Mean wave height in non hydrostatic mode

Figure 4.26: Mean wave height in pocket beach under normal incident waves from a wave spectrum

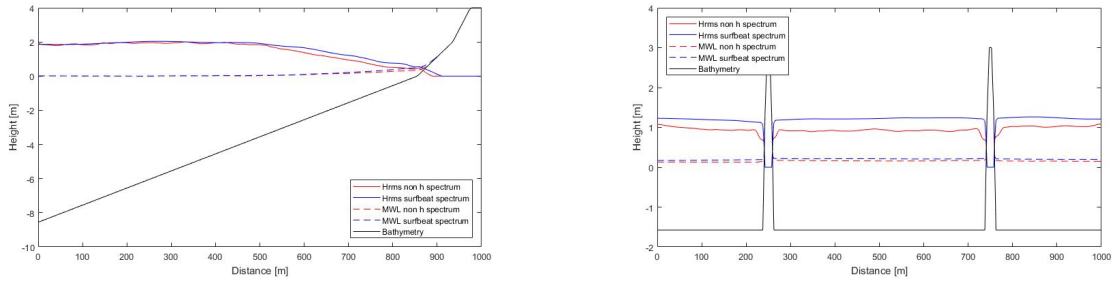

(a) Cross-shore profile AA of the mean wave height

(b) Alongshore profile BB of the mean wave height

Figure 4.27: Cross- and alongshore profiles of the mean wave height in pocket beach with normal incident waves of a spectrum

In case of oblique incident waves the wave height development in cross-shore direction in the middle of the pocket (figure 4.29a) is very similar to the normal incident case. From x=550 m onwards the non hydrostatic

case decreases faster. However, more variations can be found within the embayment and especially within the shadow zone. In figure 4.29b the wave height of the two simulations can be seen in alongshore direction. The shadow zone can be recognized by the drop of wave height in the surfbeat simulation (at about x=780 m). All short waves are blocked in this area, so only the long wave motion is still present. This means an abrupt drop of 60% of the original wave height. In the non hydrostatic mode the wave height in the shadow zone also decreases, however, not that much and much more gradually.

The ratio of the local wave height to the incoming wave height can be seen in appendix D. In figure 3.8a in section 3.3.4 the diffraction diagram for a wave spectrum with a spreading of s=75 could be seen. However, this diagram is not exactly valid for these simulations, since the diagram is not for a shallow, changing water depth and the spreading of the simulations is much smaller with a value of s=800. Therefore, an exact comparison is not possible between the simulation results and the diagrams from literature but the patterns can be compared to recognize the diffraction process. It could be noticed that diffraction is a dominant process in the offshore half of the embayment in the non hydrostatic results (figure D.1b) when comparing the simulation results (appendix D) and the diagram from literature (figure 3.8a). In the onshore half of the embayment other processes, like wave breaking, become dominant over diffraction. The pattern of the ratio of the local wave height to the incoming wave height is more or less parallel to the depth contours again. For the non hydrostatic mode, the wave height drops to about 70% of the incoming wave height in the most offshore part of the shadow zone. In the surfbeat mode the wave height in the shadow zone decreases abrupt to 40% of the incoming wave height. Furthermore, it can be seen that just outside the shadow zone, the wave height decreases a bit as well compared to the area further away from the shadow zone. This lowering of the mean wave height can be found till about half way the embayment. In both modes the wave height at the exposed groyne is high.

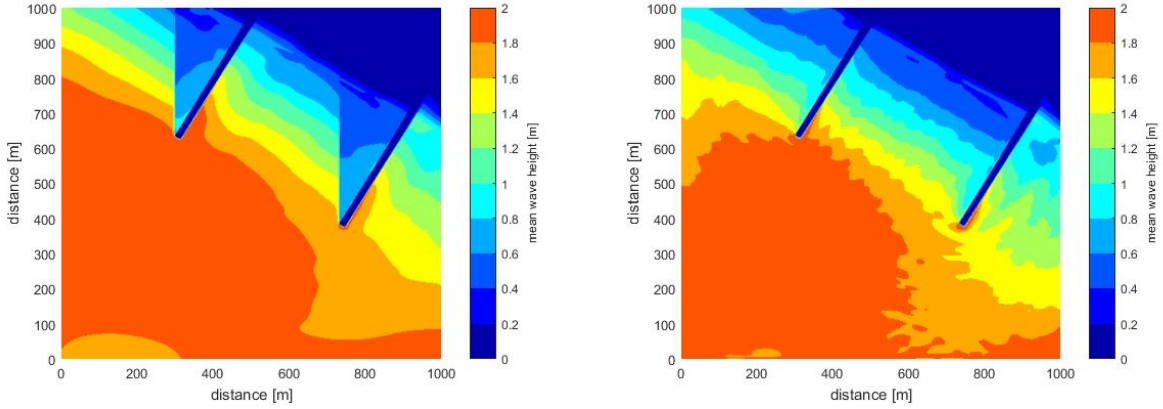

(a) Mean wave height in surfbeat mode

(b) Mean wave height in non hydrostatic mode

Figure 4.28: Mean wave height in pocket beach under oblique incident waves of a spectrum

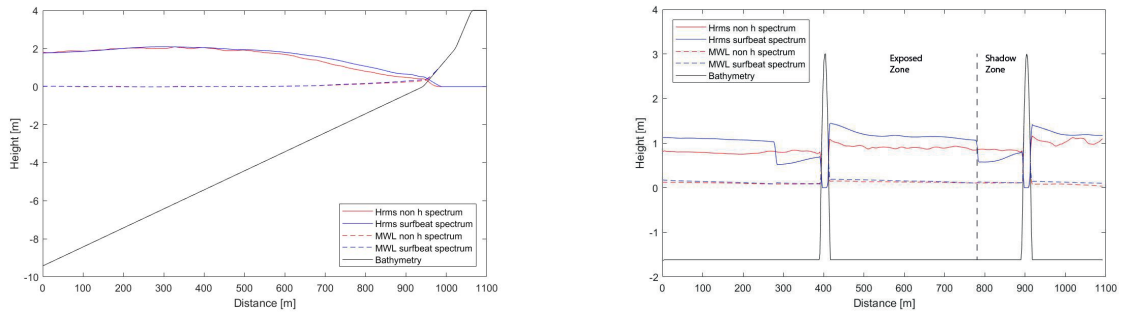

(a) Cross-shore profile AA of the mean wave height

(b) Alongshore profile BB of the mean wave height

Figure 4.29: Cross- and alongshore profiles of the mean wave height in pocket beach with oblique incident waves of a spectrum

4.5.4. Circulation Patterns

The velocities within the pocket beach in case of normal incident waves show similar patterns in both modes (figure 4.30). These circulation patterns are similar to the ones shown before in this chapter; a strong inflow along the groynes and weak outflow over a wide area in the middle. This is not what is expected based on the known cellular circulations (section 3.4). As mentioned before, this is probably caused by the high inflow at the groynes. The velocities in the non hydrostatic mode are a bit higher than the velocities in the surfbeat mode. This is similar to the velocity results on the plain beach. However, the differences are in general very small. The relatively higher values at the shoreline compared to the values in front of the shoreline, have been seen before in the plain beach case. It can be recognized in both modes, although, the velocities in the surfbeat are higher at and just behind the shoreline (figure 4.31).

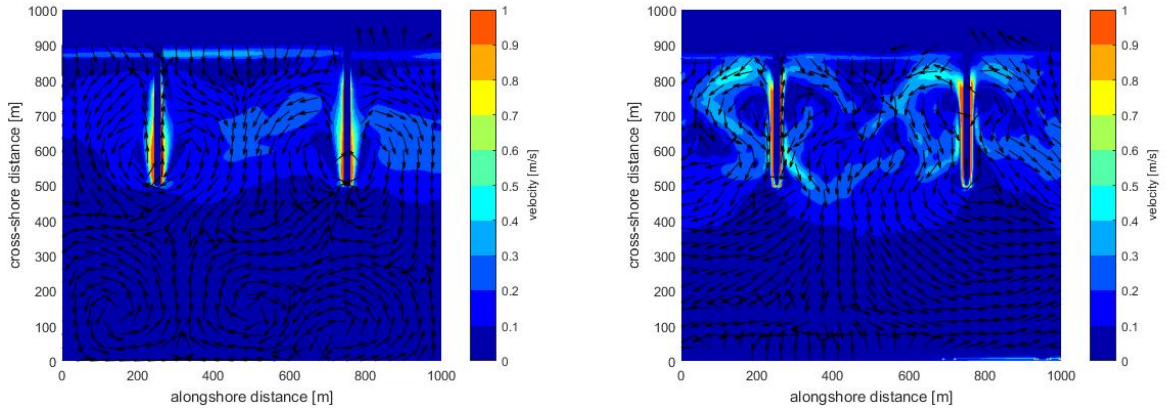

(a) Mean velocities in surfbeat mode

(b) Mean velocities in non hydrostatic mode

Figure 4.30: Mean velocities in pocket beach under normal incident waves of a spectrum

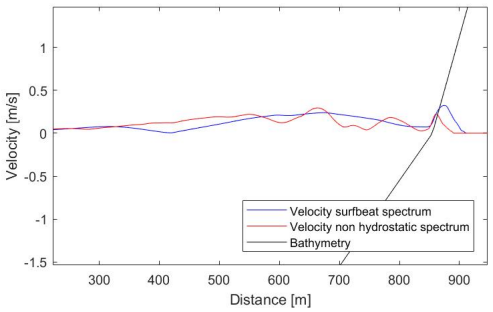

Figure 4.31: Mean velocities in surfbeat mode and non hydrostatic mode both with a wave spectrum

The circulation patterns in the cases with oblique incident waves are shown below in figure 4.32. The expected circulation pattern (section 3.4.1), of a flow from the exposed zone into the shadow zone close to the coast and an outflow from the shadow zone offshore, can be recognized in both simulations. However, clearly the patterns are different from each other. The circulation in the surfbeat mode (figure 4.32a) is a local circulation pattern covering half or less of the embayment in alongshore direction. The results of the non hydrostatic simulation (figure 4.32b) show a much wider circulation cell. In figure 4.33 the mean alongshore and mean cross-shore velocity components of both modes are shown in the alongshore profile BB. Based on the alongshore velocity direction the circulation cell length at the middle of the pocket beach has been determined. In figure 4.34 it can be seen the circulation cell in the surfbeat mode has a width of about 35% of the embayment length and the circulation cell of the non hydrostatic simulation has a width of 90% of the embayment length.

The magnitudes of the velocities throughout the embayment show some differences as well. The velocities in the circulation pattern are more constant in the non hydrostatic mode than in the surfbeat mode. The total magnitude of velocity in the exposed zone is similar in the surfbeat and the non hydrostatic mode in

the middle of the pocket beach (profile AA). However, in figure 4.33 it can be seen that in most part of the embayment (exposed zone) the non hydrostatic velocity is dominated by an alongshore velocity (about 70% of total) and the surfbeat velocity is cross-shore dominated (about 70% of total). The velocities in both modes are highest in the outflow from the shadow zone. The maximal total outflow velocity at the alongshore profile in the surfbeat mode is 0.9 m/s and in the non hydrostatic mode this is 0.6 m/s. The outflow velocity of the non hydrostatic mode is 33% lower than in the surfbeat mode. In the surfbeat mode the velocities in the shadow zone are 450% higher than in the exposed zone in the middle of the pocket beach. In the non hydrostatic case this is 300%. Furthermore, in the exposed corner of the embayment the velocities around the shoreline in the surfbeat mode are higher than in the non hydrostatic mode.

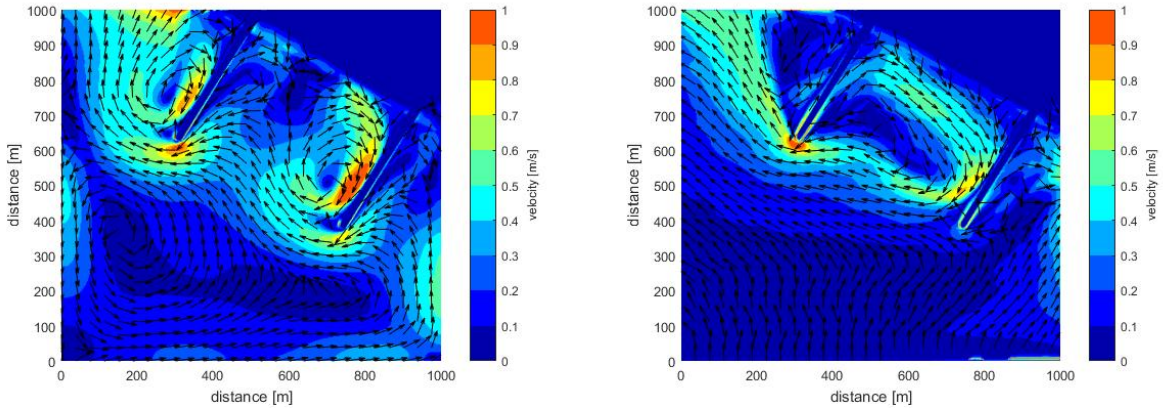

(a) Mean velocities in surfbeat mode

(b) Mean velocities in non hydrostatic mode

Figure 4.32: Mean velocities in pocket beach under oblique incident waves of a wave spectrum

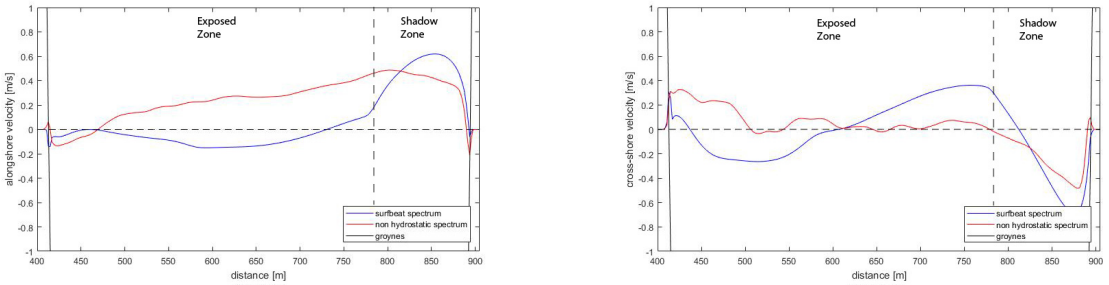

(a) Mean alongshore velocity components in surfbeat and non hyrostatic mode in profile BB

(b) Mean cross-shore velocity components in stationary and surfbeat mode in profile BB

Figure 4.33: Mean alongshore and cross-shore velocity components in surfbeat and non hyrostatic mode with a wave spectrum in profile BB

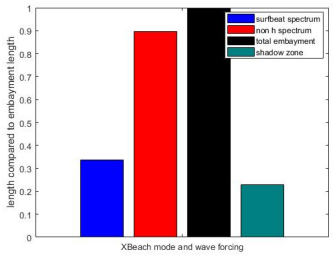

Figure 4.34: Relative cell length based on alongshore velocity components for the surfbeat and non hyrostatic mode with a wave spectrum

4.5.5. Initial Sediment Transport

In this section the initial sediment transport patterns and magnitudes are examined. In the cases with normal incident waves (figure 4.35), the magnitudes along the groynes are very high in both cases. Furthermore, the magnitudes around the shoreline are relatively high in the surfbeat case. In general, the magnitudes are a bit higher in the surfbeat simulation than in the non hydrostatic simulation. However, the red band at the shoreline indicates a larger difference than the overall difference. The difference at the shoreline is about a factor two ($4*10^{-5}$ and $7.5*10^{-5}$). This variation in impact on the shoreline can be explained by the higher wave height at the shoreline (see figure 4.29a). More wave action means that more sediment is stirred up and the combination with the higher velocities means more sediment transport.

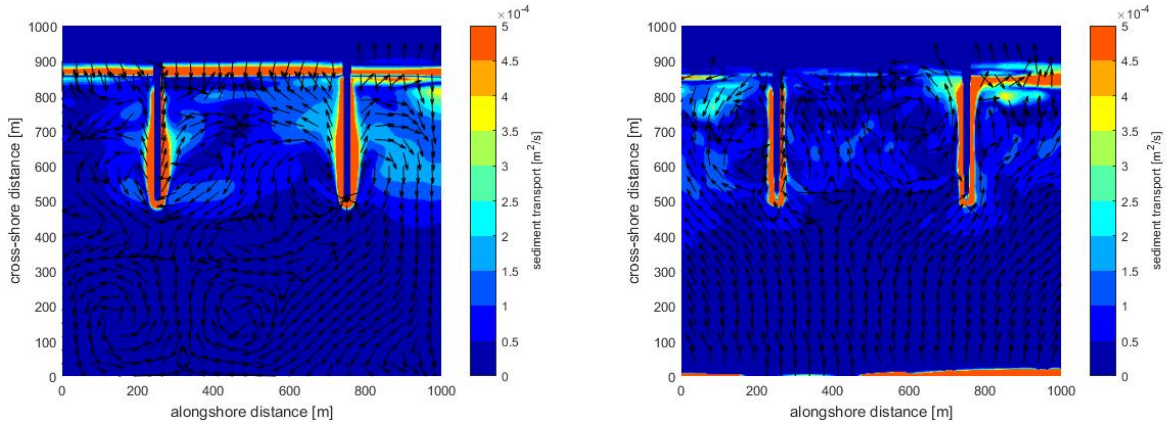

(a) Mean initial sediment transport in surfbeat mode

(b) Mean initial sediment transport in non h mode

Figure 4.35: Mean initial sediment transport in pocket beach under normal incident waves of a wave spectrum

In figure 4.36 the mean sediment transport results with oblique incident waves are shown. The direction of the sediment transport is similar to the before shown circulation patterns. Furthermore, the sediment transport is high at the exposed side of the groynes in both simulations. In the surfbeat simulation the circulation of sediment transport is around the shadow zone. The magnitudes just outside the shadow zone are considerably higher than just inside the shadow zone. Just outside the shadow zone, the wave action results in sediment stirring up. In the shadow zone the wave action has decreased significantly, so considerably less sediment is stirred up which causes a low concentration of sediment. The concentration difference and the set-up difference cause a high inflow into the shadow zone. The non hydrostatic circulation of sediment transport is covering the entire embayment with very equal magnitudes throughout the embayment, in or outside the shadow zone does not make a significant difference in magnitude of sediment transport. This can be explained by the fact that the decrease in wave height and set up is much more gradual over the entire width of the embayment.

In both results a relatively strong outflow of sediment can be noticed at the offshore boundary of the shadow zone. Furthermore, around the shoreline, the sediment transport is higher at the exposed part than at the shadow part. This is also similar to the circulation patterns.

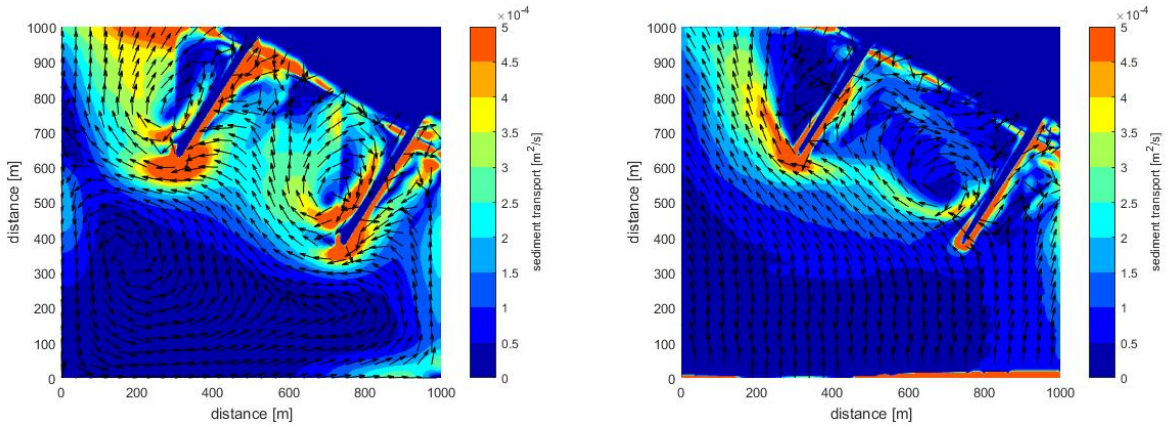

(a) Mean initial sediment transport in surfbeat mode

(b) Mean initial sediment transport in non h mode

Figure 4.36: Mean initial sediment transport in pocket beach under oblique incident waves of a wave spectrum

4.5.6. Results

In this section the two more realistic cases, including long waves, are researched with the surfbeat and non hydrostatic modes of XBeach imposed with a wave spectrum. The contribution of short wave diffraction has been examined based on the following hypothesis:

The short wave diffraction widens the circulation pattern compared to only long wave diffraction and including short wave diffraction lowers the impact on the exposed beach.

In the above comparisons of surfbeat and non hydrostatic simulations, could be seen that the circulation pattern and therewith the sediment transport pattern of both modes are different. The surfbeat mode, in which short wave diffraction is not included, shows a local circulation pattern covering about 35% of the embayment length. The surfbeat mode shows high magnitudes of sediment transport just outside the shadow zone directed into the shadow zone. Furthermore, the impact on the exposed beach is rather high. The non hydrostatic mode, in which short wave diffraction is included, the circulation pattern is spread over the entire embayment. The circulation cell covers about 90% of the embayment length. Like in the surfbeat mode, the exposed shoreline is impacted more than the shadow zone shoreline. Although, a real quantitative comparison is not possible between the two modes, it can be seen that the sediment transport is more gradual dispersed. In conclusion, the hypothesis can be confirmed.

4.6. Morphological Development

In this section the effect of short wave diffraction on the sedimentation and erosion patterns has been examined. These morphological developments are researched for the the two cases from section 4.5 since, these are the most realistic ones. The same model set up has been used as in section 4.5; the surfbeat and non hydrostatic modes are used, imposed with a wave spectrum. The previous sections have shown that the wave height development is very similar in these two cases and the effect of long wave diffraction is negligible compared to the effects of short wave diffraction.

To research the morphological development, first the initial sediment transport has been examined into more detail and has been made ready to compare more quantitatively than before. Second, the bed level changes after 5 days have been looked into. For a good overview, the variations in the two used modes of XBeach are shown in table 4.2.

	Surfbeat mode (left figure)	Non hydrostatic mode (right figure)
Long waves	+	+
Diffraction	-*	+

Table 4.2: Variations in included processes in simplified pocket beach simulations (*only long wave diffraction)

4.6.1. Initial Sediment Transport

In figure 4.37 the initial sediment transport in the two modes of XBeach is shown. These have been shown before in section 4.5, however, the non hydrostatic results have experienced a small modification. As mentioned before in section 4.2, the magnitudes of sediment transport of different modes can not be compared quantitatively because the non hydrostatic mode has not been validated extensively on sediment transport (Deltares, 2017). To be able to compare the sediment transport quantitatively a factor has been used for the sediment transport magnitudes of the non hydrostatic simulations. The factor is based on the sediment transport magnitudes in a pocket beach with normal incident waves in the surfbeat mode and the non hydrostatic mode, both imposed with a wave spectrum. In appendix E this is explained in more detail. The sediment transport factor that has been found is 1.5 to bring the non hydrostatic results to a comparable value. In figure 4.37 this factor is implied on the non hydrostatic results (figure 4.37b).

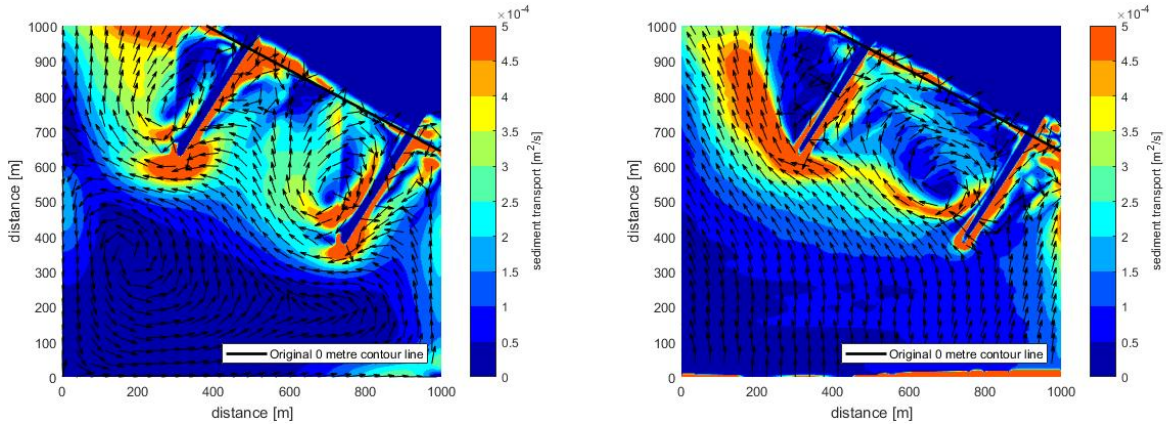

(a) Mean initial sediment transport in surfbeat mode

(b) Mean initial sediment transport in non h mode

Figure 4.37: Mean initial sediment transport in pocket beach with oblique incident waves of a wave spectrum. Simulations in various XBeach modes, a factor (1.5) has been applied for the non hydrostatic mode. With indication of original shoreline (black line)

It can be seen that the results show some similarities and some differences. First of all, at the exposed sides of the groynes, the initial sediment transport is large in both cases. However, it is expected this will stop after some time due to deepening and therewith a decrease in sediment transport. Besides, in both pocket beaches a sediment transport outflow in the shadow zone from beach to offshore can be distinguished. Furthermore, the magnitudes of sediment transport at the shoreline are quite high in the exposed zones. It is expected that this influences the morphology, the shoreline will erode. The erosion is expected to be largest in the exposed zone of the surfbeat mode, since the sediment transport magnitudes are highest.

The magnitudes of sediment transport are high outside and low just inside the shadow zone in the surfbeat mode simulation (figure 4.37a). Erosion is expected in the exposed zone and a lot of sediment is transported just into the shadow zone. This abrupt change of high to low sediment transport is clearly visible at the boundary of the exposed to the shadow zone (x=780 metres) in figure 4.38, where the sediment transport drops with 95%. At this location also an abrupt change could be seen in the velocity profiles in section 4.5. The magnitudes of sediment transport in the non hydrostatic mode are more gradually dispersed from outside to inside the shadow zone. Therefore, a more gradual distribution of erosion and sedimentation areas is expected.

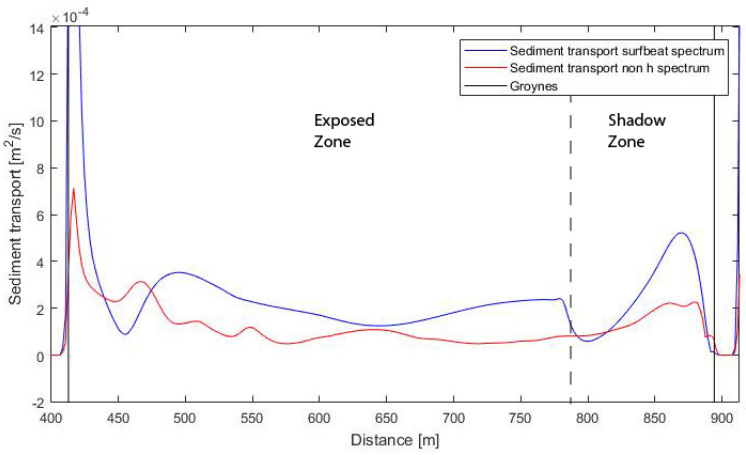

Figure 4.38: Alongshore profile BB of the mean initial sediment transport within the simplified pocket beach

4.6.2. Bed Level Changes

Below the results of morphological simulations after 5 days are shown and analysed. In figure 4.39 the initial bed level is shown. The wave input is the same as used before. Also, the factor of 1.5 for sediment transport in the non hydrostatic case has been used for the simulation of the morphological development. Furthermore, a morphological acceleration factor has been used. This factor speeds up the morphological time scale compared to the hydrodynamic time scale (Roelvink et al., 2015). In these cases the morfacopt is set to 0, which means all the hydrodynamic parameters are left unchanged and the morphological acceleration factor (morfac) is set to 10. This makes the morphological time scale 10 times larger than the hydrodynamic time scale set in to the model.

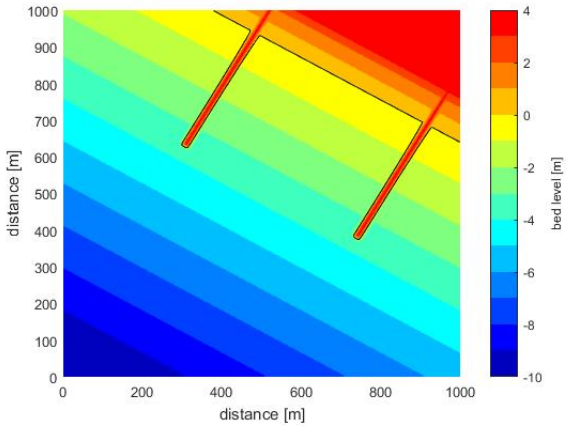

Figure 4.39: Initial bed level of simplified pocket beach with the 0 metre contour line (black line)

The morphological simulations are conducted for 5 days. The results shown in figure 4.40 are the morphological changes after these 5 days. The black line indicates the original 0 metre contour line. This could be helpful in the detection of changes. The blue lines indicate the location of the profiles that are shown in figures 4.42 and 4.43. Furthermore, the differences between the initial bed level and the bed level after 5 days of simulation are shown in figure 4.41.

In both cases a regression of the shoreline can be noted, the yellow zone has extended behind the black line (figure 4.40). In the surfbeat mode this is clearly visible over the entire exposed zone, in the non hydrostatic mode this is only clearly visible in the corner close to the groyne of the exposed zone. This difference is also clearly visible in figure 4.41. In figure 4.41a heavy erosion has taken place over a larger area (twice as large) as in figure 4.41b, which can be seen in the dark blue areas behind the shorelines.

Furthermore, sedimentation in the shadow zone can be seen in both cases but the patterns are different. In the surfbeat mode an abrupt transition into the sedimentation zone can be noticed. In the non hydrostatic mode, deposition zone is more gradual dispersed over the embayment (figure 4.41b). A comparison of the bed levels half way the embayment (profile BB), in these two modes, can be seen in figure 4.42.

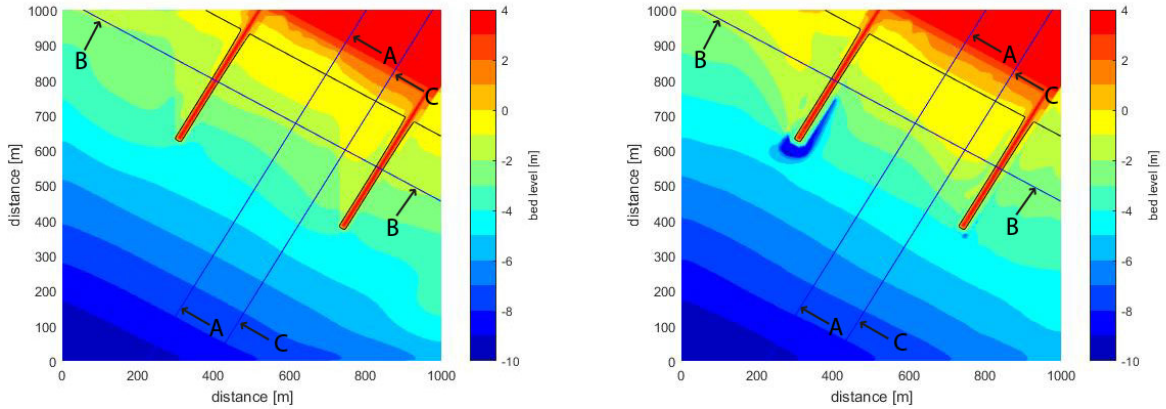

(a) Bed level after 5 days in surfbeat mode

(b) Bed level after 5 days in non hydrostatic mode

Figure 4.40: Bed level in pocket beach after 5 days. Simulations forced with oblique incident waves, in various XBeach modes. With indication of 0 m contour line (black) and the profile lines (blue)

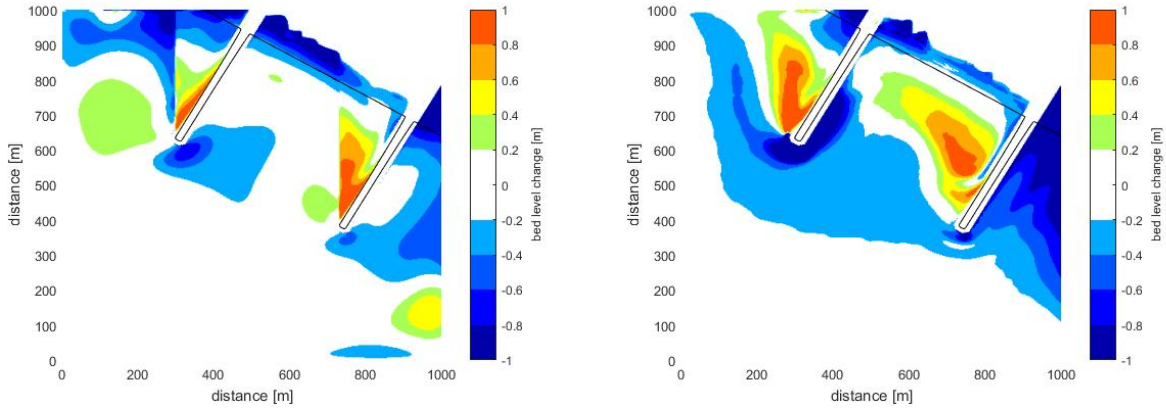

(a) Bed level changes after 5 days in surfbeat mode

(b) Bed level changes after 5 days in non h mode

Figure 4.41: Bed level changes in pocket beach after 5 days. Simulations forced with oblique incident waves, in various XBeach modes. With indication of original shoreline (black line)

In figure 4.42 the gradual sedimentation of the non hydrostatic mode from far into the exposed zone into the shadow zone is very clearly visible. Also, the abrupt change at the shadow zone boundary in the surfbeat mode is obvious. The abrupt increase into the shadow zone is a vertical difference in bed level of about one metre. It arrests some attention that the bed levels of the non hydrostatic mode are very high over this entire profile.

Figure 4.41 gives the idea that the erosion behind the shoreline in the shadow zone of the non hydrostatic mode is more than in the surfbeat mode. Therefore, two cross-shore profiles are made to compare the bed levels. In figure 4.43 two cross-shore profiles are shown (profiles AA and CC). The left figure (4.43a) is a cross-shore profile in the middle of the pocket beach (profile AA), this is in the exposed zone. It can be seen that the surfbeat mode impacted the beach behind the coastline (x=852 m) more than the non hydrostatic mode. Higher in the profile the erosion is 3 times more severe. In figure 4.43b the cross-shore profile through the shadow zone is shown (profile CC). At this location in can be seen that especially the erosion of the surfbeat

simulation is considerably less than in the exposed zone (figure 4.43a). The erosion at the shoreline is similar in the surfbeat and non hydrostatic mode. In front of the shoreline the surfbeat mode erodes a bit more than the non hydrostatic mode. Higher up in the profile, behind the shoreline, the erosion of the non hydrostatic mode is about two times larger than the erosion of the surfbeat mode. Furthermore, an abrupt change in the bed level can be seen at x=650 m. That is again a transition between shadow and exposed zone.

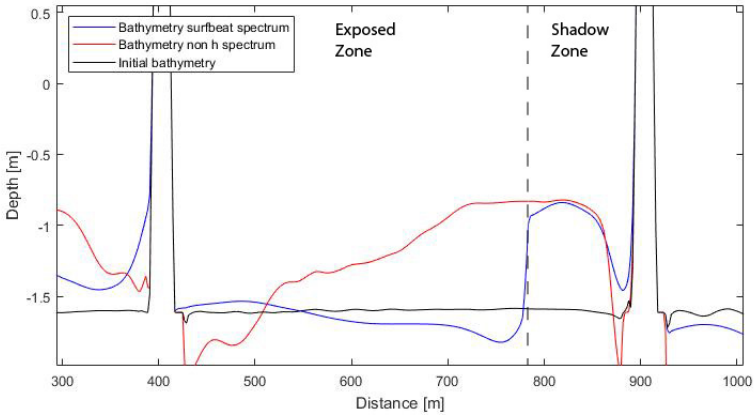

Figure 4.42: Alongshore profile BB of the bed level after 5 days of simulation in the surfbeat and non hydrostatic mode with a wave spectrum

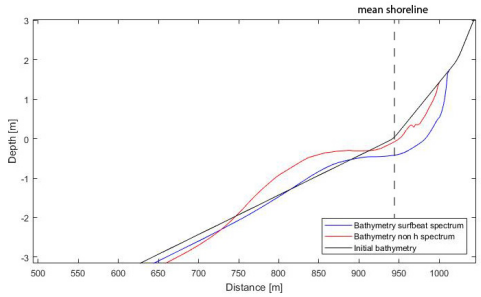

(a) Cross-shore profile AA through exposed zone of pocket beach

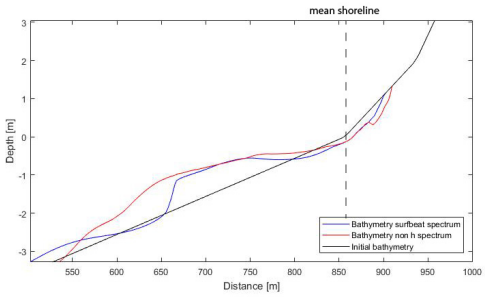

(b) Cross-shore profile CC through shadow zone of pocket beach

Figure 4.43: Cross-shore profiles of bed level after 5 days of simulation in the surfbeat and non hydrostatic mode with a wave spectrum

The volume changes after 5 days of simulation in both modes have been examined. The pocket beach has been divided in four areas. These areas are shown with green lines in figure 4.44a. The shadow zone and the exposed zone are both divided in a shoreline and in an embayment part. The shoreline area is from +2 metres till -0.5 m of the initial bed levels. The embayment part is chosen from -0.5 m to - 2.5 m of the initial bed levels. This offshore boundary is chosen based on surfzone area. The areas on top of the bed level changes and the mean bed changes per area can be seen in appendix F. The volume changes per area and in total for both the surfbeat mode and the non hydrostatic mode can be seen in figure 4.44b. The volume changes in the non hydrostatic mode relative to the volume changes in the surfbeat mode can be seen in table 4.3.

	1. Embayment Exposed	2. Embayment Shadow	3. Shoreline Exposed	4. Shoreline Shadow	Total
Volume change in non hydrostatic mode relative to surfbeat mode	+540%	0%	-40%	-10%	-50%

Table 4.3: Volume changes in the non hydrostatic mode relative to the surfbeat mode for the simplified pocket beach after 5 days (*large due to small volume change in surfbeat mode)

The most outstanding differences can be seen in the exposed zone. In the shadow zones the differences are really small. Although, no real difference in the total amount of erosion in the shadow shoreline area can be found, in figures 4.41 and 4.43 a difference can be noticed. The main body of erosion in the surfbeat mode is located close to the exposed zone and in front of the shoreline. In the non hydrostatic mode the erosion is more gradually dispersed over the shadow shoreline area. The main part of the erosion is located behind the shoreline.

The exposed shoreline erodes 40% less in the non hydrostatic mode than in the surfbeat mode. In the exposed embayment part the difference is largest. In the non hydrostatic mode the volume change is 540% larger than the volume change in the surfbeat mode. It should be noted that this difference is very large due to the low value in the surfbeat mode. The volume change in the surfbeat mode is really small, much smaller than the volume change in other areas. Furthermore, it is striking the volume change is opposite in direction in the exposed embayment area. In this area the non hydrostatic mode shows sedimentation and the surfbeat mode shows a small erosion. This was already clearly visible in 4.41.

In the final column the total volume change can be seen. The amount of moved material in the surfbeat mode is about twice the the amount of moved material in the non hydrostatic mode. Furthermore, the surfbeat mode results in a total loss of sediment in the pocket beach and the non hydrostatic mode results in a total gain of sediment. The total loss of sediment in the surfbeat mode is about 12790 m^3 and the total gain of sediment in the non hydrostatic mode is about 6850 m^3. A gain of sediment is very unlikely under storm conditions and should therefore not be trusted.

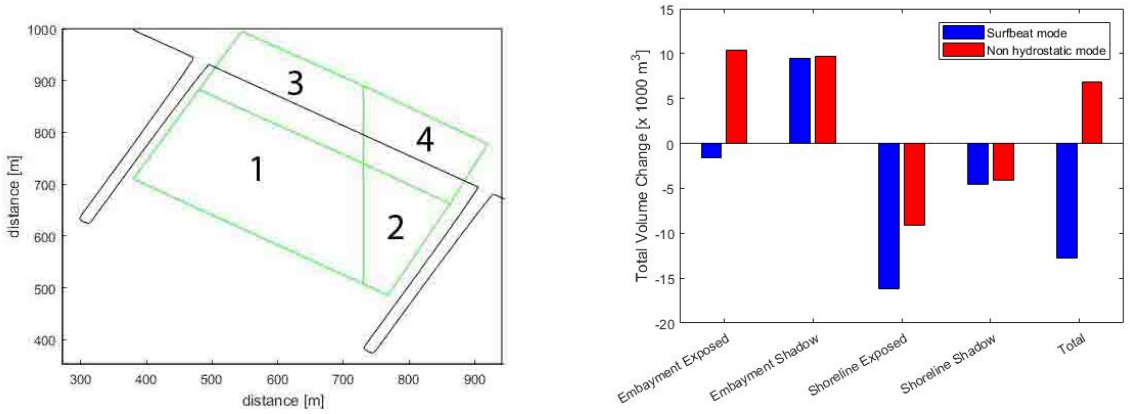

(a) Overview calculation areas simplified pocket beach

(b) Total volume change of surfbeat and non hydrostatic simulation

Figure 4.44: Morphological change calculation of simplified pocket beach

To compare the behaviour of the different areas independently of their size, the mean differences are examined as well. The mean volume changes per area can be found in figure F.2 in appendix F. In table 4.4 the mean accretion and erosion in the shadow zone, relative to the exposed zone for both modes can be seen. Within the surfbeat mode the variations are much larger than in the non hydrostatic mode. The smaller variations indicate the more gradual transition of the beach from exposed to shadow zone within the non hydrostatic mode. At the shoreline the mean erosion in the shadow zone is 40% less with diffraction and 60% less without diffraction. For the embayment zones, the difference between shadow and exposed zone are larger. Although, this is caused by the very low value of mean volume change in the exposed embayment zone of the surfbeat mode.

	2. Embayment Shadow	4. Shoreline Shadow
Non hydrostatic mode	+230%	-40%
Surfbeat mode	+1930%	-60%

Table 4.4: Mean accretion and erosion in the shadow zones relative to mean accretion and erosion in the exposed zone for the simplified pocket beach

4.7. Findings

In this chapter simplified artificial pocket beaches have been researched with a focus on diffraction under storm conditions. A relatively small pocket beach of 500 metres and a shadow zone of 30% of the total embayment has been examined with various modes of XBeach. First, the effect of short wave diffraction and long waves on the hydrodynamics and sediment transport have been looked into separately. From the first tests (section 4.3) it could be found that short wave diffraction influenced the circulation and therewith the sediment transport patterns. The circulation cell widened from 55% to 75% of the embayment. From the second tests (section 4.4) on long waves it could be seen that long waves expose more energy on the coast, the mean wave height, mean velocity and mean sediment transport values are higher at and especially behind the shoreline. This indicated an important effect in erosion patterns. Furthermore, the effect of long wave diffraction on the circulation cell does not enhance the effect of short wave diffraction. The circulation cell even narrows from 55% to 35%. These findings make it interesting to combine those processes into more realistic cases.

The short wave diffraction has been researched while in both cases long waves are incorporated. These comparison has been made for the dynamics in velocity, sediment transport and morphology. The results of these simulations show a widening of the circulation cell due to short wave diffraction. Without short wave diffraction the circulation cell takes up 35% of the embayment. With short wave diffraction the circulation cell covers 90% of the embayment. The difference in circulation cell length is 55% of the embayment. Furthermore, the velocities in the exposed zone are dominated by alongshore transport in the non hydrostatic mode (with short wave diffraction) and dominated by cross-shore transport in the surfbeat mode (without short wave diffraction). The outflow velocities in the shadow zone are 33% lower in the non hydrostatic mode relative to the surfbeat mode.

For the morphological development the sediment transport in the non hydrostatic mode has been multiplied with a factor (1.5) to be able to compare the results of the surfbeat and non hydrostatic mode more properly. The patterns of initial sediment transport are very similar to the circulation patterns. Most outstanding is the sudden drop of sediment transport at the boundary of the shadow zone in the surfbeat mode (without short wave diffraction). Just outside the shadow zone, the sediment transport value is high and just inside the value is low. The magnitude decreases with 95% at this location. The non hydrostatic mode shows a gradual sediment transport increase into the shadow zone. The bed level changes within the pocket beach are especially different in the exposed zones. Some qualitative differences can be seen in the dispersion of erosion in the shadow shoreline area, however, the volume changes are very similar in both modes. In the exposed embayment zone, the volume change in the non hydrostatic mode is 540% of the volume change in the surfbeat mode. Furthermore, the exposed shoreline shows 40% less erosion in the non hydrostatic mode relative to the surfbeat mode. The total volume change in the surfbeat mode comes down to a sediment loss of 18400 m^3 and the total volume change in the non hydrostatic mode is a sediment gain of 9900 m^3. This total difference is mainly caused by the large erosion of the exposed shoreline in the surfbeat mode and the large accretion of the embayment in the non hydrostatic mode. A total gain of sediment for a storm condition is unlikely.

5

Case Study Constanta

5.1. Introduction

In this chapter, the two ways of simulating a pocket beach, used in section 4.5 and 4.6, are applied on a real pocket beach. The two modes, the surfbeat mode and the non hydrostatic mode, imposed with a wave spectrum are able to simulate most realistic circumstances. For this research beaches at the coast of Constanta are chosen as case study location. This research is mainly focussed on the differences between the surfbeat and the non hydrostatic results. Which show the differences with and without diffraction. A comparison with reality is only possible to a very limited level. Some data on the real beach development is available, however, far too less to be able to validate the model results. To start with, the case study location will be clarified. Thereafter, the circumstances on layout of the beaches and wave data are discussed. Further, the beach evolution from the available data is analysed. Finally, the results of the XBeach simulations are shown and analysed.

Along the North West side of the Black Sea, Romania has a coastline of more than 200 kilometres (figure 5.1). The past few decades the coast of Romania is subject to large beach erosion and cliff instability. These major changes along the shore affect the coastal safety and recreational value. Therefore, local interventions are carried out in the coastal system to maintain the safety and values for the inhabitants. One of the locations where these problems occur is at the shore of Constanta, a city located at the Black Sea (see figure 5.1).

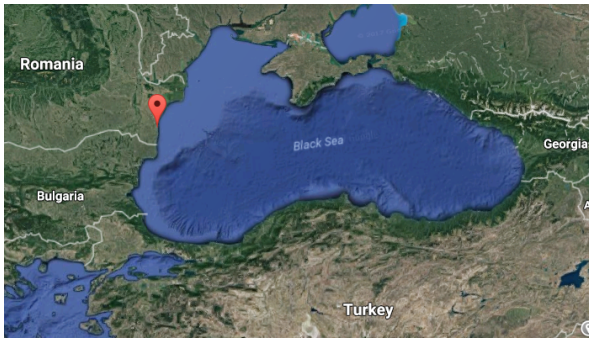

Figure 5.1: Location of Constanta (red pin) (Google Map Data , 2017)

To take action on the problems at the coast of Constanta, van Oord was contracted in 2013 for the design and construction of coastal defences. A stretch of coast of 6 kilometres was the focus of this project. The coastline has been divided into four lots, Tomis North, Tomis Centre, Tomis South and Eforie North (figure 5.2). Using XBeach a low maintenance solution consisting of soft sea defences (beaches) and coastal structures (groynes and breakwaters) was designed. These pocket beaches were constructed in 2014 and 2015. These beaches were designed and constructed to be stable, so the nett sediment transport was aimed to be small. The beaches before and after construction can be seen in figure 5.2. In 2015, just after construction, and in 2016, one year after construction, bathymetric measurements are conducted. These measurements are also called surveys.

The influence of the structures on the dynamics within the pocket beach is important in this research. The processes close to the structures can influence the dynamics and patterns in the whole pocket beach since, these are relatively small beaches. The Tomis Centre and South beaches (figure 5.2c) are researched because, in these cases, the effect without offshore breakwaters can be researched. This is more comparable to the extensive tests of the simplified pocket beaches.

(a) Tomis beaches before construction (Google Earth Pro V7.1.8.3036, 2006)

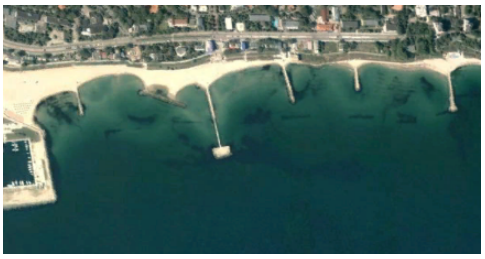

(b) Eforie beaches before construction (Google Earth Pro V7.1.8.3036, 2006)

(c) Tomis beaches after construction (Google Earth Pro V7.1.8.3036, 2017b)

(d) Eforie beaches after construction (Google Earth Pro V7.1.8.3036, 2017b))

Figure 5.2: Tomis and Eforie beaches before and after construction (North is right)

5.2. Circumstances

5.2.1. Layouts

Tomis Centre and Tomis South consist of four beaches in total which are subject of this research. The four beaches can be found in figure 5.3. In this figure, west is above and north is right. The outer beaches are more closed than the two middle beaches. The left beach has an orientation perpendicular to north-east. The two middle beaches are both orientated from north to south, so perpendicular to an east direction. The beach at the right side of the figure, has an orientation a little bit more to the south than the two middle ones, so perpendicular to south-east east. The size of the opening, measured parallel to the beach, are quite similar. Beach two and four (seen from left) have an opening of about 450 metres, beach three has an opening of about 490 metres. The opening of beach one is about 300 metres. In the first and the fourth beach the width of the beach is about twice the size of the opening. The shoreline is even longer because the shoreline shape is not straight but curved. The width of beach two and three is equal to the opening width. However, these ratios of beach width to opening width can change due to variations in wave direction. In front of beach four an offshore submerged breakwater is located which makes the opening width even smaller.

Figure 5.3: Overview of the layouts of Tomis Centre and Tomis South beaches (North is right) (Google Earth Pro V7.1.8.3036, 2016a)

5.2.2. Wave Data

In this section the available wave data of Constanta have been analysed. The wave data have been collected offshore from the first of January 1992 till the end of August 2016. Every three hours a value is given of several parameters such as wave height, direction and wave period. The data are collected at a location of about 70 kilometres offshore of Constanta (44°00'N, 29°30'E).

The probability of occurrence of combinations of wave height and wave direction, based on all available data, is shown in figure 5.4a. The highest waves and the waves with the highest probability of occurrence have a wave angle between 0 and 120 degrees from North. Around 200 degrees from North also a high probability is present, however, these waves can not reach the shore of Constanta. Waves with an angle of more than 180 degrees can not reach the coast of Constanta therefore, only the waves of 0 to 180 degrees are of interest. In figure 5.4b the probability of occurrence of combinations of wave height and wave direction for the period between the two surveys are shown. The areas with high probability match more or less in the figures of the total available data and the data of the period between the two surveys. Focussing on the interesting wave angles for the Constanta beaches, it can be seen that in both cases the highest probability of occurrence is between 0 and 115 degrees from North. A wave angle of 90 degrees would be perpendicular to the coast. So, most of the time the waves come from almost perpendicular or more from the North. Furthermore, it should be realised that the wave data are collected offshore. Waves are influenced by processes, like refraction, as they approach the shore. Furthermore, it can be seen in figure 5.4 that the often occurring wave heights are below 2 metres and the most occurring wave heights are below 1 metre. Less occurring wave heights are below 4 metres in the period between the surveys (figure 5.4b). The total amount of data give a maximum wave height of 7 metres, however, waves above 5 metres have a probability of occurrence of less than $2*10^{-4}$ whereas the the lowest probability of occurrence in the survey period is more than $4*10^{-4}$.

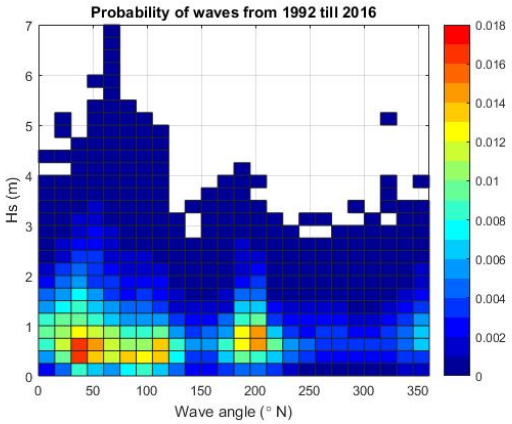

(a) Probabilities of occurrence in survey period (1992 till 2016)

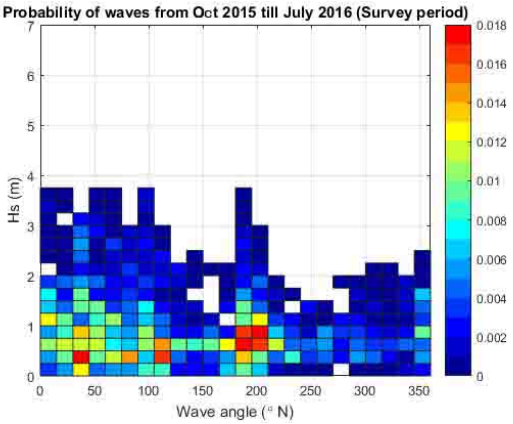

(b) Probability of occurrence in survey period (Oct 2015 till July 2016)

Figure 5.4: Probabilities of occurrence of wave heights and directions at Constanta (offshore measurements)

The wave heights come with a wave period. The wave data give significant wave heights and periods. Below, in figure 5.5, the correlation between H_s and T_p can be seen. On the background, with black dots, the correlation can be seen of all available data. On top of these dots, the trend line is shown in red.

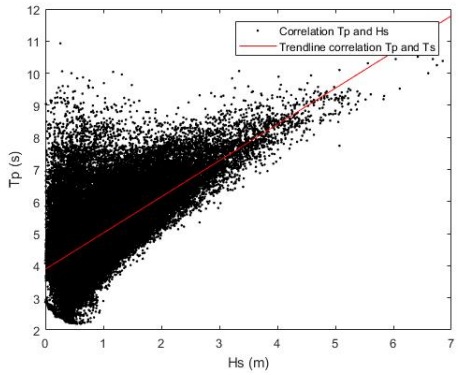

Figure 5.5: Scatter plot of H_s and T_p of all wave data and the trend line of these data

Higher waves have more energy and have therefore more influence on sediment transport. Chapter 3 described that storm conditions and long waves are important in sediment transport processes in pocket beaches. In the design of the beaches of Constanta an equilibrium beach has been designed based on perpendicular orientation to the wave energy flux. The long term sediment losses are calculated with storm conditions. Several storm conditions are modelled with XBeach to be able to see what the impact of these storms is on the long term losses of sediment out of the pocket beach. The near shore wave conditions during these storm conditions can be seen in table 5.1.

Return Period [yr.]	H_{m0} [m]	T_p [s]	Dir [◦ N]
1	3.06	8.112	60
2	3.50	9.198	60
5	3.90	9.974	60
10	4.48	10.729	60
20	4.62	11.245	60
50	4.78	11.830	60
100	5.14	12.566	60

Table 5.1: Statistical maximum wave conditions during storm conditions already transformed to onshore conditions(Steetzel et al., 2014)

A storm event contains a building-up period, a peak of the storm and a decreasing part. In figure 5.6 the development of a storm with a return period of 100 years can be seen. It is assumed that all the storms from the above table (table 5.1) have a similar development.

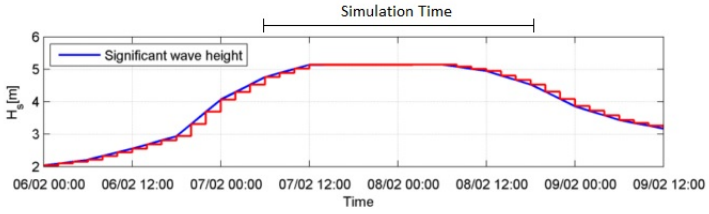

Figure 5.6: Storm development of storm with return period of 100 years (Steetzel et al., 2014) with the indication of the used simulation time for this research

5.3. Analysis Beach Evolution

In this section the evolution of the Tomis Centre and Tomis South beaches are analysed. First, this is done only based on the coastlines visible in Google Earth images. Second, the measurements of the bed level of two subsequent years are compared.

5.3.1. Satellite Images

Below in figure 5.7 the coastline evolution of the Tomis beaches in Constanta can be seen from 2015 till 2107. On the left an overview is shown and on the right the four beaches are shown separately and larger to be able to see the changes better. Due to variations in wave direction the shadow zones are not all the time the same. However, some places are more often a shadow zone than others. In section 5.2.2 it could be seen that most wave energy is coming from 0 to 115 degrees and the storm wave heights come from 60 degrees North. Due to the position of the groynes and the wave directions it is expected that the most northern and most southern part of Tomis, close to the groynes are often shadow zones. In the top left and bottom right pictures of figure 5.7 it can be seen that the shoreline is moving more offshore in these areas. In the most southern pocket beach (bottom right) onshore movement can be seen in the northern part of this beach; the shoreline is rotating. The other beaches show small variations but not so clear a trend in movement of the coastline can be distinguished. The position of the coastlines is very stable in the middle beaches with straight groynes (top right and bottom left figures). The beach cells with large diffraction zones show more variation. The predicted energy on the coast in the northern part of the southern beach is underestimated in the design phase, because this shoreline shows regression. In the northern part of the northern and the southern part of the southern beaches (often the shadow zones), the energy is over-estimated, since these parts of the shoreline are moving offshore. So, probably the real wave directions were different than the design wave directions.

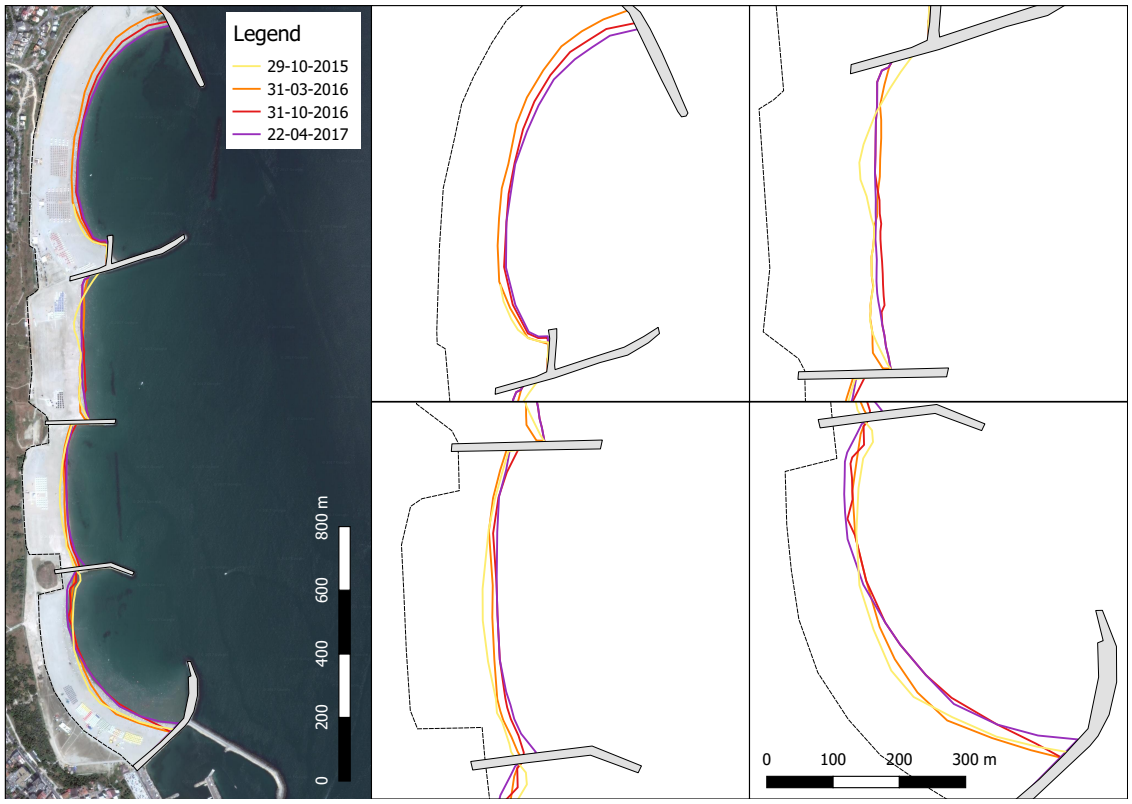

Figure 5.7: Coastline evolution from 2015 till 2017 of Tomis Centre and Tomis South beaches based on google earth images (Google Earth Pro V7.1.8.3036, 2015, 2016a,b, 2017a) (North is above)

5.3.2. Measurements

The measurements of the bed level in October 2015 and July 2016 are analysed. The differences between the two bed levels can be seen in figure 5.8. The green areas indicate accretion from the first to the second measurements, the red areas indicate erosion. It is noticeable that at almost all beaches a band of accretion

is located more onshore (around the shoreline) and a band of erosion can be found more offshore. Several phenomena play a role in the morphological changes of this beach. Erosion during storm conditions and recovery of the profile during calm conditions. Furthermore, just after construction, settlement of the sand and steepening of the shore face could influence the bathymetry measurements. The most southern beach, the left beach in figure 5.8, does not show this bands of erosion and sedimentation over the entire beach width. It does show more sedimentation at the left side and more erosion on the right side. In the other beaches small areas of accretion can be found close to the groynes. This could indicate an effect of shadow zones. In figure 5.9 the October 2015 and July 2016 coastlines are shown to be able to see in more detail the shift of the coastline. Here also the offshore movement of the shoreline is clearly visible in the most northern and most southern corners like noticed in the satellite images.

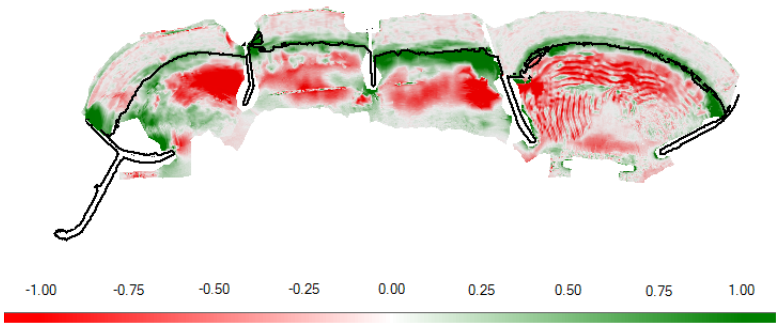

Figure 5.8: Bed level differences between survey at October 2015 and July 2016 and the initial coastline of October 2015 (black line)(North is right)

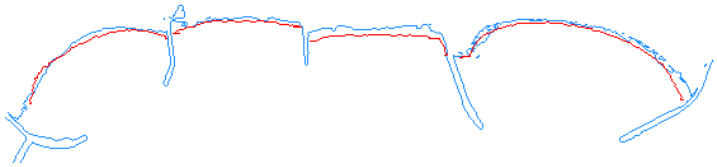

Figure 5.9: Coastlines at October 2015 (blue) and July 2016 (red) based on survey data (North is right)

5.4. XBeach Simulations

From above section (section 5.3) it could be seen that the most northern and southern beaches have areas which are most of the time within the shadow zones due to the curved groynes and mean wave direction. Because shadow zones and diffraction are important within this research, these beaches are most interesting to do further research on. In the simplified pocket beach simulations, sedimentation and erosion can be seen in the shadow zones of the structures and outside the shadow zones. Furthermore, the coastlines from 2015 till 2017 drawn from the satellite images show a significant coastline change in Tomis South. Besides, the measurements of 2015 en 2016 show a movement of the shoreline and the beach slope below the mean water level which is very clear in the most southern pocket beach. These findings together make the most southern beach most interesting to research with XBeach simulations.

The simulations are conducted in the surfbeat and the non hydrostatic mode of XBeach, like in sections 4.5 and 4.6. In reality always a wave spectrum is imposed on a beach, it could be with a small spreading or a large spreading. However, always some spreading is present in real cases. Furthermore, from section 4.4 it turns out that long waves play a significant role in the coastline development within a pocket beach. Therefore, it is important to incorporate this phenomena.

Based on the results of the simplified pocket beaches (section 4.6) the expectation is that the differences and similarities pop up with the various XBeach simulations. In both simulations erosion of the coastline is expected. Furthermore, the short wave diffraction, which is included or not, will cause a difference in the circulation, sediment transport and sedimentation and erosion pattern within the pocket beach.

5.4.1. Model set up

Based on the beach evolution analysis and the findings of the simplified pocket beach simulations, Tomis South is chosen as the most interesting beach of Constanta. Since storm events are high energetic events and therefore important in the sediment transport, a storm condition is selected for these simulations. A storm with a return period of 10 years is chosen for this research. The significant wave height is 4.5 metres and the peak period is 10.7 seconds (see table 5.1). This model input results in two shadow zones, one small shadow zone in the northern part and one larger shadow zone in the southern part. The total shadow zone area is about 40% of the whole embayment area, 75% of this shadow area is the southern shadow zone. All model input can be seen in table 5.2. Below more explanation is given on the parameters.

Angle [° N]	60
H_s [metres]	4.5
T_p [seconds]	10.7
s	100
t [days]	1.5
Cross shore distance [metres]	1500
Alongshore distance [metres]	900

Table 5.2: The characteristics of the simulations of Tomis South beach

The storm condition with a return period of 10 years is extreme for the year 2015/2016, however, the processes will be clearly visible with this condition. Furthermore, a trade off had to be made between grid cell size and wave length. With a small grid cell size also small wave lengths can be modelled without wave dissipation, however, the computation time will be large. According to the sensitivity analysis of the wave dissipation (appendix B.2) a too large grid cell size relative to the wave length causes wave dissipation. In the simplified pocket beaches this wave dissipation was clearly visible with wind waves on a grid of 5 by 5 metres therefore, a grid of 2.5 by 2.5 metres was chosen for the simplified pocket beach research. For this case study a grid cell size of 3 by 3 metres is chosen. A peak wave period of 10.7 seconds means a peak wave length of about 93 metres. With 34 points per wave length, a grid cell size of 3 metres is minimal. A tread off between representative storm wave conditions and computational time determines this model input.

In above section 5.2.2 the development of a storm condition has been shown. For this case study no variations are imposed in the wave conditions. It is assumed that the interesting developments in the bathymetry could be seen with a simplified storm condition as well. The period of simulation is therefore reduced to the peak period (figure 5.6) with constant values for wave height, wave period and wave direction.

The sensitivity analysis of the boundary conditions shows a limited influence of the boundary conditions on the processes within the pocket and a limited influence of a non uniform offshore boundary (section B.1). Since these influences are limited and it is impossible to use cyclic boundaries, the best option is to rotate the grids like has been done before with the simplified pocket beaches as well. This prevents oblique waves from reflecting on the boundaries. The grid is rotated 60 degrees and the waves are imposed perpendicular on the grid. Due to the grid rotation of 60 degrees the pocket beach is rotated a bit from its position in reality. The waves are imposed perpendicular to the y-axis and along the x-axis from right to left, which is a wave direction of 60 degrees from North. The total size of the grids are 300 by 500 grid cells, which means 900 by 1500 metres.

This storm condition is simulated with the surfbeat mode and the non hydrostatic mode of XBeach. These two ways of simulating looked promising in the simplified pocket beach simulations and with these two it can be distinguished what the influence of short wave diffraction is on the dynamics within an artificial pocket beach including wave groups and long waves.

5.4.2. Wave Height

The mean wave height in the beginning (first 6 hours) of the simulations can be seen in figure 5.10. The waves are imposed from the right side. In general it can be seen that the waves of the surfbeat mode decrease a bit later than the waves in the non hydrostatic mode. Furthermore, in the surfbeat mode the shadow zones can be easily recognized by the abrupt decrease in wave height. In the non hydrostatic mode the shadow zones can be recognized as well, however, the decrease in wave height goes much more gradually. Especially in the

offshore half of the shadow zone the diffraction pattern is visible. In figure D.2 in appendix D the ratio of the local wave height to the incoming wave height is shown for both cases. The diffraction patterns are easier to recognize in these figures. At the boundary of the shadow zones the mean wave height decreases to 60% in the non hydrostatic mode. This a real value since it is between 50% and 70% which are values mentioned in literature for wave spectra with a small to a large spreading (section 3.3.4). The mean wave height in the surfbeat mode decreases abruptly to about 40% of the incoming wave height.

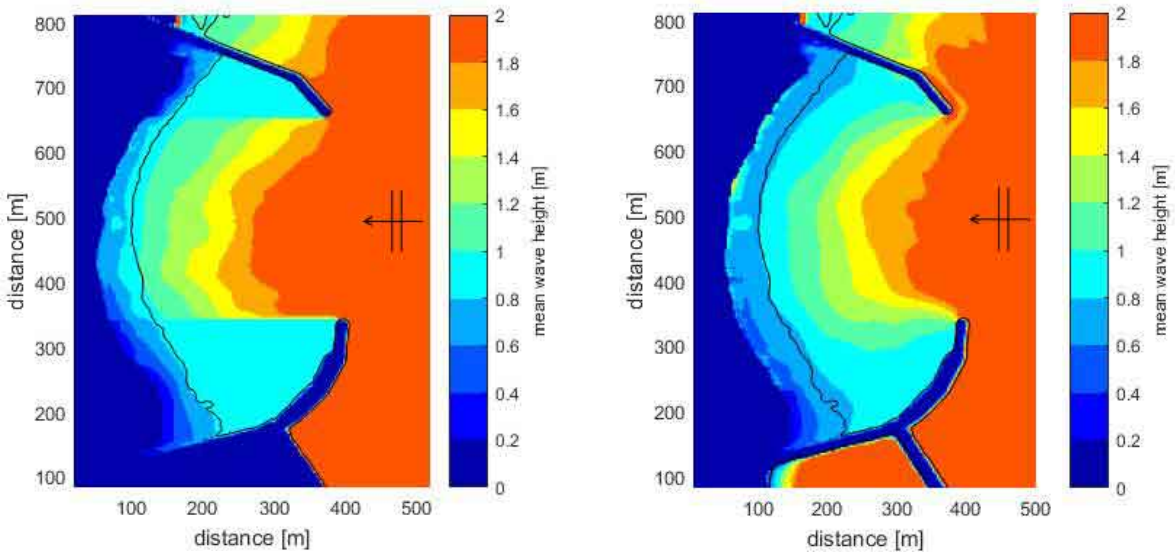

(a) Mean wave height in the surfbeat mode

(b) Mean wave height in the non hydrostatic mode

Figure 5.10: Mean wave height in the surfbeat and the non hydrostatic mode for Tomis South

5.4.3. Circulation Patterns

In this section the circulation patterns and velocities are analysed. In figure 5.11 the mean velocities over the first 6 hours are shown. The distinction between alongshore and cross-shore direction is not as clear as in the simplified pocket beaches since the shoreline is not a straight line. However, the u and v direction are a good indication for alongshore and cross-shore velocities. In the surfbeat mode two circulation patterns can be distinguished; one small circulation pattern around the northern shadow zone and one large circulation pattern into the southern shadow zone. In the results of the non hydrostatic simulation only one clear circulation pattern can be seen; directed towards the southern shadow zone. The total length of the circulation cells relative to the embayment length can be seen in figure 5.12. The surfbeat mode shows a large circulation cell of about 80% of the embayment length. The other 20% is a circulation cell around the smaller shadow zone. The non hydrostatic mode has only one circulation cell which covers about 95% of the embayment. The length of these circulation cells and embayment is based on a line trough x=1200 metres in figure 5.11. In the shadow zones this line corresponds with a depth of 1.5 meters, which was also used in the simplified pocket beach analysis.

The maximum velocities in the shadow zones have been looked at as well. The same line as for the cell length has been used (x=1200 m). For the surfbeat mode the maximum velocities are in both shadow zones about 0.8 m/s. In the non hydrostatic mode the southern shadow zone gives a higher velocity than the northern shadow zone, which can also be seen by the colors in figure 5.11b. The southern shadow zone gives a velocity of 0.6 m/s and the northern shadow zone shows a maximum velocity of 0.45 m/s. In the southern shadow zone the velocity in the non hydrostatic mode is 25% lower relative to the velocity in the surfbeat mode. In the northern shadow zone the non hydrostatic velocity is 45% lower than the surfbeat velocity.

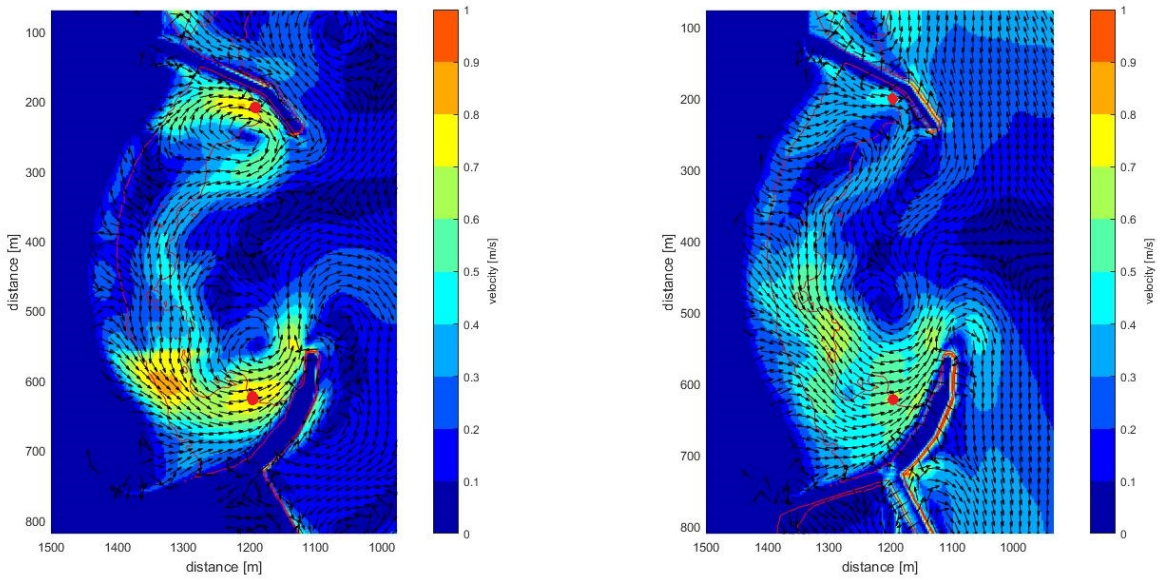

(a) Mean velocities in surfbeat mode

(b) Mean velocities in non hydrostatic mode

Figure 5.11: Mean velocities in surfbeat and non hydrostatic mode (red lines are the 0 m and -1.5 m contour lines and red dots are the locations of maximum velocities)

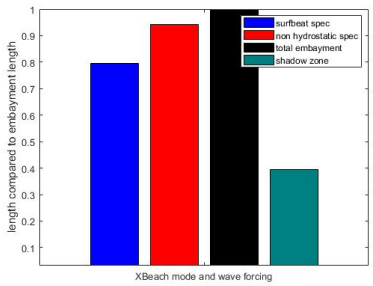

Figure 5.12: Relative cell length based on alongshore velocity direction for the surfbeat and non hyrostatic mode (based on profile at x=1200 m of figure 5.11)

5.4.4. Sediment Transport

In this section the sediment transport is analysed. The mean sediment transport values of the first 6 hours are shown in figure 5.13. In these simulations the bed level is updating therefore, the results are not really initial sediment transport values but close. The same patterns as in the circulation cells can be recognized. Furthermore, the sediment transport behind the shoreline (between the 0 and 1 m contour line) is high in both models. In the surfbeat mode it can be seen these high values are concentrated in the exposed zone. In the non hydrostatic mode this sediment transport behind the shoreline can be found over the entire length of the beach. The sediment transport magnitudes out of the shadow zones is a bit higher in the non hydrostatic mode. However, large part of the flow along the groynes is directed back into the embayment. Besides, it can be recognized in the surfbeat results that some areas, just inside the shadow zones, have very low sediment transport values compared to the surrounding sediment transport values. These areas are coloured dark blue en can be found around y=240 m and y =580 m. The comparison with the non hydrostatic mode can best be made in the southern shadow zone since both modes show a circulation pattern into this zone. Within the black box the difference in decrease in sediment transport can be seen clearly. In the surfbeat mode the sediment transport decreases with 95% in the black box and in the the non hydrostatic mode the sediment transport decreases with 60%. In both modes, within the shadow zone the sediment transport increases again towards the groyne.

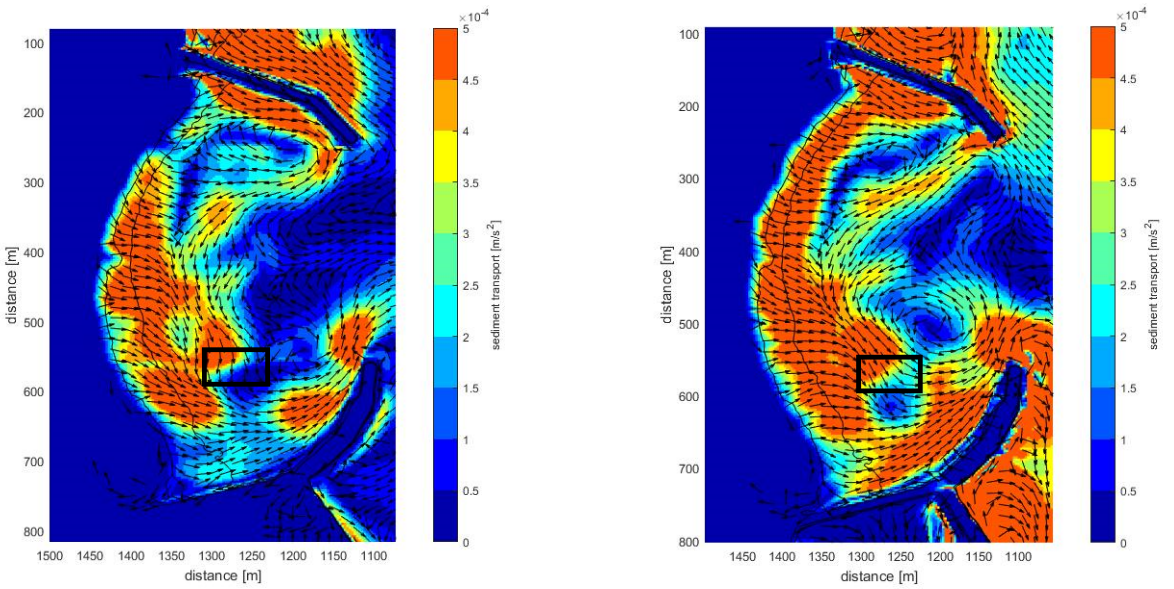

(a) Sediment transport in the surfbeat mode

(b) Sediment transport in the non hydrostatic mode

Figure 5.13: Mean sediment transport in the surfbeat and the non hydrostatic mode (black lines are the 0 m and 1 m contour lines)

5.4.5. Morphological Development

In this section the results of the morphological simulations can be seen. For the sediment transport in the non hydrostatic mode the same factor has been used as before for the simplified pocket beaches. The explanation on the determination of this factor can be found in appendix E. The initial bed level is shown in figure 5.14. In this figure also the 1, 0 and -2 metres contour line are shown. For the analysis of the results it is useful to realize the incoming waves have a direction perpendicular to the y axis. This mean the shadow zones are formed below y=350 m and above y=650 m in the figures.

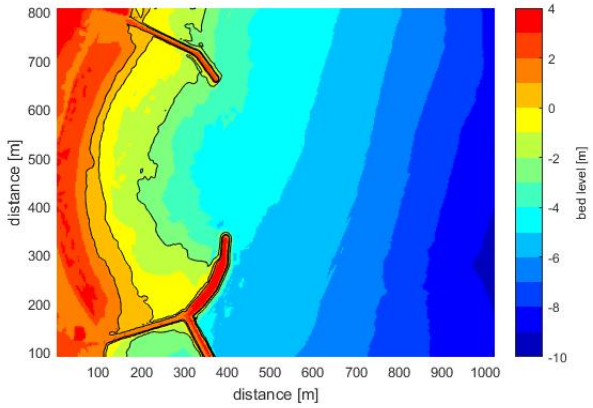

Figure 5.14: Initial bed level of Tomis South beach with 1, 0 and -2 m contour lines (black lines)

In figure 5.15 the bed level and bed level changes are shown after 1.5 days of morphological simulation. The top figures (figures 5.15a and 5.15b) show the results of the surfbeat mode. The bottom figures, (figures 5.15c and 5.15d) show the results of the non hydrostatic mode. In all figures the same initial contour lines are presented as in the above shown initial bed level figure (figure 5.14). The contour lines and the figures of the bed level change (5.15b and 5.15d) make the morphological development more clear.

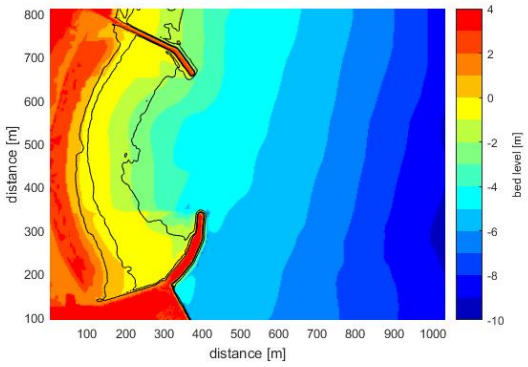

(a) Bed level after 1.5 days storm condition simulated with surfbeat mode

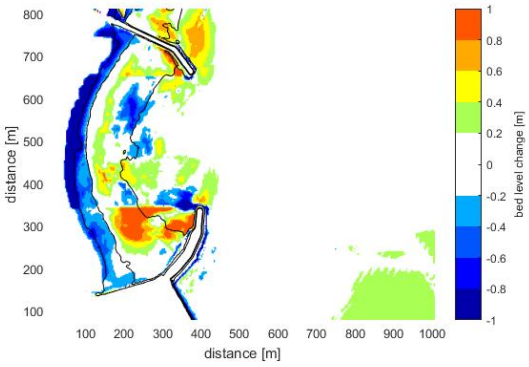

(b) Bed level change after 1.5 days storm condition simulated with surfbeat mode

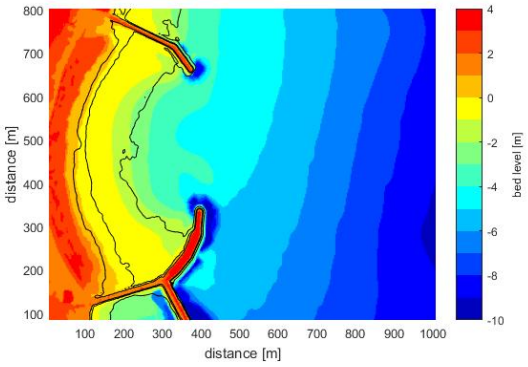

(c) Bed level after 1.5 days storm condition simulated with non hydrostatic mode

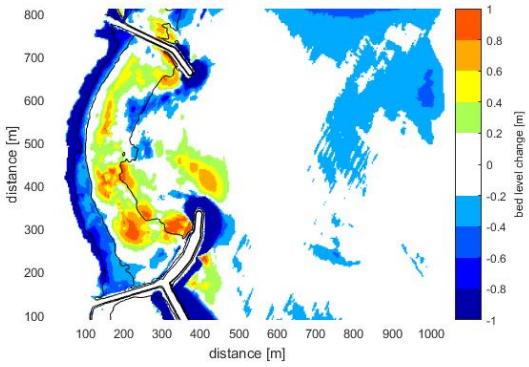

(d) Bed level change after 1.5 days storm condition simulated with non hydrostatic mode

Figure 5.15: Bed level and bed level differences of Tomis South after 1.5 days storm condition simulated with two different modes of XBeach. The black lines indicate the original 1, 0, and -2 m contour lines.

The erosion of the coastline, which can be seen clearly by the blue area left of the black line in figures 5.15b and 5.15d, is according to the expectations for a storm condition. The amount of coastline erosion on several location shows variations. In the surfbeat mode (figure 5.15b) a darker blue color can be seen between y=350 m and y=650 m. In this area in figure 5.15a also the largest regression of the coastline can be seen. From y=650 m up and from y=350 m down in the figure, the regression of the coastline is less than in the area between y=350 m and y=650 m. In figure 5.15a this is visible by an abrupt change in color at x=350 m and x =650 m. In the non hydrostatic case (figure 5.15d) the band of erosion is more dispersed over the entire coastline. This blue band of erosion is almost equal from y=200 m till y=720 m. Within the shadow zones (from y=350 m and y=650 m to the ends) the erosion in the non hydrostatic mode seems to be more than in the surfbeat mode.

The bed level just below mean water level, from 0 to -1 (yellow in figures 5.15a and 5.15c), extends not only in onshore direction (this is the coastline erosion discussed above) but also in offshore direction in both cases. In the exposed area, between y=350 m and y=650 m, the area extends further in the non hydrostatic mode than in the surfbeat mode. In the shadow zones it is the other way around. This can also be seen in figures 5.15b and 5.15d, where in the surfbeat mode in the exposed zone primarily a green band can be noticed and in the non hydrostatic mode more yellow and orange can be noticed in this band of sedimentation. Within the shadow zones, especially in the southern shadow zone, the accretion is large in the results of the surfbeat mode (red colored area in figure 5.15b.

In the top figures in figure 5.15 it can already be noticed that in the surfbeat mode (without short wave diffraction) the transition of sedimentation and erosion patterns is very abrupt at the shadow zone boundary compared to the transitions in the non hydrostatic mode (with short wave diffraction). The non hydrostatic mode shows a much more gradual dispersed sedimentation and erosion pattern. This difference in transitions is

very clearly visible in figure 5.16, where left the contour lines of 1, 0, -1 and -2 metres of both modes are shown and right an alongshore profile at x=210 metres. In figure 5.16a it can be seen that the differences in contour lines locations is larger at the -1 m and -2 m contour lines than at the 0 m and 1 m contour lines. In the exposed zone (between x=250 m and x= 550 m in this figure) the contour lines of the surfbeat simulation are located more onshore than the non hydrostatic mode, which indicated a larger depth. In the shadow zone, especially in the southern shadow zone (x>550 m in this figure) the contour lines of the surfbeat simulation are more offshore located. In the alongshore profile (figure 5.16b) the bed levels at this location after 1.5 days of simulation are shown compared to the initial bed levels. A clear difference of sedimentation in the shadow zones and erosion in the exposed zones can be seen. The surfbeat mode shows this to a greater extent and more abrupt transitions can be seen than the non hydrostatic mode. In the surfbeat mode, an abrupt vertical bed level elevation of about one metre is visible just inside the southern shadow zone.

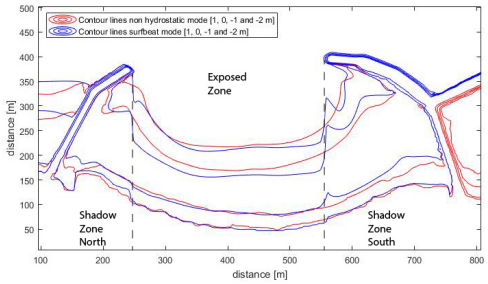

(a) Contour lines after 1.5 days of simulation

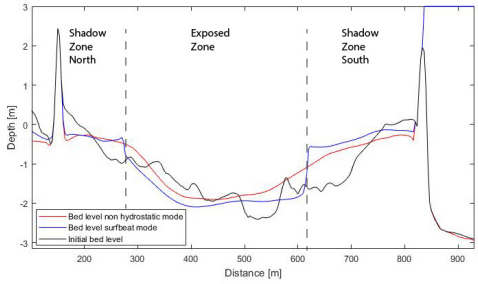

(b) Alongshore profile at x=210 m of Tomis South beach

Figure 5.16: Contour lines and profile after storm simulation on Tomis South with non hydrostatic (red) and surfbeat mode (blue)

The above mentioned differences can also be found in the volume changes of the Tomis South beach after 1.5 days of simulation. The beach has been divided into 6 areas. The exposed zone and the two shadow zones are divided into a shoreline and an embayment part. These areas are shown with green lines in figure 5.17a. The shoreline parts are chosen with the same boundaries as in section 4.6; from +2 m till -0.5 m. The embayment part is chosen from -0.5 m till -3 m. The offshore boundary of the pocket beach is determined based on the breaking depth and the groyne length. In this case the breaking depth is located outside the pocket beach due to the high waves, therefore -3 metres is chosen as the boundary. The areas on top of the bed level changes and the mean bed changes per area can be seen in appendix F. The volume changes per area for the surfbeat and the non hydrostatic mode can be seen in figure 5.17b. The volume changes in the non hydrostatic mode relative to the volume changes in the surfbeat mode can be seen in table 5.3.

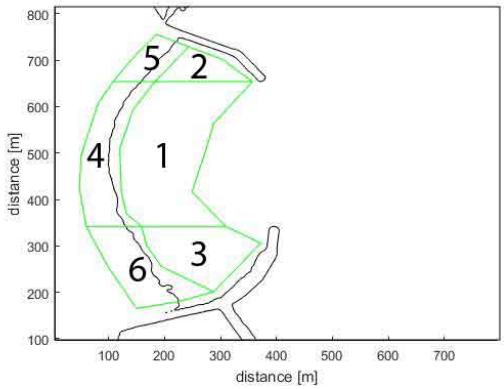

(a) Overview calculation areas Tomis South

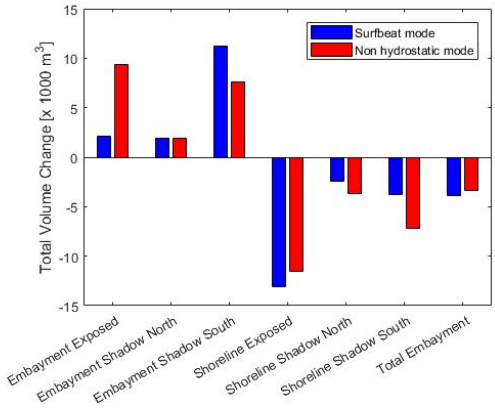

(b) Volume change of surfbeat and non h simulations

Figure 5.17: Morpholocical change calculation of Tomis South beach

	1. Embayment Exposed	2. Embayment Shadow North	3. Embayment Shadow South	4. Shoreline Exposed	5. Shoreline Shadow North	6. Shoreline Shadow South	Total
Volume change in non hydrostatic mode relative to surfbeat mode	+350%*	0%	-30%	-10%	+50%	+90%	-10%

Table 5.3: Volume changes in the non hydrostatic mode relative to the surfbeat mode for the Tomis South beach (*large value due to small volume change in surfbeat mode)

In figure 5.17b it can be seen that all embayment areas, shadow as well as exposed, show accretion and all shoreline areas show erosion. The largest differences in amount of volume between the surfbeat and the non hydrostatic mode can be found in the exposed embayment. The non hydrostatic mode shows 350% more accretion relative to the surfbeat mode. In the exposed shoreline area the erosion of the surfbeat mode is more severe than the non hydrostatic mode, which is 10 % less relative to the surfbeat mode. The shadow shoreline areas both show a larger erosion in the non hydrostatic mode, 50% or even 90% relative to the surfbeat mode. The difference is larger (90%) in the larger shadow zone (southern shadow zone). The accretion in the embayment shadow zones is similar in both modes in the northern shadow zone. In the southern shadow zone, the volume change in the non hydrostatic mode is 30% less than the volume change in the surfbeat mode.

The total volume change in both modes comes down to a loss of sediment. The surfbeat mode shows larger losses than the non hydrostatic mode. The difference is about 10%. The total loss in the surfbeat mode is calculated at 3900 m^3 and the total loss in the non hydrostatic mode is calculated at 3400 m^3 for this storm condition with a return period of 10 years and a duration of 1.5 days.

It is also interesting to look at the mean bed level changes since, the sizes of the areas are very different. The diagram with mean bed level changes can be found in appendix F. The mean bed level changes in the shoreline areas show very similar results in the non hydrostatic mode but very inconstant results in the surfbeat mode. The non hydrostatic results show the largest difference of 20%, whereas the surfbeat results show a difference up to 60%. The mean changes in the shadow zones relative tot the exposed zone can be seen in table 5.4. The larger differences between exposed and shadow zone endorse the abrupt transitions between the zones in the surfbeat mode.

	Shoreline Shadow North	Shoreline Shadow South
Non hydrostatic mode	0%	-20%
Surfbeat mode	-40%	-60%

Table 5.4: Mean shoreline erosion in shadow zones relative to mean shoreline erosion in the exposed zone

For the accretion in the embayment areas a similar comparison can be made. The mean accretion in the shadow zones is in both modes lowest in the exposed zone and highest in the southern shadow zone (figure F.5). However, the ratio between exposed and shadow zone is very large in the surfbeat mode and much less in the non hydrostatic mode. The accretion in the southern shadow zone relative to the exposed zone is more than 10 times as much in the surfbeat mode and only twice as much in the non hydrostatic mode (table 5.5).

	Embayment Shadow North	Embayment Shadow South
Non hydrostatic mode	+30%	+100%
Surfbeat mode	+490%	+1238%

Table 5.5: Mean embayment accretion in shadow zones relative to mean embayment accretion in the exposed zone

5.5. Findings

In this chapter the case study of Constanta has been examined with the focus on the influence of short wave diffraction on the hydrodynamics and morphodynamics under a storm condition. The layouts and development of several beaches and the wave conditons have been looked at. Finally, one beach, Tomis South, has been simulated with the surfbeat and the non hydrostatic mode of XBeach.

The wave action on the Tomis beaches is most of the time directed from the north west (0 tot 110 degrees from North). The main direction for storm conditions is found at 60 degrees North. In the beach development analysis it turned out most beaches were quite stable. However, some variations could be noticed, especially in the zones which are often shadowed from incoming waves. Close to the groynes in shadow zones accretion could be noticed. Furthermore, the most southern beach of Tomis showed also erosion. The general pattern of sedimentation around the shoreline and erosion in front of the shoreline is not valid for the this beach.

Tomis South is chosen to simulate in two modes of XBeach. Like in the previous chapter the surfbeat and non hydrostatic mode are compared on a relatively small pocket beach to research the influence of diffraction, under a storm condition with a return period of 10 years. In the surfbeat mode two circulation cells can be distinguished; a small and a large one. The large one covers 80% of the embayment length, the other 20% is covered by the small circulation cell. In the non hydrostatic mode, only one circulation cell could be seen with a length of 95% of the embayment length. The circulation cell length is 15% of the embayment length larger in case short wave diffraction is included. Furthermore, in both modes the velocities in the exposed zone are dominated by alongshore directed velocities but these are stronger in the non hydrostatic mode. The maximum velocities in the shadow zones are higher in the surfbeat mode compared to the non hydrostatic mode. In the northern, smaller shadow zone the velocity in the non hydrostatic mode is 45% lower relative to the surfbeat mode. For the southern, larger shadow zone the decay is 25% for the non hydrostatic mode relative to the surfbeat mode. The sediment transport pattern shows similar circulation patterns. Furtermore, an abrupt decrease of 95% of the magnitude in sediment transport can be found at the boundary of both shadow zones in the surfbeat mode. In the non hydrostatic mode also a decrease in magnitude can be found at the boundary of the southern shadow zone, however this decrease is less (60%) and much more gradually.

For the morphological development in the pocket beach a factor has been applied on the sediment transport in the non hydrostatic mode. This makes it possible to compare the results of the surfbeat and non hydrostatic mode. It could be seen that in the non hydrostatic mode erosion and deposition areas are more gradually distributed over the pocket beach. In the surfbeat mode the transitions between shadow and exposed zone are more abrupt. In both modes the shoreline areas show erosion and the embayment areas show accretion. The difference in volume change is especially large in the exposed embayment where the accretion in the non hydrostatic mode is 350% more relative to the surfbeat mode. The erosion is most severe at the exposed shoreline, the non hydrostatic mode shows 10% less erosion than the surfbeat mode. In both shorelines in the shadow zones the erosion is stronger in the non hydrostatic mode; 50% and 90% more volume change in the non hydrostatic mode relative to the surfbeat mode. The variation in the embayments is less, 0% and 30% less sedimentation in the non hydrostatic mode relative to the surfbeat mode. The total volume change is in both modes a loss of sediment out of the pocket beach, with a difference of about 10%. The surfbeat mode shows a total loss of 3900 m^3 and the non hydrostatic mode shows a total loss off 3400 m^3. Relative to the exposed zone the mean erosion in the shadow zones has decreased to maximal 60% in the surfbeat mode and to maximal 20% in the non hydrostatic mode. The mean accretion in the shadow zones relative to the exposed zone is increased more than 10 times in the surfbeat mode and twice in the non hydrostatic mode.

When the model results are compared to the measurements one should not look at the green band of accretion along the coastline and the red band of erosion in front of the coastline. These are cross-shore processes of steepening which could not be modelled with XBeach very well. However, the variations within these bands are interesting. In the southern part a lot of sedimentation has been measured interrupting the band of erosion (figure 5.8). This pattern can be found in both simulations (figure 5.15), but the surfbeat mode shows very abrupt changes and extreme sedimentation just inside the shadow zone, which can not be found in the measurements. The coastlines in both models are very similar, except from the southern shadow zone. The coastline in the surfzone mode has eroded less than the shoreline in the non hydrostatic mode. This corresponds better with the shoreline development in the satellite images. However, the satellite images show the reorientation of the coastline due to a different wave angle of incidence over almost one year instead of the result of a single storm. Therefore, this can not be related exactly. Over the entire beach, the shoreline has eroded more in the simulations than in the measurements and satellite images. This is in line with the expectations since the simulations only show the result of a single storm condition and the measurements show the result of a year of different wave conditions including a lot of mild, beach recovering conditions.

6
Discussion

Throughout this research the results are evaluated and discussed to come up with findings. The causes, consequences and limitations of the results are mainly found in hydrodynamic and sediment processes by diffraction, model differences or the measurements used for the case study.

The individual effects of processes on the dynamics in artificial pocket beaches has been rarely researched (Dehouck et al., 2009; Scholar et al., 1998). A better understanding of the processes that influence the erosion and sedimentation patterns in pocket beaches can make more sustainable beaches possible in the design phase. From this research it turns out that diffraction plays an important role in the sedimentation and erosion processes within the pocket beach.

The influence of diffraction has been examined by a literature study, the simulation of a simplified pocket beach and a case study beach. The similarities and differences of the results of the simulations are discussed below. First, the differences are discussed in detail per main interested processes within the pocket beaches for this research. Circulation patterns, sediment transport patterns and morphological development are discussed below one by one. The results found in the simplified pocket beach and the case study show similar patterns however, also differences are found. Furthermore, some general causes of differences are mentioned for the beaches and models used in this research.

6.1. Circulation Patterns

First of all, the effect of diffraction on the circulation patterns has been examined with various modes of the XBeach model. It should be noted that initial circulation patterns are examined, so influence of bed level changes is not incorporated. The patterns are in general the same, inflow into the shadow zone close to the beach and outflow along the groyne. This is similar to the measured circulation patterns in the research of Pattiaratchi et al. (2009). In both beaches the circulation cell widens when short wave diffraction is included in the simulations. Long wave diffraction does not enhance the effect of short wave diffraction on the circulation cell. Next to long wave diffraction also, long waves, groupiness and some spreading has been introduced to the simulations. In the simplified pocket beaches the difference in circulation cell length with or without short wave diffraction is larger than in the case study. Probably this is related to the shape of the bays. The case study beach has a curved shape and therefore, the alongshore direction into the circulation cell is the direction with lowest resistance. In the simplified pocket beach the circulation cell direction is opposite to the natural alongshore direction. The widening of the circulation cell means another influencing factor has been found on the number of rips within an embayment. In previous studies it has been found that higher waves and shorter embayments decrease the number of rips (Ab Razak et al., 2014; Daly et al., 2011; Short and Masselink, 1999). Diffraction widens the circulation cells and therewith increases the distance between rips. The circulation patterns are quantified by the magnitude of alongshore and cross-shore currents, in a long circulation cell the alongshore directed velocities are dominant. In the smaller circulation cells cross-shore directed velocities are dominant.

From previous research it is known that in an embayment dominated by the end effects one or at most two 'natural' rips occur at the boundaries (Short and Masselink, 1999). In this research in all simulations a rip current was present along the groyne in the shadow zone and no rips where found in the middle of the beach. So,

both the simplified and the case study beach show circulation patterns of the cellular type. This is probably caused by the size of the pocket beach, the pocket beach is relatively narrow. In the results of the simplified as well as the case study beach, the velocities in the rip currents are lower in case diffraction is included. On average the velocities are 34% lower with diffraction relative to the cases without diffraction. The northern shadow zone of the case study beach does not have a own circulation cell due to diffraction in the non hydrostatic mode. The circulation cell of the southern shadow zone has become dominant over the northern shadow zone. Therefore, for the processes within the dominant circulation cell, reduction values of 25% and 33% are found. For the northern shadow zone, the velocities in the non hydrostatic mode are 45% less than in the surfbeat mode. The larger difference is probably caused by the existance of a circulation cell in the surfbeat mode, but no circulation cell in the non hydrostatic mode. The other variations (25% and 33%) are very small relative to each other in spite of the differences in bed level, shadow zone size or wave height. This finding on the influence of diffraction on the outflow velocities may influence previous research results. Some research has been done on current patterns and rip current with an XBeach surfbeat model (Ab Razak et al., 2014; Castelle and Coco, 2013). It should be noticed that the values of the outflow within the rip currents is probably overestimated in these cases since diffraction is not included in these model simulations.

6.2. Sediment Transport

Secondly, the effect of diffraction on sediment transport patterns have been investigated. Just like the circulation patterns, the sediment transport values are initial values, without the influence of bed level updates. The sediment transport patterns have similarities with the circulation pattern, but also some differences. In general the direction of the sediment transport and the size of the circulation cell are comparable to the circulation patterns. These similarities can be explained by the fact that horizontal velocities of the water play an important role in the sediment transport. The magnitudes of sediment transport do not always correspond to the velocity values in the circulation patterns. This is caused by another important influencing factor; the sediment concentration. This is very clear at the boundary of the shadow zone in case diffraction is not included in the simulations. The sediment transport magnitudes decreases with 95% from just outside to just inside the shadow zone in both the simplified and the case study beach. Without diffraction in the simulation no wave action is present within the shadow zone. This means almost no sediment stir up and therefore, the sediment concentration is very low within the shadow zone. In case diffraction is included, the simulations show a more gradual course of the magnitude of sediment transport. However, the simplified and the case study beach do not show exactly the same. In the simplified beach the sediment transport is gradually increasing towards the maximum outflow along the groyne but in the case study the the sediment transport decreases first just inside the shadow zone and than increases again towards the outflow along the groyne. The different bed levels at several places and for the simplified and the case study beach could cause this. The similarity in cases with diffraction is the gradual more gradual transition. The amount of sediment transported is apparently not only linked to the velocities. The high velocities in the rip current indicate the amount of material that can be transported offshore (Short and Masselink, 1999). However, the amount of material available has an influence on the amount of material which will flow out along the groyne. In the simplified pocket beach the outflow of sedment is significantly larger in the surfbeat mode than in the non hydrostatic mode. In the case study pocket beach the sediment transport value is not larger along the groyne, however, probably the amount of out flowing material is due to the more outward directed rip current. The rip current and flow of transport along the groyne have not been researched into detail.

6.3. Morphological Development

Finally, the influence of diffraction on the morphological developments in both beaches has been researched. Again similar patterns of more or less erosion and sedimentation can be seen in the results of the simulations. However, the simplified and case study beach show some differences as well. The total morphological behaviour has been examined and the total area is also divided and assessed based on two criteria, is it a shadow or an exposed zone and is it in the embayment or around the shoreline.

The total surface areas of the beaches are similar; 146000 m^2 for the simplified and 123000 m^2 for the case study beach, however, the shadow zone surface areas are different. The ratio exposed to shadow zone in the simplified beach is 70%/30% and in the case study beach it is 60%/40%. The 40% shadow zone in the case study beach is divided in a small shadow zone (10%) at the north side and a large shadow zone (30%) at the south side. This different ratios of the shadow zones probably already cause disparities in the amount of sed-

imentation and erosion. This can already be seen in the case study, the disparities between the two shadow zones are visible. In the larger shadow zone the sedimentation and erosion values with and without diffraction vary more than in the smaller shadow zone. Although, this is probably caused by the more dominant behaviour on the dynamics of the southern shadow zone. The circulation cell of the southern shadow zone is dominant over the northerns shadow zone in the non hydrostatic mode.

6.3.1. Erosion and Sedimentation Pattern

The case study beach shows a total loss of sediment with and without diffraction. Since a severe storm conditions has been modelled this is in line with the expectations. Storm conditions with high and long waves cause erosion of the shoreline areas. Material from around the shoreline is transported more offshore into the surf zone (Bosboom and Stive, 2015a). This sediment can be brought back to the shoreline during mild conditions unless it is permanently lost offshore or in alongshore direction. The total loss of sediment with diffraction is 10% less than without diffraction. In the simplified pocket beach the volume changes are much more severe. This can be explained by the fact the initial beach is not in equilibrium. The case study beach has been designed as an equilibrium beach whereas the simplified is not. The total mean volume change in the case study beach without diffraction is 60% less than the simplified beach without diffraction. With diffraction the case study beach shows a mean volume change of 40% less. Furthermore, the simplified beach with diffraction has not lost sediment but has gained sediment in the beach during the storm condition. The storm condition of the simplified beach is less severe than the case study storm, however, an increase in sediment and especially with these amounts is unlikely and not according to literature (Bosboom and Stive, 2015a). Probably, this is caused by the overestimation of erosion in the current dominated areas within the non hydrostatic mode of XBeach. The sediment transport of the non hydrostatic mode performs good in a wave dominated area, however, in the current dominated areas it does not perform as well. The sedimentation in the simplified pocket beach with diffraction is therefore over-estimated.

A prominent difference in the results of both beaches is the abrupt transition between sedimentation in the shadow zones and no sedimentation in the exposed zones in case diffraction is not incorporated in the model (surfbeat mode). The transition is very clearly visible with an abrupt change in bed level, a line at the border, in both the simplified as well as the case study beach. At both beaches, the bed level abruptly increases with about one metre at the boundary of the exposed to shadow zone. This abrupt change could also be found in the sediment transport at these locations, where the magnitude drops with 95% without diffraction. This abrupt decrease in sediment transport explains the abrupt transition from no sedimentation to a lot of sedimentation. In case diffraction is incorporated in the simulations (non hydrostatic mode) the sedimentation and erosion is gradually dispersed over the area. The sediment transport patterns also show more constant and gradually increasing and decreasing transport values, which explains the more gradual dispersion of sedimentation and erosion. Furthermore, the variations between the exposed and the shadow zone endorse the more gradual transitions. With diffraction the differences between exposed and shadow zone are much smaller, maximum 40% decrease and 230% increase with diffraction and maximum 60% decrease and almost 2000% increase without diffraction. However, this last value is very large due to a very small value in the exposed embayment are of the surfbeat mode.

6.3.2. Shoreline Response

The shorelines erode in all cases, this is as expected since storm conditions are modelled. During storm conditions, material from around the shoreline is transported more offshore (Bosboom and Stive, 2015a). The amount of erosion of the shorelines is different in the various cases. In both beaches, simplified as well as case study, the erosion at the exposed shoreline is less severe with diffraction incorporated in the simulations compared to simulations without diffraction (10%). This can be related to the dominant alongshore instead of cross-shore velocities and sediment transport directions. Also, the higher waves in the surfbeat mode compared to the non hydrostatic mode might be the cause of a difference in erosion at the exposed shoreline. Furthermore, a difference is existent between the simplified and the case study beach. The simplified beach erodes 40% less with diffraction relative to without diffraction. The case study beach only erodes 10% less with diffraction relative to without diffraction. The larger difference in the simplified beach could be related to the fact it is an unstable beach, not yet adapted to the main wave direction. Whereas the case study beach is designed as a stable beach. Furthermore, the circulation cell in the surfbeat mode of the case study beach covers a larger area than in the simplified beach, whereby also the surfbeat mode has more alongshore directed velocities and sediment transport.

The shoreline areas within the shadow zones show in most cases more erosion with diffraction than without diffraction. However, in the simplified case this difference is not visible over the entire shadow shoreline area. The total volume of lost material is a bit less with diffraction however, in a cross-shore profile at the middle of the shadow zone (figure 4.43) it can be seen the case with diffraction shows more erosion higher up in the profile and at the shoreline the amount of erosion is equal. In the top view figures (4.41a and 4.41b) it can be seen the erosion without diffraction is primarily located close to the exposed shoreline and the erosion with diffraction is more dispersed over the total shadow shoreline. The larger erosion without diffraction in the simplified beach is probably correlated to the massive erosion in the exposed zone, which initiated erosion from the shadow shoreline towards the exposed shoreline. The shadow shoreline of the simplified beach erodes 10% less with diffraction. Whereas, at the case study beach the shoreline in the shadow zones erodes with respectively 90% and 50% more with diffraction. This enormous increase in erosion at the shoreline can be related to the larger sediment transport rates and the larger wave impact at this part of the beach due to diffraction. Without diffraction these beaches are not impacted by waves. With diffraction waves can enter the shadow zones and therewith cause more sediment transport along the shoreline.

6.3.3. Embayment Response

In general the shoreline zones show erosion and the embayment zones show accretion. As one should expect during a storm condition (Bosboom and Stive, 2015a). One exception can be seen in the simulations in this research; the exposed embayment of the simplified pocket beach without diffraction. In this area a small loss of sediment can be recognized. This erosion originates from the groyne erosion. This erosion is also visible in case diffraction is incorporated, however, this is negligible compared to the amount of sedimentation in this case. No sedimentation at all in the surf zone area during a storm condition is unlikely. In the case study beach the exposed embayment zones both show sedimentation, however, this is significantly more with diffraction than without diffraction (350% more). The circulation and sediment transport patterns are wider in the cases with diffraction and the velocities and magnitudes of sediment transport are dominated by alongshore directions in the exposed area. This results in less losses in cross-shore direction, therefore, more sediment stays in this area.

The embayment shadow zones all show a lot of accreation, which is as expected. Mangor (2004); Ab Razak et al. (2013); Fredsoe and Deigaard (1992) already mentioned that sheltered areas are sedimentation areas in their researches. With and without diffraction the shadow zones are sheltered from incoming waves but to a different extent. Without diffraction the wave height is reduced more than with diffraction. The sedimentation in the various embayment shadow zones differs from almost no difference to 30% less sedimentation with diffraction relative to without diffraction. The largest shadow zone shows the largest difference, so this could be an explanation for the difference. The smallest shadow zone, does not show a difference. Furthermore, a cause could be found in the overestimation of the sedimentation of the simplified beach with diffraction. The simplified pocket beach shows a total accretion of the embayment areas for the non hydrostatic simulation, which is very unlikely during storm conditions. Outside the pocket beach a lot of erosion can be seen, which is maybe initiated by model properties. Therefore, the accretion within the simplified pocket beach might be overestimated in case diffraction is incorporated. This overestimation could explain the small variation between the sedimentation in the surfbeat and the non hydrostatic mode.

6.3.4. Result Morphological Development

All in all the simplified beach results for the sedimentation and erosion values are found less reliable than the case study results. The simplified beach is an unstable beach and shows a implausible sedimentation of the area during a storm condition in the non hydrostatic mode. The case study results are more reliable and match better with expectations based on literature. The northern shadow zone is small and the dynamics within the pocket beach are dominated by the southern shadow zone. Therefore, the results of the southern shadow zone are expected to be more representative on the dynamics within an artificial pocket beach simulation.

Designs for pocket beaches are nowadays based on the combination of an equilibrium coastline oriented perpendicular to the direction of the wave energy flux and a total weighted sediment loss per year. These sediment losses are determined on several storm event simulations with the surfbeat model of XBeach. For reliable long term predictions it is therefore necessary to simulate the storm events as accurate as possible.

In this research a new mode, XBeach non hydrostatic, has been used to simulate storm events within pocket beaches. The results of this research show that surfbeat sometimes overestimates and sometimes under estimated sedimentation and erosion and in general overestimated the losses out of the pocket beach. This has an influence on the total weighted sediment loss per year in the designs. The total amount of material needed in the construction and maintenance of the beach is therefore probably overestimated with the surfbeat mode.

6.4. Model

Next to all the above mentioned differences, also some general discontinuities play a role in results of the simulations. The input for the model simulations and the characteristics of the model cause variations in the results that should be kept in mind. Already some of the differences are mentioned above but for completeness are discussed here as well.

First of all the the two beach sections, the simplified and the case study beach, already are different from each other on several aspects. The total surface area and length of pocket beach is about the same, however, the layout, beach shape and the shadow zone surface area is different for both beaches. The case study has a larger shadow zone compared to the simplified beach. Besides, the simplified beach is not designed to be stable. Adaptation to the incoming wave direction is not clearly visible due to the strong influence of diffraction in this small artificial pocket beach. On contrary the case study beach has been designed as a stable beach. This can also be seen on the characteristic curved shape of the beach (Silva et al., 2010). Next to the bathymetry input in the model simulations, the input variables for the storm conditions are different. The storm condition in the simplified beach is milder but takes longer than the storm condition in the case study beach. The wave height, wave period and duration are therewith different in both beaches. However, it is not expected these difference influence the differences between the cases with or without diffraction significantly. The exact volume changes could be different, but the general patterns should be similar within a storm condition.

Furthermore, the different modes of XBeach used in this research bring in some differences. The different modes are used for the examination of the influence of diffraction and on a small scale the influence of long waves on the dynamics in artificial pocket beaches. However, these modes contain more differences than only diffraction or long waves. Therefore, some results of the simulations could be explained by differences in these modes. First of all, the wave resolving level is different for all three modes. This implies several differences in the initiation of processes. Furthermore, two important differences are the way breaking of waves is included in the models and the sediment transport formulations. The breaking of waves is coupled to the ratio of water depth to wave height within the surfbeat model and to the steepness of waves in the non hydrostatic model. This can have consequences for the moment of wave breaking. Therewith the wave heights and set-up differences can variate in the results of different modes of XBeach. This could be seen in the extensive tests of the simplified beaches and introduces differences between the surfbeat and the non hydrostatic mode. The mean wave height in the non hydrostatic mode decreases a bit earlier than the mean wave height of the surfbeat mode. The mean wave height of the stationary mode with monochromatic waves decreases much earlier, however, these results are not used in the later stage of the research and this larger variation is therefore less important. Furthermore, the sediment transport formulations are different in all modes. For the stationary and surfbeat mode these has been properly validated, however, for the non hydrostatic mode this has not been done yet. In this research a factor has been used to bring the sediment transport in the non hydrostatic mode more to the level of the surfbeat mode. Nevertheless, this does not take out all the possible errors in the sediment transport of the non hydrostatic mode. It is known that the sediment transport results are good in wave dominated areas, however, in current dominated areas the sediment transport is not that well. The overestimation of sedimentation within the non hydrostatic simulation of the simplified pocket beach shows this limitation. The waves in the case study are much larger and therefore, the area outside the pocket beach is more wave dominated. Which results in a more reliable result of the sedimentation and erosion. In this research the results of the case study simulations could not be validated but no very strange results are found, the results look promising. Therefore, the sediment transport within the non hydrostatic mode is valued reliable enough to conclude on the influence of diffraction on the behaviour within artificial pocket beaches.

Finally, the groynes are modelled as hard, reflective, non erodible structures. The structures are not able to absorb energy of the waves. In reality these structures are made of stones not as one big concrete structure. Due to the different ways of wave breaking and the different level of wave resolving the effect is different in the various modes. In general it can be noticed that the processes along the groynes are not modelled correctly due to the simplification of the groynes and the effects of this on the dynamics within the pocket beach. For example, in the non hydrostatic mode more reflection could be recognized in the mean wave height results. Furthermore, in all simulations the velocities really close to the groynes are high, especially in the cases with normal incident waves. the cases with normal incident waves, parallel to the groynes, are not very important for the influence of diffraction. Therefore, this restriction is not of large impact for the results of this research.

6.5. Measurements Case

Within the case study, conducted in this research, the pocket beach of Tomis South has been looked at in detail with model simulations. These simulations cover a period of 1.5 days. It is assumed that several of these storm conditions would be representative events to explain morphological dynamic processes within the pocket beach on the long term. Most sediment is moved during these conditions. A general comparison has been attempted to be made on the morphological changes. However, it is difficult to compare the simulation results with measurement results. Within the measurements, more processes play a role which can not be found in the model results. Recovery of the beach profile during calm conditions and transverse changes are not incorporated in the XBeach model. Besides, especially from the satellite images of two years after construction, it can be noticed that the beach has been reorientated. Which can be explained by a different angle of mean wave direction compared to the design angle. Furthermore, some settling of the sediment could have taken place within the interval of the measurements because the measurements are conducted just after construction. A reliable comparision of the measurement results and simulation results is therefore not possible.

7
Conclusion

7.1. Introduction

The main objective of this research was to gain better insight in the dynamics of artificial pocket beaches initiated by diffraction. The dynamics that have been looked at are hydrodynamic, sediment transport and morphodynamics by comparing various modes of XBeach including diffraction or not. The insights in these processes and the effect of these processes on the sedimentation and erosion within artificial pocket beaches is important for the design of dynamic stable pocket beaches. To achieve this objective the research has been conducted by means of three parts; a literature study, simplified pocket beach simulations and a case study. In all three parts the focus was on the three main processes, appointed in the sub questions, which are used to answer the main research question. The main research question for this research is:

How does the morphological behaviour of artificial pocket beaches change when diffraction is included in simulations and why does it change?

7.2. Circulation Patterns

What is the effect of diffraction on general circulation patterns within an artificial pocket beach?

In artificial pocket beaches often the groyne length relative to the beach length is large. This results in relatively large shadow zones. Therewith, the structures influence the waves within the embayment significantly. These variations in wave height induce a set-up difference within the embayment, which initiate circulation patterns. Without short wave diffraction, relatively local circulation cells occur. On the contrary, with short wave diffraction, relatively wide circulation cells occur. In a straight unstable simplified pocket beach with a shadow zone surface area of 30% of the total embayment area, the cell length with diffraction is 55% larger relative to the embayment length. In the stable designed, curved case study beach in Constanta, with a shadow zone covering 40% of the total embayment surface area, the circulation cell with diffraction is 15% larger relative to the embayment length. In both cases with diffraction the circulation cell covers almost the entire embayment length (at least 90%). The effect of long wave diffraction on the circulation cell is not significant. When imposing a spectrum on the beach consequently, including wave groups and long waves, the circulation cell lengths with and without diffraction differentiate even more.

Furthermore, the velocities in the outflow currents along the groynes in the shadow zone are different in case short wave diffraction is included or not. On average with diffraction the velocity is about 30% lower than with diffraction. In the simplified case the outflow velocities are 33% less with short wave diffraction and in the case study beach the main shadow zone shows a velocity 25% smaller with short wave diffraction.

7.3. Sediment Transport

What is the effect of diffraction on general sediment transport patterns within an artificial pocket beach?

The general initial sediment transport patterns are very similar to the water circulation patterns; with short wave diffraction the circulation is wider than without short wave diffraction. However, the magnitudes do not always correspond with the circulation patterns. The magnitude of sediment transport is not only influenced by the velocity, it is also influenced by the sediment concentration. Without short wave diffraction the magnitude of sediment transport is high just outside the shadow zone and low just inside the shadow zone. Further into the shadow zone the sediment transport magnitude increases again. In both, the simplified as well as the case study beach, an abrupt decrease of the sediment transport rate of 95% could be noticed at the boundary of the shadow zone. In case diffraction takes part, the magnitude of sediment transport just inside and outside the shadow zone does not show the large differences, it gradually develops into the shadow zone.

On the outflow magnitudes no clear conclusion can be given. In the simplified pocket beach the outflow without diffraction was significant larger than with diffraction but in the case study beach the outflow was larger in the case with diffraction. The outflow in the case study beach circulates back into the beach again, whereas, the outflow in the surfbeat mode is more directed out of the pocket beach.

7.4. Morphological Development

What is the effect of diffraction on the general sedimentation and erosion within an artificial pocket beach?

The morphological development within an artificial pocket beach is different in case diffraction is taken into account from when it is not taken into account. To analyse the morphological development the pocket beach has been divided into four types of areas based on two characteristics. The depth determines if it is a shoreline area or an embayment area. Furthermore, distinction has been made between shadow zone and exposed zone. In general, all areas around the shoreline show erosion and all embayment areas show sedimentation during storm conditions. However, the transitions between areas and the volume changes per area are different due to diffraction. The case study beach has been found most reliable concerning morphological changes since it best fits the expectations based on literature. The southern largest shadow zone of this beach is most representative since it is dominant over the smaller one.

The sedimentation and erosion pattern is more gradually spread over the pocket beach area in case diffraction is included as a process. In case diffraction is not included, the transitions between shadow zone and exposed zone are very abrupt. Without diffraction almost all gained material in the shadow zone is located just inside the shadow zone. The material has been piled up next to the boundary of the shadow to exposed zone with a steep difference of approximately one metre. These abrupt transitions can also be indicated by the differences in volume change between exposed and shadow zone, within one simulation. The variation in volume changes are larger when short wave diffraction is not taken into account than when it is. With the exposed area as a reference the shoreline area erodes 20% less with diffraction and 60% less without diffraction. For the embayment area, the shadow zone gains two times more sediment with diffraction and more than 10 times more sediment without diffraction, relative to the exposed zone.

Presence of diffraction within the simulation changes the sedimentation and erosion in various areas. The erosion around the coastline is overestimated in the exposed zone and underestimated in the shadow zone in case short wave diffraction is not incorporated in the simulation. The volume changes with short wave diffraction relative to without short wave diffraction are summarized in table 7.1 for a stable designed curved beach with a shadow area of 40% of the total pocket beach area. The erosion at the exposed shoreline is 10% less with diffraction than without diffraction. The erosion of the shadow shoreline is 90% more with diffraction. The sedimentation in the shadow embayment area is 30% less with diffraction. Furthermore, in the exposed embayment the differences are very large, with diffraction 350% more sediment is accumulated in this area. It should be noted that this value is large due to the very limited volume changes in the case without diffraction in this area.

In total the pocket beach losses are 3900 m^3 of sediment without diffraction and 3400 m^3 with diffraction, for a storm with a return period of 10 years and a duration of 1.5 days. For this storm event, with a significant

wave height of 4.5 metres on a pocket beach with 40% shadow zones, including short wave diffraction reduces the total sediment loss with 10%.

	Shadow Shoreline	Shadow Embayment	Exposed Shoreline	Exposed Embayment	Total
With diffraction (non hydrostatic mode) relative to without diffraction (surfbeat mode)	+90% erosion	-30% sedimentation	-10% erosion	+350% sedimentation	-10% erosion

Table 7.1: Results morphological changes with short wave diffraction

7.5. Behaviour in Artificial Pocket Beaches

How does the morphological behaviour of artificial pocket beaches change when diffraction is included in simulations and why does is change?

XBeach is a two-dimensional model which is used for the near shore area, beaches and dunes during storms. It has several modes to do the simulations with, with all a different level of wave resolving. The stationary mode is a wave-averaged mode which neglects wave-group variations and thereby infragravity waves. Wave-groups and long waves are incorporated in the other two modes. The surfbeat mode solves the variation of waves on the wave-group scale. The short waves are still averaged. This mode includes long wave diffraction, however, short wave diffraction is not included. Short and long waves are resolved in the non hydrostatic mode. Therewith, short and long wave diffraction are included in this model. Since storm conditions (including long waves) are important for the morphological development of pocket beaches, the surfbeat or non hydrostatic mode are used. Furthermore, diffraction appeared to influence the dynamics within an embayment significantly. Simulations with diffraction show that erosion at the exposed zone decreases, erosion at the shadow shoreline increases, sedimentation at the exposed embayment increases and sedimentation in the shadow embayment area decreases relative to simulations without diffraction. The total loss of sediment after a storm decreases with 10% when diffraction is incorporated compared to when diffraction is not incorporated in the model simulations. Furthermore, the transitions are very abrupt without diffraction. The results found with the non hydrostatic mode show more realistic bed level shapes.

The areas of sedimentation and erosion are similar in both ways of simulation. However, the transitions and quantities are different. These differences can be explained by the hydrodynamic and sediment transport dynamics within the pocket beach caused by diffraction. It could be seen that the circulation cell length is significantly larger with diffraction than without diffraction. Furthermore, the outflow velocities along the groynes in the shadow zone are lower with diffraction than without diffraction. Due to the wide or narrow circulation cell, the dominant direction of the velocity or sediment transport is different. With diffraction, the velocities and sediment transport in the exposed zone are dominated by alongshore directions in the direction of the shadow zone. The magnitudes are very constant from outside to inside the shadow zone. Due to these gradual circulation and sediment transport patterns, the sedimentation and erosion patterns are also smooth. Without diffraction the cross-shore direction is more dominant in the exposed zone and velocities and sediment transport outside the circulation cell are also directed in opposite alongshore direction. This causes more erosion in the exposed zone without diffraction. Furthermore, much more variation can be noticed in the magnitudes of the velocity and sediment transport. Especially, just inside the shadow zone the sediment transport magnitudes drop with 95% which causes the abrupt accumulation of approximately one metre of sediment just inside the shadow zone.

A validation with measurements was not possible, the amounts of sedimentation and erosion after a storm could therefore not be checked properly. However, the patterns of the non hydrostatic mode, which includes short wave diffraction look much more natural than the results of the surfbeat mode, which neglects short wave diffraction. For the design of pocket beaches, the losses of sediment out of the pocket beach and the retreat of the shoreline are important. In this research it has been identified that significant differences in these areas appear by the influence of short wave diffraction. With short wave diffraction (non hydrostatic mode) the erosion of the exposed shoreline reduces with 10%, the erosion of the shadow shoreline increases with 90% and the total loss of sediment out of the pocket beach reduces with 10% .

8

Recommendations

8.1. Validation

In this research, it has been mentioned that the sediment transport of the non hydrostatic mode of XBeach has not been extensively validated. In this thesis the sediment transport of the non hydrostatic simulations has been adapted to the results of the surfbeat mode with a factor based on the mean initial sediment transport within the groynes with normal incident waves. However, still some erroneous results are shown in the sedimentation and erosion. Especially in the current dominated areas, the results are not as expected. The reliability of the results of this research would improve if the sediment transport of the non hydrostatic mode would be more reliable. So, a more extensive validation of the non hydrostatic mode can improve the results. Since this problem is not easy to solve, a more reliable result could be achieved by determining a factor based on several cases to come up with a more robust factor till the non hydrostatic mode is validated extensively.

For the beach case study in this research, a storm with a 10 year return period is simulated. The attempt to compare these results with reality has been done with bathymetry measurements and satellite images. However, these measurements and satellite images have an interval of almost one year. The conclusions about differences in morphological changes in storms by incorporating diffraction or not would be more reliable if measurements of a comparable period are available to validate the simulation results. Furthermore, the measurements are conducted right after construction. It is hard to verify the results, since steepening of the beach profile, rotation to the equilibrium coastline and settling of nourished sediment has all taken place in this interval. For example, measurements around a storm, a year after construction would improve the reliability.

8.2. Variations

For this thesis first an orientating study has been done on the processes within a relatively small pocket beach. This resulted in the research on diffraction on the dynamics within an artificial pocket beach. It has been proved that diffraction has effect on the sedimentation and erosion patterns within the embayment. However, more research could be done on the degree of influence of diffraction under several conditions. For this research all parameters are kept as identical as possible, to be able to conclude on a difference in hydrodynamic, sediment transport and morphodynamics in case diffraction is included within simulations. The degree of impact could be influenced by wave period, wave height and wave spreading. Several variations in this parameters and combinations could give a better understanding of the degree of importance of diffraction under several circumstances.

Next to the wave characteristics also the degree of influence of several pocket beach layout variations is interesting to do subsequent research on. Shadow zones are important conditions to get diffraction and since it has been found that diffraction significantly affects the dynamics within pocket beaches, it is interesting to look more into detail of relation of layout to the degree of influence. Probably, the ratio of shadow zone to beach length influences the degree of influence of diffraction on the dynamics within the pocket beach. The size of the shadow zone is determined by wave angle of incidence and the geometry of the groynes relative to the beach. Long or curved groynes on a relatively small beach create relative large shadow zones.

8.3. Processes Close to Groynes

In the results of the simplified pocket beaches, it attracts attention that the velocities and magnitudes of sediment transport are very high close to the groynes. Especially, the cases with normal incident waves show very high velocities and magnitudes of sediment transport along the groynes. Nevertheless, also in the oblique incident wave cases high magnitudes of sediment transport can be found along the exposed side of the groyne. In the normal incident wave cases it maybe even influences the patterns. This effect is not that strong in the oblique incident wave cases, however, the balance of sediment transport within the pocket beach can be disturbed. In the case study of this research also straight groynes are present. These are not examined into detail, however, for future design processes it is important to know how to model with straight groynes. The influences of the effects of the groynes due to problems in model simulations should be minimised. The sediment losses out of the embayment are important for the design of such beaches. Therefore, it is important to improve the model results close to the groynes. For example, it could be tried to use smaller grid cells at the slope of the groynes or change the roughness of the groynes.

Bibliography

Ab Razak, M. S., Dastgheib, A., and Roelvink, D. (2013). Sand bypassing and shoreline evolution near coastal structure, comparing analytical solution and xbeach numerical modelling. *Journal of Coastal Research*, 65(sp2):2083–2088.

Ab Razak, M. S., Dastgheib, A., Suryadi, F. X., and Roelvink, D. (2014). Headland structural impacts on surf zone current circulations. *Journal of Coastal Research*, 70(sp1):65–71.

Baquerizo Azofra, A., Losada, M., and L. Ortega, J. (2002). Rip currents in semi-elliptic bays. In *28th International Conference Coastal Engineering*, volume 1, pages 718–726.

Bemmelen, C. V. (2017). Long Term Process-Based Morphological Modelling of Pocket Beaches. Master's thesis, Technical University Delft.

Bird, E. C. F. (1985). *Coastline changes. A global review*. John Wiley and Sons Inc., New York, NY.

Bosboom, J. and Stive, M. J. (2015a). Coastal dynamics i, lecture notes cie4305.

Bosboom, J. and Stive, M. J. (2015b). Lecture slides coastal dynamics 1 (cie4305.

Bowen, A. J. (1969). Rip currents: 1. theoretical investigations. *Journal of Geophysical Research*, 74(23):5467–5478.

Bowman, D., Rosas, V., and Pranzini, E. (2014). Pocket beaches of elba island (italy)–planview geometry, depth of closure and sediment dispersal. *Estuarine, Coastal and Shelf Science*, 138:37–46.

Castelle, B. and Coco, G. (2012). The morphodynamics of rip channels on embayed beaches. *Continental Shelf Research*, 43:10–23.

Castelle, B. and Coco, G. (2013). Surf zone flushing on embayed beaches. *Geophysical Research Letters*, 40(10):2206–2210.

Castelle, B., Scott, T., Brander, R., and McCarroll, R. (2016). Rip current types, circulation and hazard. *Earth-Science Reviews*, 163:1–21.

Daly, C., Bryan, K. R., Roelvink, J., Klein, A., Hebbeln, D., and Winter, C. (2011). Morphodynamics of embayed beaches: the effect of wave conditions. *Journal of Coastal Research*, (64):1003.

Daly, C. J., Bryan, K. R., and Winter, C. (2014). Wave energy distribution and morphological development in and around the shadow zone of an embayed beach. *Coastal Engineering*, 93:40–54.

de Santiago González, I. n. (2014). *Storm inpact on engineered pocket beaches*. PhD thesis, L'Université de Pau et des pays de l'adour.

Dehouck, A., Dupuis, H., and Sénéchal, N. (2009). Pocket beach hydrodynamics: The example of four macrotidal beaches, brittany, france. *Marine geology*, 266(1):1–17.

Deigaard, R., Jakobsen, J. B., and Fredsøe, J. (1999). Net sediment transport under wave groups and bound long waves. *Journal of Geophysical Research: Oceans*, 104(C6):13559–13575.

Deltares (2017). Xbeach skillbed report, revision 5123, status update trunk default revision: 5123. Technical report, Deltares, Rotterdamseweg 185 Delft The Netherlands.

Dunham, J. W. (1965). Use of long groines as artificial headlands. In *Proceedings Santa Barbara specialty conference*. ASCE.

Fredsoe, J. and Deigaard, R. (1992). *Mechanics of coastal sediment transport*. World Scientific Publishing Co. Pte. Ltd.

Goda, Y. (2010). *Random seas and design of maritime structures*. World scientific.

Google Earth Pro V7.1.8.3036 (2006). Constanta, Romania. DigitalGlobe 2017 http://www.earth.google.com. 44°10'51.33" N, 28 °39'27.99" W, Eye alt 1.16 km.

Google Earth Pro V7.1.8.3036 (2015). Constanta, Romania. DigitalGlobe 2017 http://www.earth.google.com. 44°11'15.21" N, 28 °39'33.07" W, Eye alt 1.89 km.

Google Earth Pro V7.1.8.3036 (2016a). Constanta, Romania. DigitalGlobe 2017 http://www.earth.google.com. 44°11'15.21" N, 28 °39'33.07" W, Eye alt 4.09 km.

Google Earth Pro V7.1.8.3036 (2016b). Constanta, Romania. DigitalGlobe 2017 http://www.earth.google.com. 44°11'15.21" N, 28 °39'33.07" W, Eye alt 1.89 km.

Google Earth Pro V7.1.8.3036 (2016c). Constanta, Romania. DigitalGlobe 2017 http://www.earth.google.com. 44°10'51.33" N, 28 °39'27.99" W, Eye alt 1.16 km.

Google Earth Pro V7.1.8.3036 (2016d). Plouarzel, France. DigitalGlobe 2017 http://www.earth.google.com. 48°24'44.35" N, 4°47'30.37" W, Eye alt 1.13 km.

Google Earth Pro V7.1.8.3036 (2017a). Constanta, Romania. DigitalGlobe 2017 http://www.earth.google.com. 44°11'15.21" N, 28 °39'33.07" W, Eye alt 1.89 km.

Google Earth Pro V7.1.8.3036 (2017b). Constanta, Romania. DigitalGlobe 2017 http://www.earth.google.com. 44°10'51.33" N, 28 °39'27.99" W, Eye alt 1.16 km.

Google Map Data (2017). Constanta, Romania. DigitalGlobe 2017 http://www.maps.google.com. 44°11'10.4" N, 28°39'21.0" W.

Harley, M., Turner, I., Short, A., and Ranasinghe, R. (2011). A reevaluation of coastal embayment rotation: The dominance of cross-shore versus alongshore sediment transport processes, collaroy-narrabeen beach, southeast australia. *Journal of Geophysical Research: Earth Surface*, 116(F4).

Holthuijsen, L. H. (2010). *Waves in oceanic and coastal waters*. Cambridge university press.

Kim, I. and Lee, J. (2009). Numerical modeling of shoreline change due to structure-induced wave diffraction. *Journal of Coastal Research*, (56):78.

Lasagna, R., Montefalcone, M., Albertelli, G., Corradi, N., Ferrari, M., Morri, C., and Bianchi, C. N. (2011). Much damage for little advantage: Field studies and morphodynamic modelling highlight the environmental impact of an apparently minor coastal mismanagement. *Estuarine, Coastal and Shelf Science*, 94(3):255–262.

Loureiro, C., Ferreira, Ó., and Cooper, J. A. G. (2012). Extreme erosion on high-energy embayed beaches: influence of megarips and storm grouping. *Geomorphology*, 139:155–171.

Mangor, K. (2004). *Shoreline management guidelines*. DHI Water and Environment, Horsholm, Denmark.

Martins, C. C., de Mahiques, M. M., and Dias, J. M. A. (2010). Daily morphological changes determined by high-energy events on an embayed beach: a qualitative model. *Earth Surface Processes and Landforms*, 35(4):487–495.

Ojeda, E. and Guillén, J. (2008). Shoreline dynamics and beach rotation of artificial embayed beaches. *Marine Geology*, 253(1-2):51–62.

Pattiaratchi, C., Olsson, D., Hetzel, Y., and Lowe, R. (2009). Wave-driven circulation patterns in the lee of groynes. *Continental Shelf Research*, 29(16):1961–1974.

Reeve, D., Chadwick, A., and Fleming, C. (2015). *Coastal Engineering: Processes, Theory and Design Practice*. CRC Press.

Reniers, A. J., Roelvink, J., and Thornton, E. (2004). Morphodynamic modeling of an embayed beach under wave group forcing. *Journal of Geophysical Research: Oceans*, 109(C1).

Roelvink, D. and Reniers, A. (2012). *A guide to modeling coastal morphology*. World Scientific.

Roelvink, D., van Dongeren, A., McCall, R., Hoonhout, B., van Rooijen, A., van Geer, P., de Vet, L., Nederhoff, K., and Quataert, E. (2015). *XBeach Technical Reference: Kingsday Release: Model description and reference guide to functionalities*. Deltares and UNESCO-IHE Institute of Water Education and Delft University of Technology.

Roy, P., Cowell, P., Ferland, M., Thom, B., Carter, R., and Woodroffe, C. (1994). Wave-dominated coasts. *Coastal evolution: Late Quaternary shoreline morphodynamics*, pages 121–186.

Scholar, D. C., Griggs, G. B., Anima, R., and Jaffe, B. E. (1998). Pocket beaches of california sediment transport along a rocky coastline. In *California's Coastal Natural Hazards: Proceedings from the Conference Hosted by the California Shore and Beach Preservation Association and the University of Southern California Sea Grant Program, November 12-14, 1997, Santa Barbara, California*, volume 1, page 65. Sea Grant Program, University of Southern California.

Short, A. and Masselink, G. (1999). Embayed and structurally controlled beaches. *Handbook of Beach and Shoreface Morphodynamics; Short, AD, Ed.; John Wiley and Sons Ltd: Chichester, UK*, pages 230–250.

Silva, R., Baquerizo, A., Losada, M. Á., and Mendoza, E. (2010). Hydrodynamics of a headland-bay beach—nearshore current circulation. *Coastal Engineering*, 57(2):160–175.

Silvester, R. (1960). Stabilization of sedimentary coastlines. *Nature*, 188(4749):467–469.

Smit, P., Stelling, G., Roelvink, D., van Thiel de Vries, J., McCall, R., van Dongeren, A., Zwinkels, C., and Jacobs, R. (2010). Xbeach: Non-hydrostatic model. *Report, Delft University of Technology and Deltares, Delft, The Netherlands*.

Steetzel, H., Jansen, M., Langeveld, C., and Hafkenscheid, J. (2014). Long term coast and beach development tomis south (improved layout) 28.3366-vosct-cl04-d-tr-3002. Technical report, Van Oord Dredging and Marine Contractors Engineering Department.

Tucker, M. (1950). Surf beats: Sea waves of 1 to 5 minute period. In *Proc. Roy. Soc. London Ser. A*, volume 207, pages 5665–573.

Turki, I., Medina, R., Gonzalez, M., and Coco, G. (2013). Natural variability of shoreline position: observations at three pocket beaches. *Marine Geology*, 338:76–89.

Turki, I., Medina, R., Kakeh, N., and González, M. (2015). Shoreline relaxation at pocket beaches. *Ocean Dynamics*, 65(9-10):1221–1234.

Wunk, W. (1949). Surf beats. *EOS, Transactions American Geophysical Union*, 30(6):849–854.

Yamashita, T. and Tsuchiya, Y. (1993). Numerical simulation of pocket beach formation. In *Coastal Engineering 1992*, pages 2556–2566.

A

Simplified Pocket Beach Variations

The four layouts that are tested can be seen below in figure 4.2. The variations in layout are combined with variations in wave characteristics to get more insight in the processes within pocket beaches.

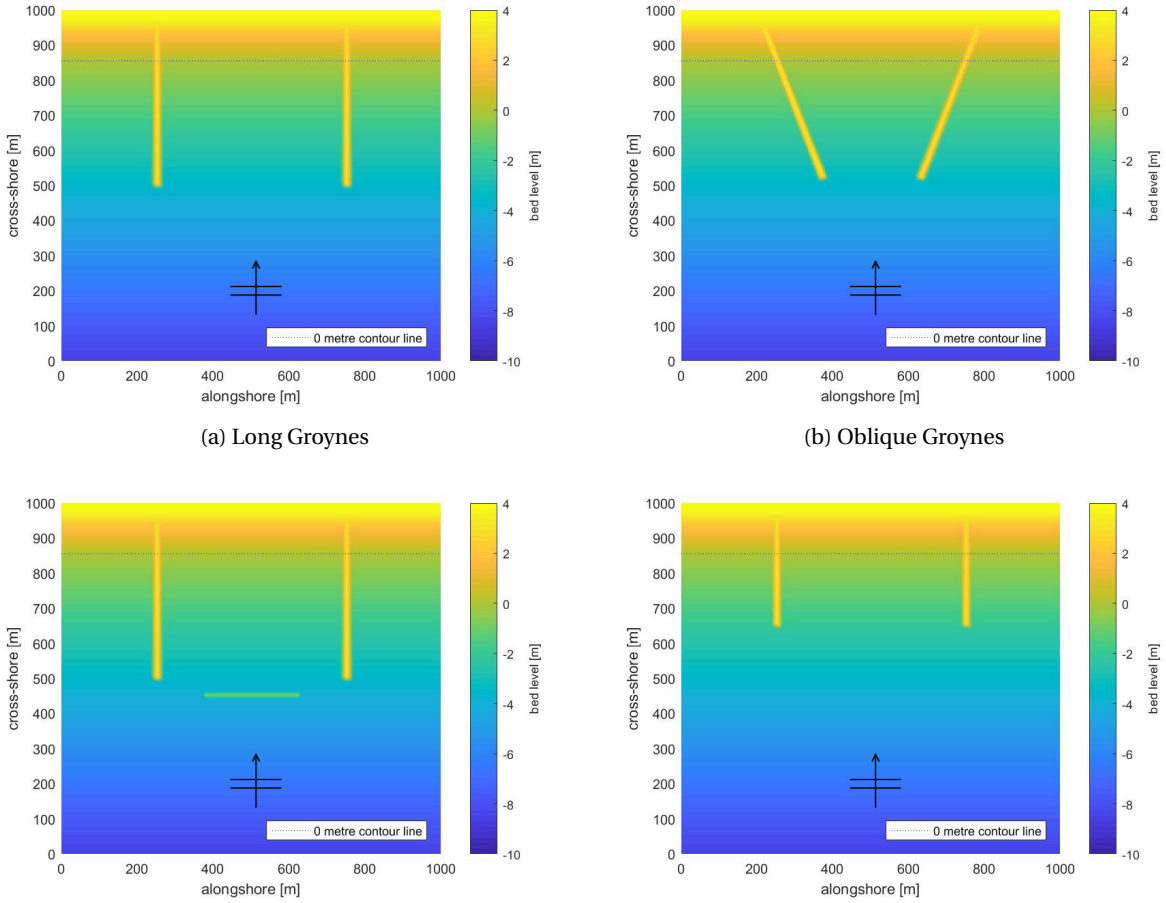

(a) Long Groynes

(b) Oblique Groynes

(c) Offshore submerged breakwater

(d) Short Groynes

Figure A.1: Bed elevation (shown in colors) of the various pocket beach layouts

The pocket beach ha a width of 500 metres at the shoreline because in chapter 3 it could be read that in beaches of 500 metres influence of structures on circulation patterns is significant. The long groynes reach about 350 metres offshore, the short groynes reach about 200 metres offshore. The offshore opening of the pocket beach with oblique groynes is halved, so an opening of 250 metres is left. The offshore submerged breakwater is located just outside the pocket beach. The length is 250 metres and the top of this breakwater

is at mean water level.

This model set up has been tested by a sensitivity analysis, which can be found in appendix B. In this sensitivity analysis the boundary effects and the effect of a non uniform offshore boundary are researched (appendix B.1). Boundary effects can be noticed however, the beaches with groynes are less effected by boundary effects than the plain beaches, the beaches without any groynes. Therefore, an area of 1000 by 1000 metres is enough to research the processes within the embayment. Though, the effects and processes outside the embayment area should not be looked at. Besides, the effect of the non uniform offshore boundary is small. The boundary effect caused by reflecting waves in case of waves initiated under an angle relative to the grid is much more. Therefore, it is chosen to work with rotated grids in this research.

To get a first impression of the hydrodynamic processes, several model runs have been done with XBeach non hydrostatic. The non hydrostatic mode of XBeach is a short-wave resolving mode. Due to this, more processes are included directly, for example skewness and asymmetry are predicted directly and not based on local approximations (Roelvink and Reniers, 2012). Additionally, short and long wave diffraction are included. This gives a broad overview of the behaviour of waves. For the following simulations a grid of 200 by 200 cells is used, with a grid cell size of 5 by 5 metres.

A.1. Wave Input

In a wave spectrum, often a wind-sea part and a swell part can be distinguished. In the simulations these two are simulated separately. In this way the effect of both kind of waves can be seen more clear. Both wave conditions are entered as a JONSWAP spectrum in XBeach. JONSWAP is one of the ways to characterise wave spectra, it relates the wind field to spectral density. For (developing) wind sea in oceanic waters a JONSWAP spectrum is characteristic (Holthuijsen, 2010). JONSWAP is used to give the wave input for the XBeach models, although, in reality not all waves and how these evolve can be characterised very well with a JONSWAP spectrum.

For swell waves the period is larger than for wind-sea waves, so the frequency is smaller. A peak frequency of 0.1 s^{-1} is used for swell waves and a peak frequency of 0.2 s^{-1} is used for the wind-sea waves. Furthermore, the directional spreading of swell waves is much smaller than for wind-sea waves, this can be expressed in the directional width σ_θ. The directional width can be converted to the width parameter of the JONSWAP spreading parameter, s. The relation between these two is shown in equation 4.2 (Roelvink et al., 2015). The swell waves have a very narrow spectrum and therefore the value 900 is used for s. The wind-sea waves have a much broader spectrum, therefore the default value for s, 10, is used. The significant wave height, H_{m0}, for both wave conditions is set to 1.5 metres.

$$\sigma_\theta = \sqrt{\frac{2}{s+1}} \qquad\qquad s = \frac{2}{\sigma_\theta^2} - 1 \tag{A.1}$$

For all the runs of a specific sea state (swell or wind sea), exactly the same time series have been used. Therefore, there is no variation because of random phase in the boundary conditions. This makes the results good comparable with each other. Furthermore, all snapshots in time shown are at the same moment in time, after 300 seconds of simulation. The wave direction is always perpendicular to the x-axis. So, waves enter the beach in vertical direction upward in all figures.

A.2. Swell Waves

The results of the four different lay outs with swell waves can be seen below in figure A.2. In general, a small directional spreading can be seen, not all the wave crest are undisturbed from left to right. Furthermore, it can be seen that the wave height decreases from the offshore boundary towards the shoreline.

In the pocket beaches with oblique groynes (A.2c) and with the breakwater (A.2d) the wave height is decreased more than in the cases with the long and short groynes. In the case of oblique groynes the water level variation is lowered over the whole area of the pocket beach. The water level variation in the pocket beach with the offshore breakwater is especially lowered just behind the breakwater. Besides, wave crests can be found

in the shadow zones. These wave crests are curved and lower than in the undisturbed areas. The lower wave heights in the undisturbed areas and the curved lower waves in the shadow zones indicate diffraction.

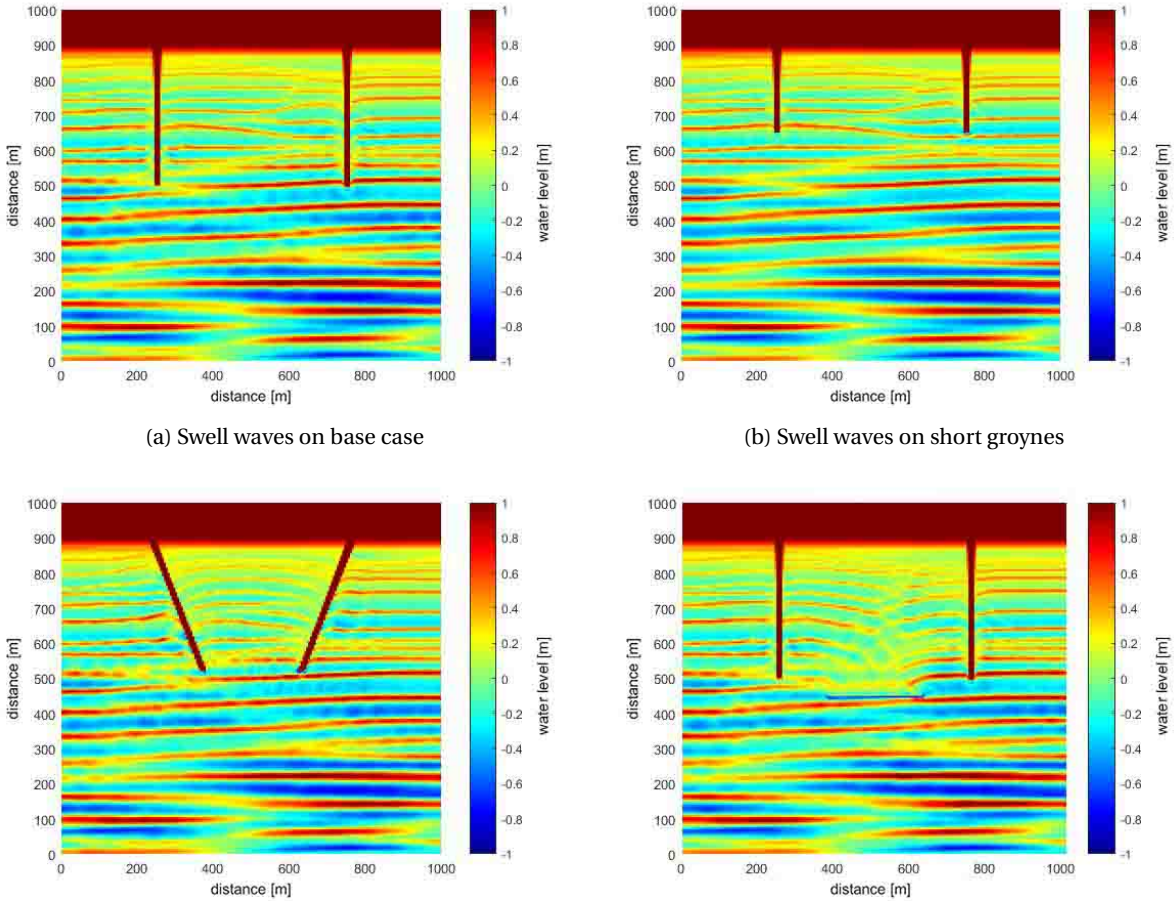

(a) Swell waves on base case

(b) Swell waves on short groynes

(c) Swell waves on oblique groynes

(d) Swell waves on detached breakwater

Figure A.2: Snapshots of surface elevations of swell waves on different layouts

A.3. Wave Direction

To research the effect of wave direction, three different main wave directions are used. One wave direction is chosen perpendicular to the coast, so 270 degrees from North (this situation is shown above in figure A.2). The second wave direction is chosen at 300 degrees, so an angle of incidents of 30 degrees from perpendicular (figure A.3a). The third wave direction is 45 degrees from the normal incoming waves, so it is set to 315 degrees from North (figure A.3b).

First, it can be seen that the wave heights on the left side decrease later than the wave heights at the right side. Also the wave crests bend when approaching the shore. This bending is stronger with waves with a larger angle of incidence from normal. These processes indicate refraction. Secondly, shadow zones can be seen at the left side of each groyne. In these areas lower wave heights and bending wave crests occur. This shadow areas are larger in the pocket beach subject to incident waves with an angle of 315 degrees from North (figure A.3b). With that also the influence of diffraction is larger in this pocket beach, the wave height in the whole pocket beach is lower. The wave energy is spread out. So, the decrease in wave height towards the shoreline and towards the groyne is larger also.

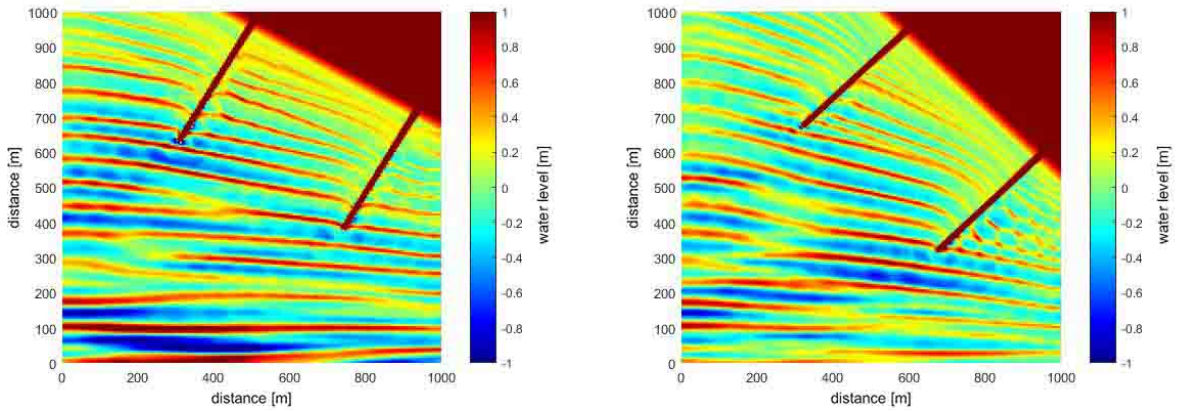

(a) Swell waves with an angle of 300 degrees from North

(b) Swell waves with an angle of 315 degrees from North

Figure A.3: Snapshots of surface elevation of swell waves for two wave directons

A.4. Wind Waves

To examine the difference between sea states, similar simulations have been done with wind sea wave forcing. These waves have smaller periods and larger directional spreading than swell waves. The results of the base layout under two main wave directions can be seen in figure A.4. Since, the variations in wave height and directions are larger in these wind wave cases than in the swell wave cases, bending of wave crests by diffraction and refraction are less clear to distinguish. However, the amount of variations in wave height on different places in the simulation can be compared. It can be observed that the wave heights decrease less at the left side in case of oblique incident waves. This is similar to the pocket beach with oblique incident swell waves and can be related to the depth.

The water level variations in these cases with wind-sea waves are much lower than in the cases with swell waves though the same significant wave height is used as input parameter. Only at the offshore boundary some water level variations of 2 metres can be seen. These variations decrease quite fast and then remain rather constant for some time. Close to the shoreline, the water level variations are not noticeable any more. Also in the shadow zone close to the groyne the water level variations become zero. It is remarkable that the wave height decrease so strong. Therefore, some test have been done to check the numerical dissipation of energy in these cases. This effect of numerical dissipation has been looked at with help of the kd value (wavenumber times waterdepth, see section 3.2) and grid cell size. These analyses can be found in appendix B.2. It has been found that the grid size is too large for this wavelength, therefore, a lot of energy has been disappeared by numerical dissipation. Especially with short waves, a larger grid cell could cause energy dissipation. Therefore, it is important for the non hydrostatic mode to use small grid sizes. For a reliable result, grid sizes of about 1 metre should be used in the simulation with wind waves and grid sizes of 2.5 metres for the swell waves, which would make it more computational demanding. For the following simulations in the next sections smaller grid sizes are used for more reliable results. For the stationary and surfbeat modes this is not that important, however, to reduce the differences in the research, all simulations have been done on a grid with smaller grid cells.

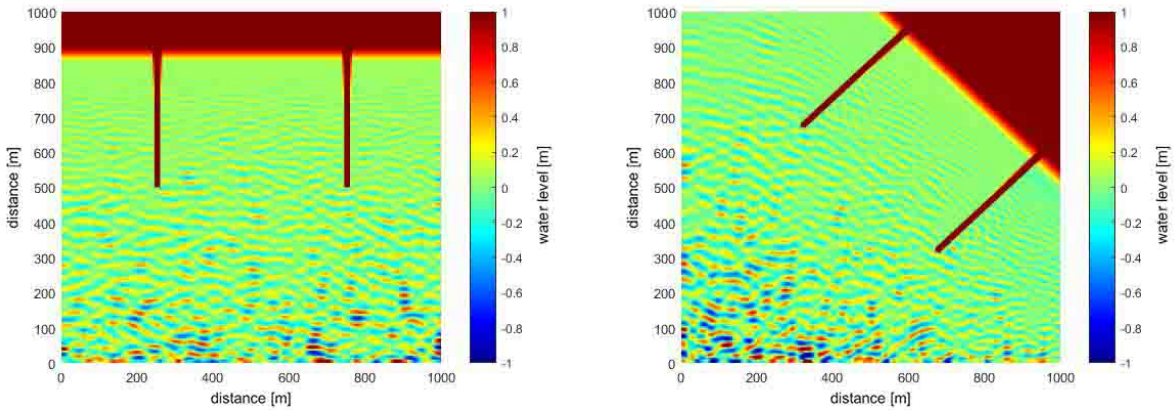

(a) Normal incident wind waves

(b) Wind waves with mean direction of 315 degrees North

Figure A.4: Snapshots of surface elevation for two directions of wind-sea waves

B

Sensitivity Simplified XBeach Models

In this chapter the sensitivity of the simplified XBeach model is discussed. The boundary effects are researched, the depth at the boundaries and the effect of grid sizes and the spreading parameter has been examined. With the results of these test more reliable conclusions can be drawn for the research with simplified pocket beaches. The non hydrostatic mode is the most sensitive mode and therefore this mode is used in these sensitivity analyses.

B.1. Boundary Effects

B.1.1. Size Area

First of all, the boundary effects are researched. To identify till where the boundary effects influence the area, a large area and a small area are compared. The large area is a grid of 500 by 500 cells and the smaller area is a grid of 200 by 200 cells. The size of the grid cells is 5 metres in all simulations. One case without and one case with groynes has been researched.

Plain Beach

Below the water level variations (figure B.1a) and velocities (figure B.1b) in the large area can be seen. In both figures it can be seen that boundary effects do play a role. In figure B.1a, the water level variations are less at the left and right boundary. Furthermore the decrease in water level variation is not the same over the whole beach length. In figure B.1b, at the boundaries higher velocities can be noticed.

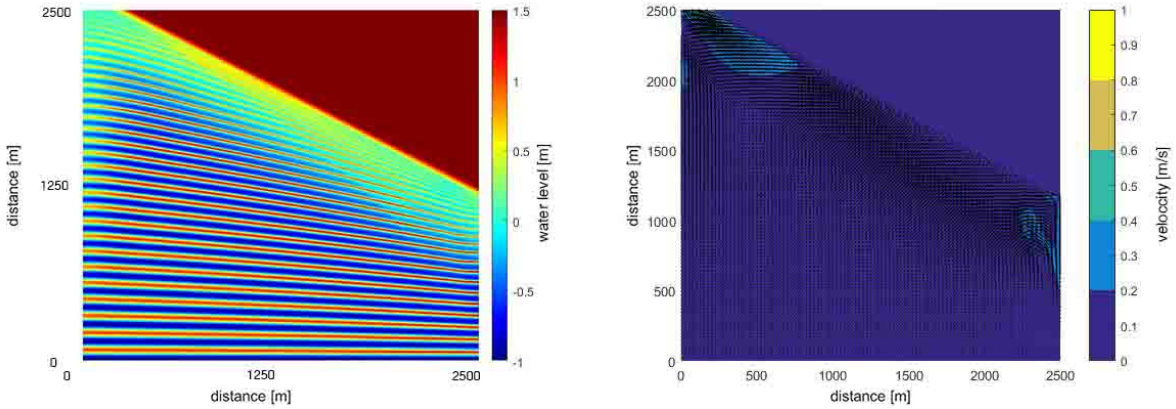

(a) Water level variations

(b) Velocities

Figure B.1: Water level variation and velocities on large grid (500x500 cells) with plain beach

More details in the area of interest can be seen when zooming in on an area similar to the smaller area simulated. In figure B.2 the zoomed in area of figure B.1 is shown. The lower water level variations at the side boundaries are not visible anymore however, the decrease in water level variation is not uniform along the beach. At the right boundary the length of decreased water level variations is larger compared to the middle and left. Furthermore, the higher velocities at the boundaries are not visible anymore. The velocity along the

beach is directed mainly towards the left and down. One should expect the velocity direction is to the left and up, alongshore. Due to the variations in the water level and the direction of the velocities it can be concluded that the boundary effects in this simulation affect the whole area, including the main area of interest.

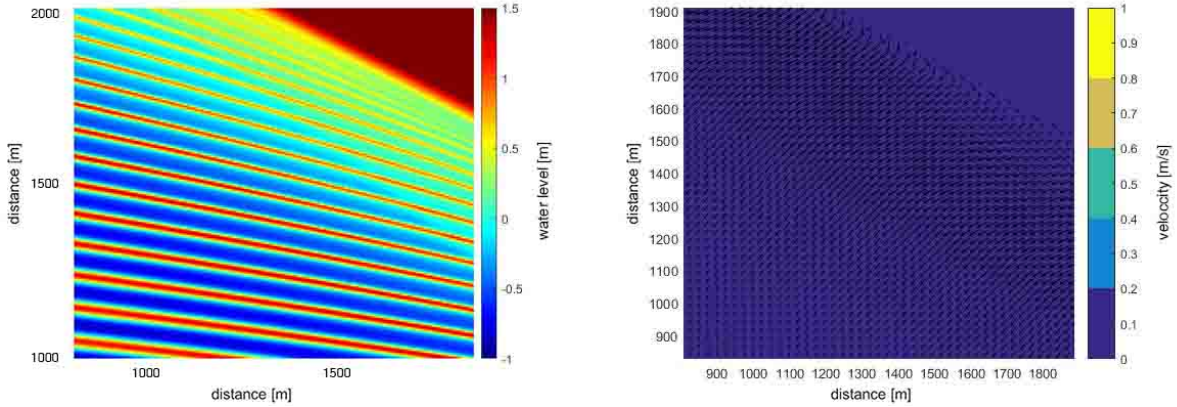

(a) Water level in section of large area (figure B.1a)

(b) Velocities in section of large area (figure B.1b)

Figure B.2: Sections of the large area (figure B.1) comparable to the small grid area with plain beach

To see if a smaller area could be used for the simulations of the plain beach also an area of 200 by 200 grid cells has been tested. The results can be seen in figure B.3. These can be compared with figure B.2 to see the differences caused by the boundary effects. In figure B.2a it can be seen that the waves are already bending due to the refraction process. Furthermore, the highest water levels close to the beach are higher in the large area (figure B.2a) than in the small area (figure B.3a). In the large area (figure B.1b) it could already be seen that the velocity at the boundaries was higher, this can be seen more clearly in the small area (figure B.3b). The direction of the velocity in the small area is towards the left. This is different than the direction in the large area. In the small area the upper boundary is not completely covered with beach, therefore the upward directed velocities are stronger than in the larger area. This could be of influence for the direction in other parts of the area.

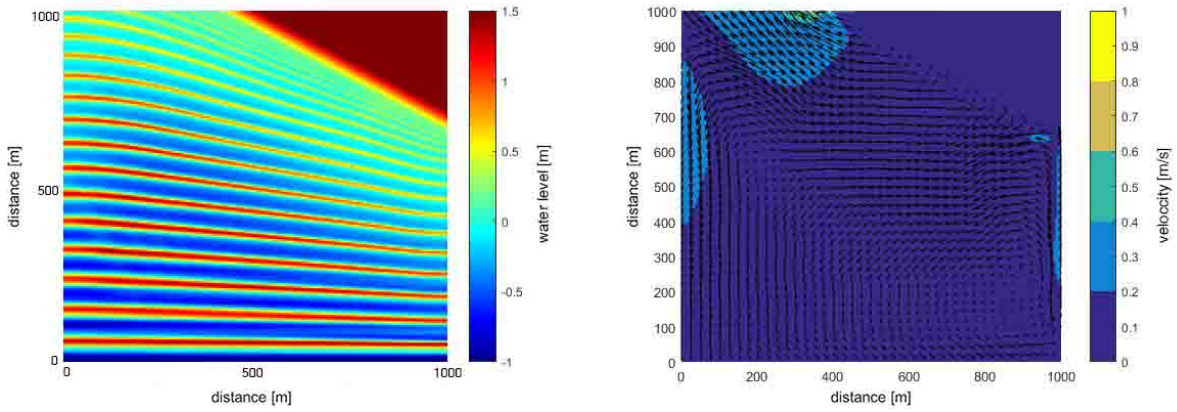

(a) Water level variations

(b) Velocities

Figure B.3: Water level variations and velocities on small grid (200x200 cells) with plain beach

From above analysis it can be concluded that in an undisturbed beach boundary effects have a lot of influence on the water level variations and the velocities. This effect is similar for a 200x200 cell layout and a 500x500 cell layout.

Pocket Beach

Since this research is about pocket beaches, it is especially important to know if the boundary effects influence the processes within a pocket beach. Therefore, the same analysis as above has been done for a beach with two groynes. In the large areas shown in figure B.4, similar phenomena can be seen as in figure B.1. With or without groynes the water level variations do look very similar on the large scale. Also, the higher velocities at the left and right boundary of the beach look very similar.

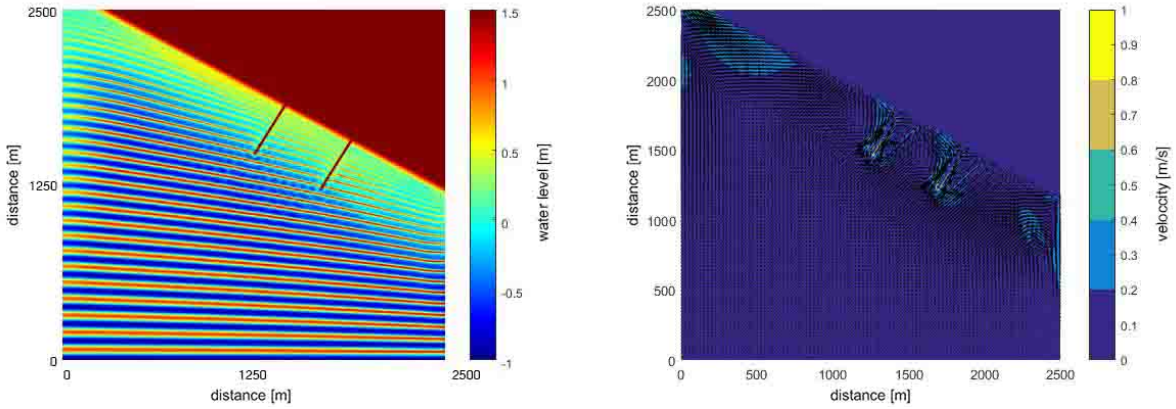

(a) Water level variations (b) Velocities

Figure B.4: Water level variation and velocities on large grid (500x500cells) with groynes

Do the boundary effects influence the water level variations and velocities within the pocket beach? This is the main question since, the pocket beach and the processes within the pocket are of main interest for this research. To be able to answer this question, a section of the large area is examined. Thereafter it is compared to the simulations of the smaller area. The middle sections out of the large area are shown in figure B.5. The water level variations and velocities of the simulations of the smaller area are shown respectively in figure B.6a and B.6b. Like in the plain beach comparison, the difference in refraction and the decrease in water level variation can be seen.

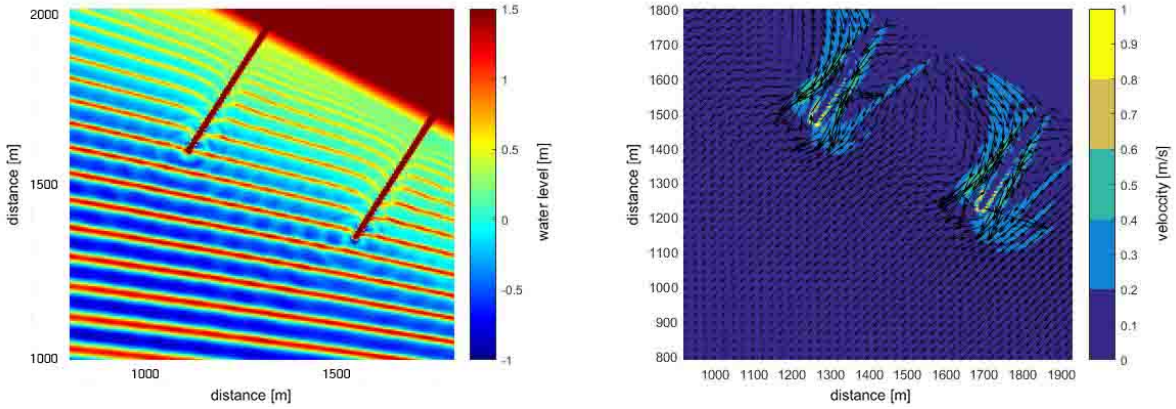

(a) Water level variations section of large area (figure B.1a) (b) Velocities section of large area (figure B.1b)

Figure B.5: Sections of the large area (figure B.4) comparable to the small grid area with pocket beach

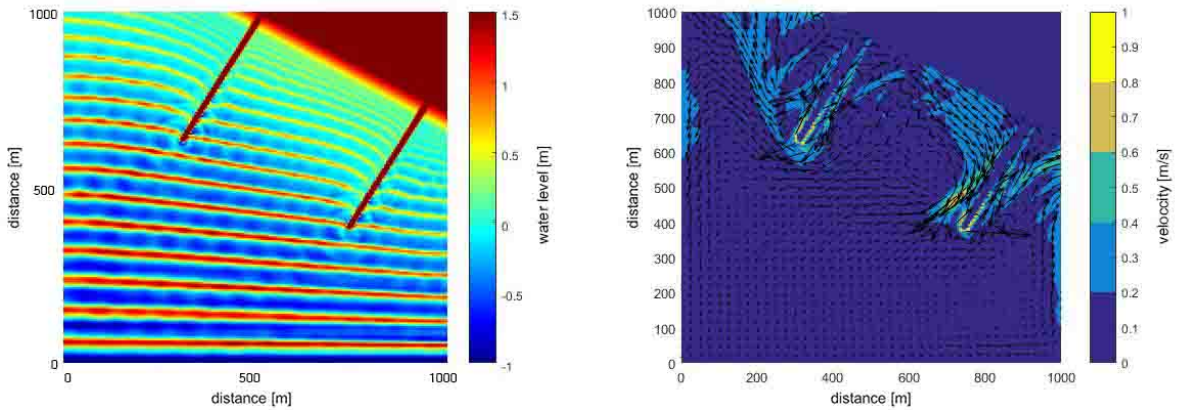

(a) Water level variations

(b) Velocities

Figure B.6: Water level variations and velocities in small area with pocket beach

The figures with the velocities show some interesting results. In figures B.5b and B.6b it can be seen that the velocity pattern in the lee side of both groynes look the same. Also velocity patterns at the other sides of the groynes are alike. In the simulation of the small pocket beach (figure B.6b), the velocity pattern inside of the pocket corresponds to the inside of the pocket in simulation of the large area (figure B.5b). It is not exactly the same but the main direction and most velocities are similar. In figure B.6b the patterns outside of the pocket beach are completely different than inside. This indicates boundary effects playing an important role outside the pocket beach. The large area should experience less boundary effects close to the pocket beach. Since, the velocity patterns within the pockets look similar on both simulations and the velocity pattern inside and outside the pocket in the large area are the same, it can be assumed that boundary effects do not play an important role within the pockets.

Conclusion
From the above simulations it can be concluded that boundary effects do not play an important role in case obstructions are located along the beach. In simulations where boundary effects are much more present (figure B.6) the velocity pattern within the pocket looks very similar to the beach where boundary effects are much less due to the larger distance to the boundary (figure B.5). Since, the groynes induce a lot of processes itself the boundary effects are blocked more and are not important for the velocity patterns within the pocket any more. In case the beach is undisturbed, so without groynes, the velocity patterns are influenced by the boundary effects to a greater extent. This makes the boundary effect on a plain beach more important in all cases than in case of a pocket beach. So, when interested in the processes within a pocket beach a simulation of a small area would be sufficient.

B.1.2. Uniform Depth at Offshore Boundary

XBeach is designed to work with uniform depth at the boundary condition. Due to the reflection at the boundaries when forcing the model with oblique incident waves it was necessary to rotate the grids. With rotated grids the waves do not reflect on the boundaries that much. However, this implies a non uniform depth at the offshore boundary, since the depth contours run parallel with the coastline. To research the effects of this non uniform depth compared to a uniform depth at the offshore boundary some simulations are done with oblique incident waves. The uniform depth at the offshore boundary is located at 5.7 metres below mean water level. The beach has a slope of 1:100 till a depth of 5.7 metres, which is the highest point on the offshore boundary. From this depth onwards the bottom is flat for the uniform depth cases and the bottom further decreases with a slope of 1:100 in the non uniform depth cases.

The oblique incident waves have been imposed on a coast with two perpendicular groynes. In figure B.7) a difference in refraction and decrease of water level variation can be seen. In case of a non uniform depth (figure B.7b) it can be seen that the water level variation offshore is larger and decreases later than in case of a uniform depth (figure B.7a). In figure B.7b the water depth is larger than in figure B.7a, this causes the higher water level variation. Furthermore, the depth contours are already under an angle to the incoming waves in

the situation a without uniform depth (figure B.7b). Therefore refraction is starting immediately in contrary to the case with uniform depth (figure B.7a), where the depth contour lines start at a depth of 5.7 metres.

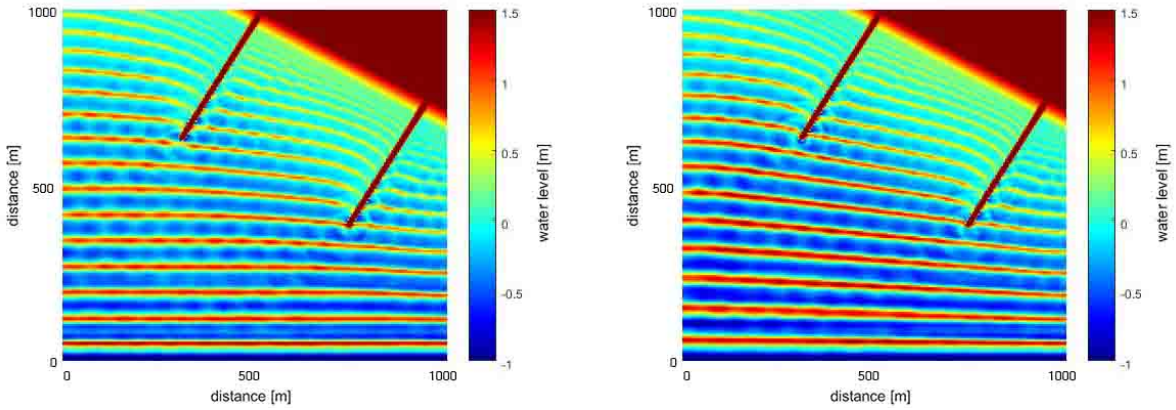

(a) Water level variations on uniform depth (z=5.7 m) at offshore boundary

(b) Water level variations on non uniform depth at offshore boundary

Figure B.7: Water level variations on a beach with a uniform offshore boundary (a) and a non uniform depth at offshore boundary (b)

Below the velocities in case of uniform offshore depth (figure B.8a) and non uniform offshore depth (figure B.8b) are shown. These velocity patterns are very alike. Some small differences in velocities can be seen. However, especially between the two groynes these differences are very small.

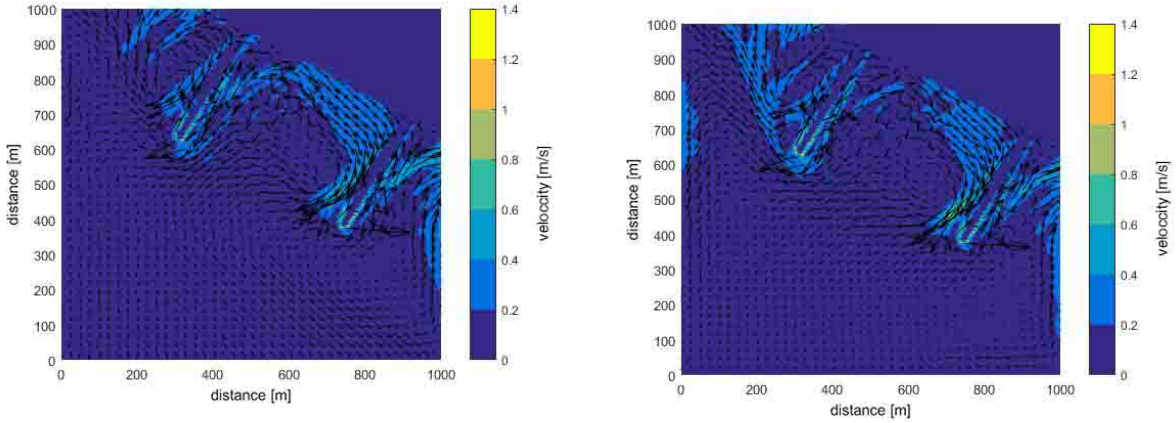

(a) Velocities on uniform depth (z = 5.7 m) at offshore boundary

(b) Velocities on non uniform depth at offshore boundary

Figure B.8: Velocities on a beach with a uniform offshore boundary (a) and a non uniform depth at offshore boundary (b)

Conclusion

From the above simulations it can be concluded that the depth itself has some effects on the water level variation and the amount and location of refraction is influenced by the different bathymetries. However, a consequence of the uniform or non uniform offshore boundary can not be found. Especially, due to the very similar velocity patterns it can be concluded it is not introducing a large error in the processes within the pocket, the area of interest.

B.2. Wave Dissipation

In the simulation of wind waves on a grid with cells of 5 metres a large amount of dissipation was found. No physical reason could be found for this dissipation of energy however, two reasons could be thought of in modelling this waves in XBeach. First, the numerical dispersion relation could be a problem since, too high values of kd could not be solved by XBeach. Second, the grid cell size could be too large. For every wave length XBeach needs a certain amount of points to calculate the the wave energy. So, too few points can cause energy dissipation. This will be tested below with a calculation and a simulation.

B.2.1. kd Value

To calculate the kd value, k and d are needed. k is the wave number and d is the depth. k can be calculated by equation B.1.

$$k = \frac{2\pi}{L} \tag{B.1}$$

So, first the wave length should be calculated. For shallow water waves, intermediate water waves and deep water waves de wave length is calculated by different formulations, which are based on the wave dispersion relation. The relative depth (depth over wave length) tells which type of wave it is. The ratios can be seen in table B.1.

Shallow water wave		d/L	<0.05
Intermediate water waves	0.05 <	d/L	<0.5
Deep water waves		d/L	>0.5

Table B.1: Water depth to wave length ratio

The equations to calculate the wave length can be found in equation B.2, B.3 and B.4. Equation B.2 for shallow water waves, equation B.3 for intermediate water waves and equation B.4 for deep water waves. For the wave length of intermediate water waves an iteration is needed.

$$L = \sqrt{gd} * T \tag{B.2}$$

$$L = \frac{gT^2}{2\pi} tanh(2\pi \frac{d}{L}) \tag{B.3}$$

$$L = \frac{gT^2}{2\pi} \tag{B.4}$$

The following parameters are used for the calculation.

- g = 9.81 m/s^2
- d = 8.55 m
- T = 5 s (used for the wind waves)

This results in a intermediate water wave with a wave length of 35.44 metres. The relative depth is about 0.24 and the wave number k is about 0.18. This results in a kd value of about 1.52.

XBeach is able to solve spectra up to kd values of 3. If the spectral peak has a kd value between 1 and 1.5 XBeach is able to solve this quite good since, most of the spectrum has values below 3. Energy is still present in the spectrum at three times the peak frequency. This means, if the peak values of the spectrum have a high kd value, a large part of the spectrum could not be solved. The kd value in this case is 1.5 which is on the maximum of the abilities of XBeach. Based on this, some of the dissipation of energy in the wind wave simulations could be explained. However, 1.5 should still be quite well so, the dissipation of energy can not be too large only due to this.

B.2.2. Grid Size

Another fact which could cause the dissipation of energy could be the grid cell size. XBeach needs a certain amount of points to calculate the energy in a wave in the non hydrostatic mode. Energy dissipation occurs when too few points are used for the calculation.

As can be seen above, the wave length for wind waves is 35.44 metres in this case. A cell size of 5 metres results in about seven cells per wave length so, seven points of information to calculate with. A cell size of 2.5 metres doubles the amount of points. In figure B.9 the results of the simulation can be seen. Left, in figure B.9a, the water level variation can be seen in case a grid with a cell size of 5 metres is used. In figure B.9b, on the right, the water level variation is shown for a cell size of 2.5 metres. Clearly, less energy dissipation can be seen in figure B.9b.

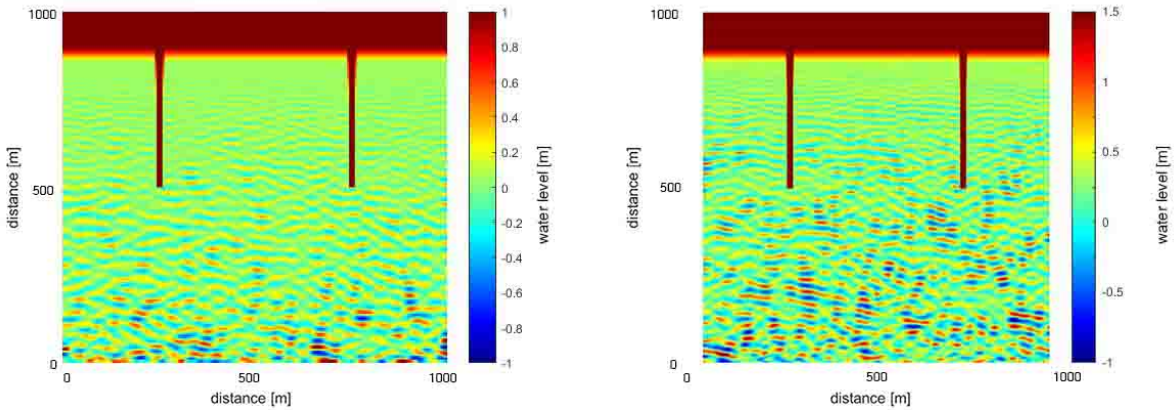

(a) Wind waves on grid with cell size of 5 metres

(b) Wind waves on grid with cell size of 2.5 metres

Figure B.9: Wind waves on gird with different grid cell sizes

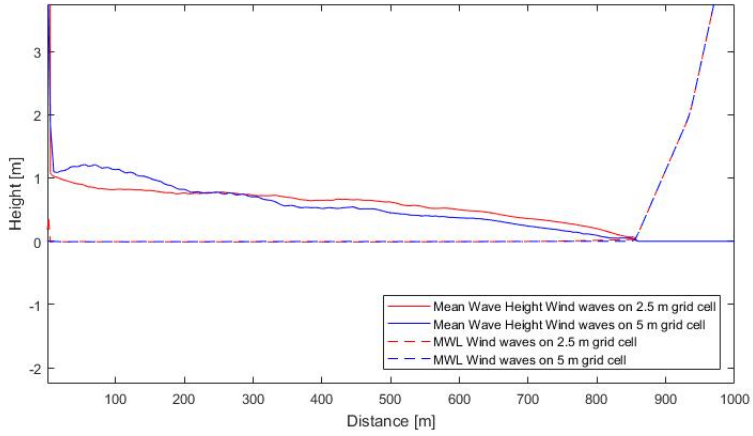

Figure B.10: Cross shore profile of the mean wind wave heights with the two grid cell sizes

The swell waves or monochromatic waves have a wave length of about 86.31 metres, which means about 17 cells with a cell size of 5 metres. So, less energy dissipation can be expected than with wind waves. However, still energy dissipation is occurring. Which can be seen clearly with a simulation of the monochromatic waves on two different grids. In figure B.11 the results of a difference between a cell size of 5 metres (figure B.11a) and a cell size of 2.5 metres (figure B.11b) can be seen. The water level variation decreases less with a smaller grid size. Furthermore, a more clear reflection pattern can be seen. So, from the results of the monochromatic waves, it follows that the wind waves need an smaller grid cell size to improve the results and prevent wave dissipation. The dissipation in the monochromatic waves looks to be brought back to a minimum with cell

sizes of 2.5 metres, which means 34 point per wave length. If the same amount of points would be taken for the wind waves, this means a cell size of 1 metres would be needed to give almost no dissipation any more.

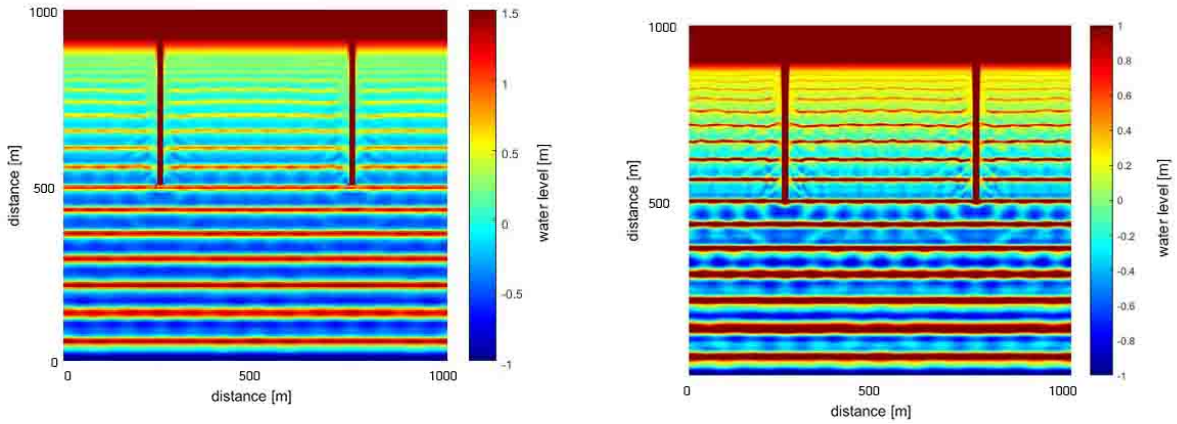

(a) Monochromatic waves on grid with cell size of 5 metres

(b) Monochromatic waves on grid with cell of 2.5 metres

Figure B.11: Wind waves on grid with different grid cell sizes

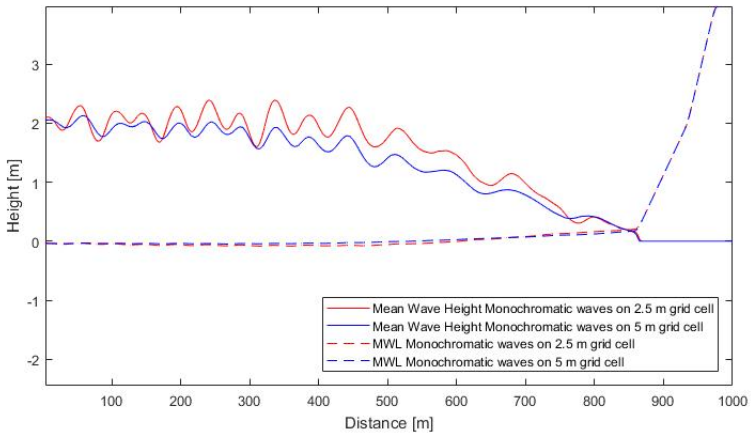

Figure B.12: Cross-shore profile of the mean monochromatic wave heights with the two grid cell sizes

B.3. Spreading Parameter Determination

To be able to compare the results of the monochromatic waves with the results of the waves from a spectrum it is important most characteristics of the waves are the same. Therefore, the wave height at the offshore boundary should be similar in both cases. Furthermore, the spreading should not be too much, since it should look like the monochromatic waves, who have no spreading at all. The results with various values of s, the spreading parameter, can be seen in figure B.13. It shows that the results of s = 800 are closest to a H_{rms} of 2 metres at the offshore boundary, which is used in the monochromatic wave simulations. Therefore, this value is chosen for the spectra to use in in the simulations for long wave research.

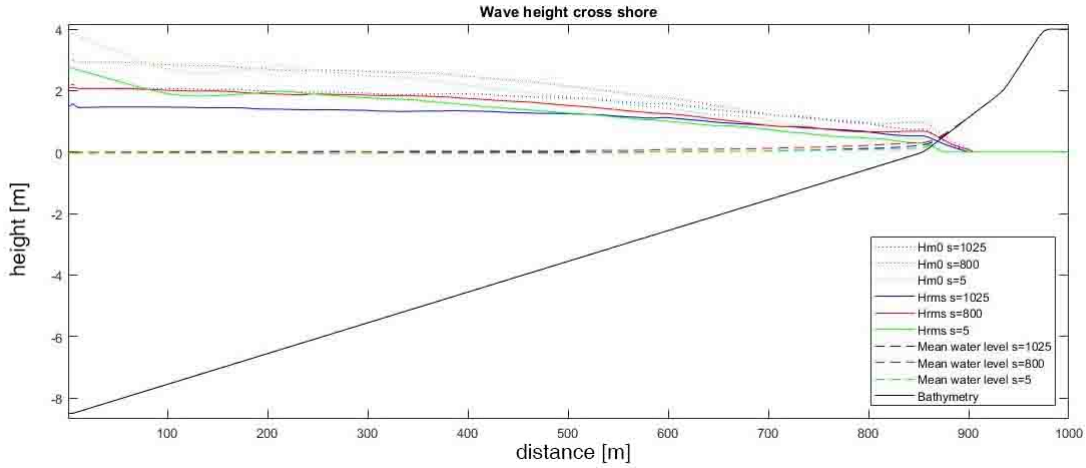

Figure B.13: Wave heights with different values of s

C

Simplified Plain Beaches

C.1. Short Wave Diffraction

A plain beach has been investigated since, the processes on the plain beach show the differences between the two ways of modelling. The non hydrostatic mode and the stationary mode of XBeach have been compared to be able to say if differences are caused by the way of calculating of the model or by the processes that are included or not.

To show the differences of wave breaking without any other differences a start has been made with a plain beach with normal incident waves. The water level variations and wave height are shown in figure C.1. A cross shore profile is shown in figure C.2 to be able to see more clear the wave height development. The non hydrostatic mode does not calculate the wave height therefore, the water level variance is used to calculate the wave height.

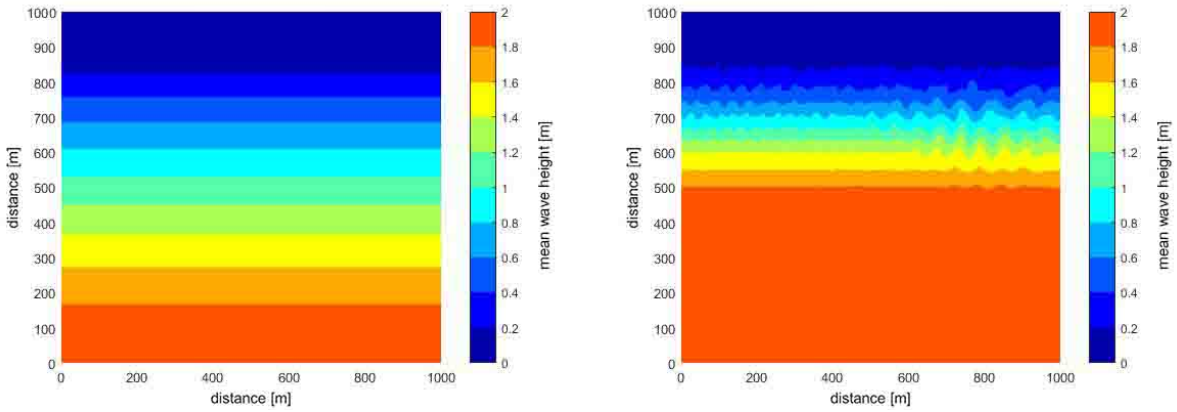

(a) Monochromatic normal incident waves in stationary mode

(b) Monochromatic normal incident waves in non hydrostatic mode

Figure C.1: Normal incident monochromatic waves in different modes of XBeach

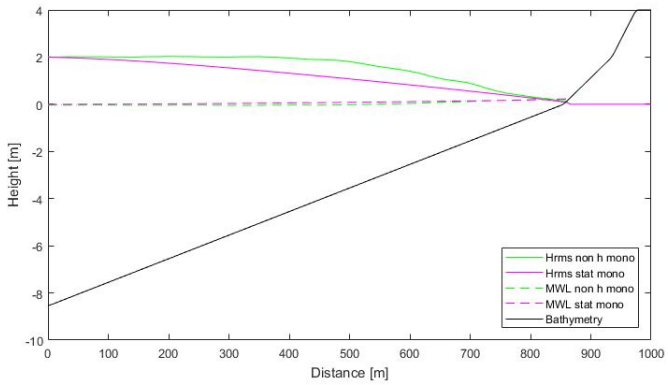

Figure C.2: Cross shore profile with wave heights in middle of the beach in case of monochromatic normal incident waves

In the above figures (C.1 and C.2) it can be seen that the wave height in the stationary mode decreases earlier than the wave height in the non hydrostatic mode. Wave breaking in the stationary mode is based on breaker formulations and a breaker index is used (Bemmelen, 2017). In the non hydrostatic mode wave breaking models are not needed due to application of momentum conservative numerical schemes (Smit et al., 2010).

Below the mean velocities (over 5 minutes) of the simulations of normal incident waves on a plain beach are shown in figure C.3. The arrows show the mean direction of the velocities and the speed can be seen with the colours, which give the speed in metres per second. The velocity patterns are very similar. The velocities of the non hydrostatic mode simulations are a little bit higher however, the difference is minimal. In the stationary mode all velocities are less than 0.1 m/s, in the non hydrostatic mode velocities of a little bit more than 0.1 m/s occur.

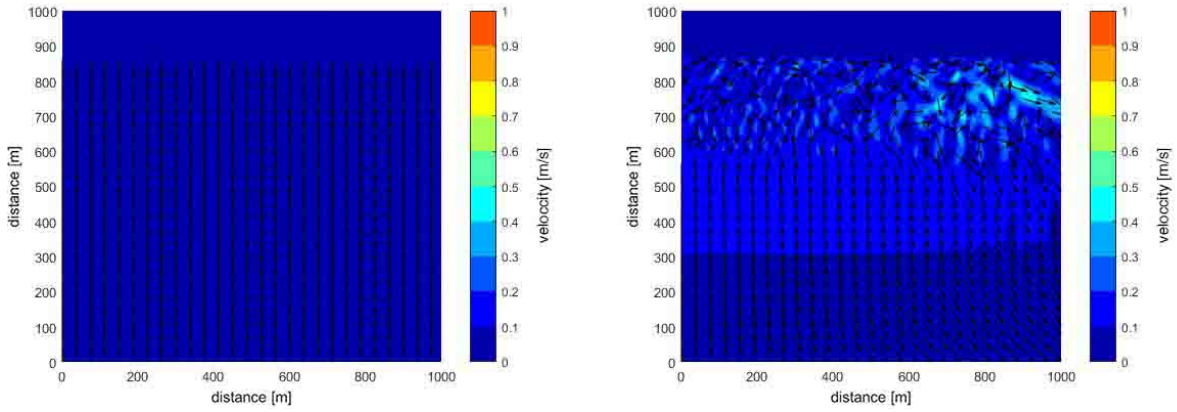

(a) Velocities on plain beach in case of normal incident waves in stationary mode

(b) Velocities on plain beach in case of normal incident waves in non hydrostatic mode

Figure C.3: Velocities on plain beach in case of normal incident waves in various modes of XBeach

After the above simulation the variation in wave breaking is known. To see the differences of wave breaking and refraction together a plain beach with obliquely incident waves is simulated. The waves make an angle of 30 degrees to normal incident waves on the coast.

In figure C.4 and C.5 results of the two model modes are shown. In figure C.4b the mean wave height of the non hydrostatic model is shown and in figure C.4a the wave height of the stationary model is shown. It can be seen that in both models the waves on the left side are higher than on the right side due the difference in water depth on the left and the right side. This variation is especially visible at some distance from the coast. Furthermore, the wave heights are quite similar on the different locations however, just like with normal incident waves, the wave height in the non hydrostatic mode is a little bit higher than the wave height in the

stationary mode. Besides, figure C.5b shows an interesting result at the left side, the wave height of the non hydrostatic mode shows some variations, probably the result of a boundary effect.

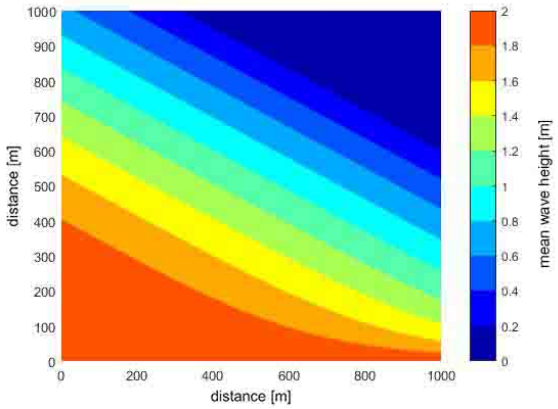

(a) Monochromatic obliquely incident waves in stationary mode

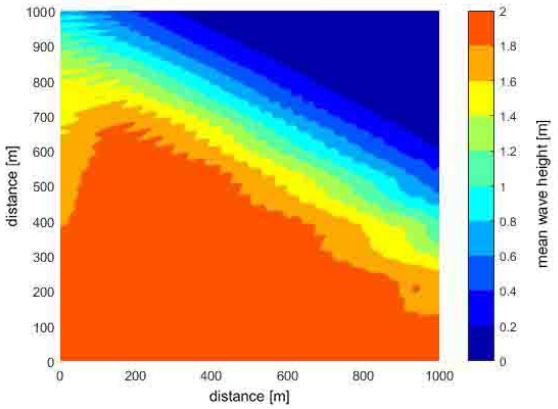

(b) Monochromatic obliquely incident waves in non hydrostatic mode

Figure C.4: Oblique incident monochromatic waves in various XBeach modes

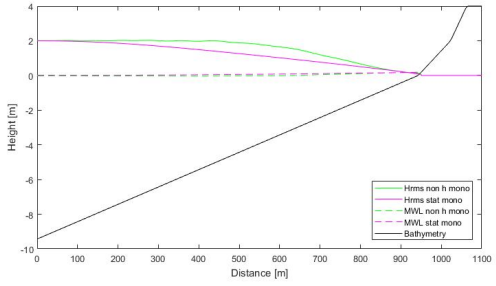

(a) Cross shore profile of wave height in middle of the beach

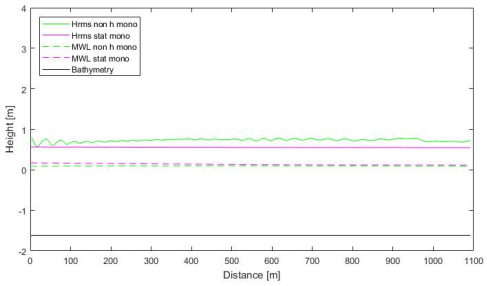

(b) Alongshore profile of wave height

Figure C.5: Cross and along shore profiles of the wave height in case of monochoromatic oblique incident waves on a plain beach

In figure C.6 the mean velocities over 5 minutes of the model run are plotted. With oblique incident waves on the coast it is expected the direction of the velocity is from right to left along the coast. This can be seen in both results. The main direction along the coast is similar however, in the non hydrostatic mode the direction is more horizontal very close to the shoreline. Furthermore, the speed at several locations, shown by the colors differ from one mode to the other. In the stationary mode the velocities close to the beach and at the offshore boundary are larger than in the non hydrostatic mode. The range of velocities is similar in both modes. Boundary effects could play a role in these variations.

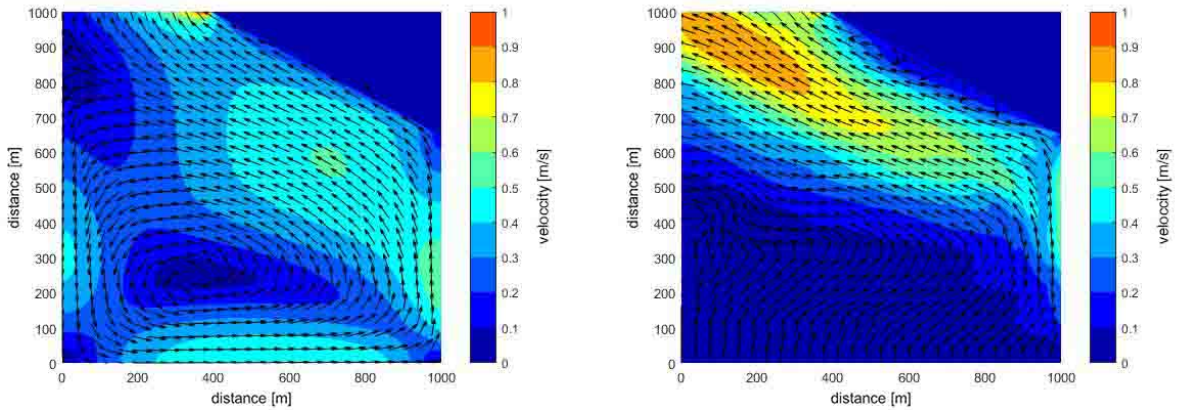

(a) Velocities on plain beach in stationary mode with monochromatic oblique incident waves

(b) Velocities on plain beach in non hydrostatic mode with monochromatic oblique incident waves

Figure C.6: Velocities on plain beach with monochromatic oblique incident waves

Below the initial sediment transport of the plain beach with normal incident waves (figure C.7) and oblique incident waves (figure C.8) can be seen simulated in the non hydrostatic mode and in the stationary mode. The plain beach with normal incident waves shows almost no sediment transport, the magnitudes are very low. In the case with oblique incident waves, the main direction of the sediment transport is more or less the same in bothe modes. However, the magnitudes of the sediment transport variate. Close to the shoreline the magnitudes are in both cases minimal. A bit further away from the shoreline and at the right boundary the non hydrostatic mode shows higher values. The result of the stationary mode shows high values at the offshore boundary. The patterns are in both cases similar to the circulation patterns.

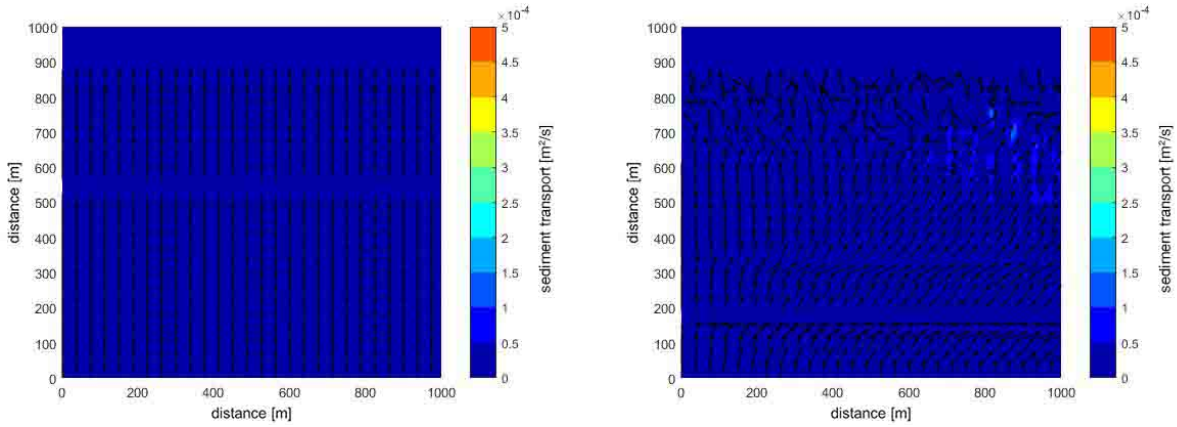

(a) Initial sediment transport in stationary mode

(b) Initial sediment transport in non hydrostatic mode

Figure C.7: Initial sediment transport under normal incident waves

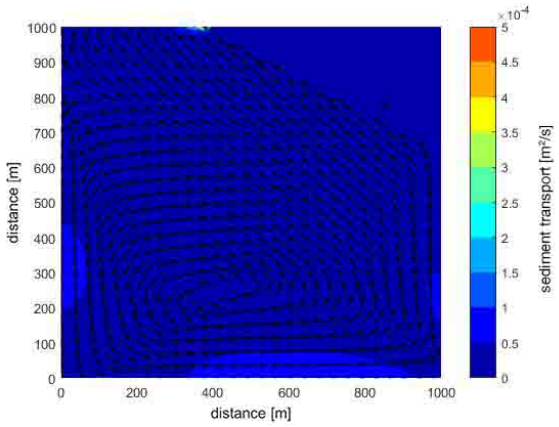

(a) Initial sediment transport in stationary mode

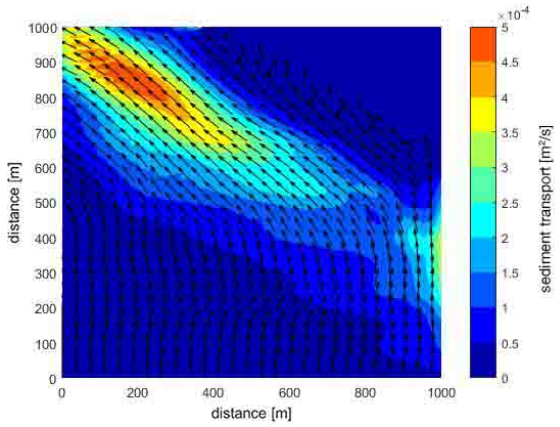

(b) Initial sediment transport in non hydrostatic mode

Figure C.8: Initial sediment transport under oblique incident waves

C.2. Long Waves

In this section the plain beaches of the stationary and the surfbeat mode are compared. The stationary mode is imposed with monochromatic waves and the surfbeat mode is imposed with a wave spectrum. With this difference the effect of long waves can be examined. In figure C.9 the top view of the mean wave height in the stationary mode (figure C.9a) and surfbeat mode (figure C.9b) are shown. In figure C.10 a cross shore profile of these mean wave heights can be seen. The wave height in the stationary mode decreases earlier than the wave height in the surfbeat mode. At a distance of x=150 m the wave height in the stationary mode decreases whereas the wave height in the surfbeat mode stays a a level of 2 metres till x=500 metres and decreases from there. At the coastline it attracts attention that the wave height and mean water level of the surfbeat mode are higher than those of the stationary mode.

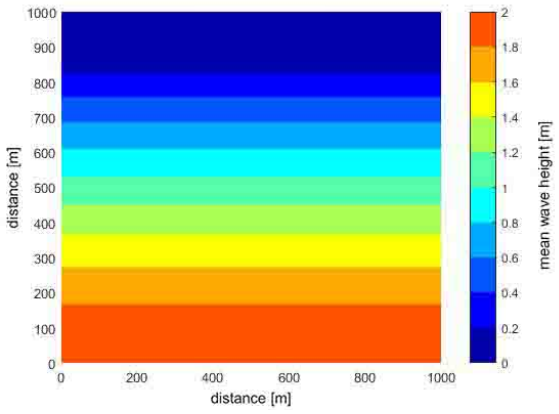

(a) Monochromatic normal incident waves in stationary mode

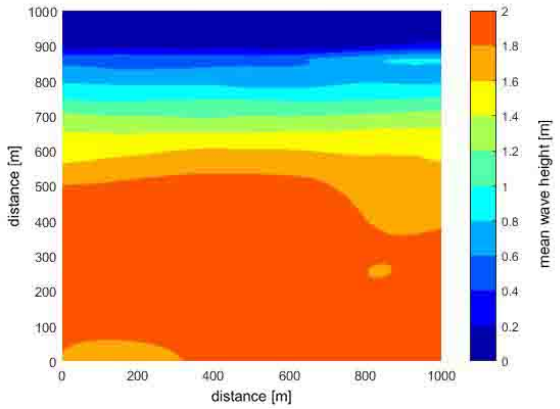

(b) Normal incident waves of spectrum in surfbeat mode

Figure C.9: Normal incident waves in different modes of XBeach

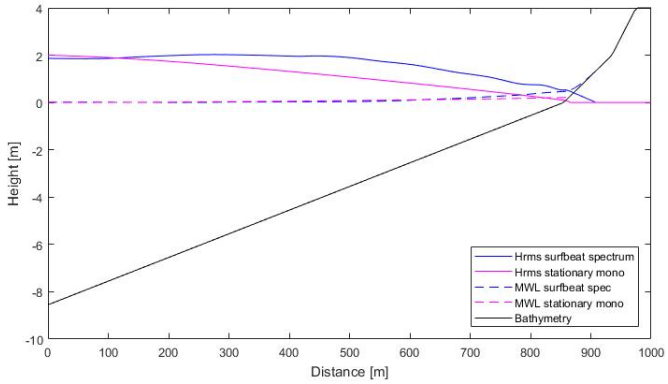

Figure C.10: Cross shore profile with wave heights in middle of the beach in stationary and surfbeat mode

In figure C.11 the top views of the cases with oblique incident waves are shown. Below, in figure C.12 the cross and alongshore profiles are shown. These figures show similar results as the case with normal incident waves. The differences in moments of decreasing wave height are the same and also the higher wave height and mean water level are higher in the surfbeat mode in this case.

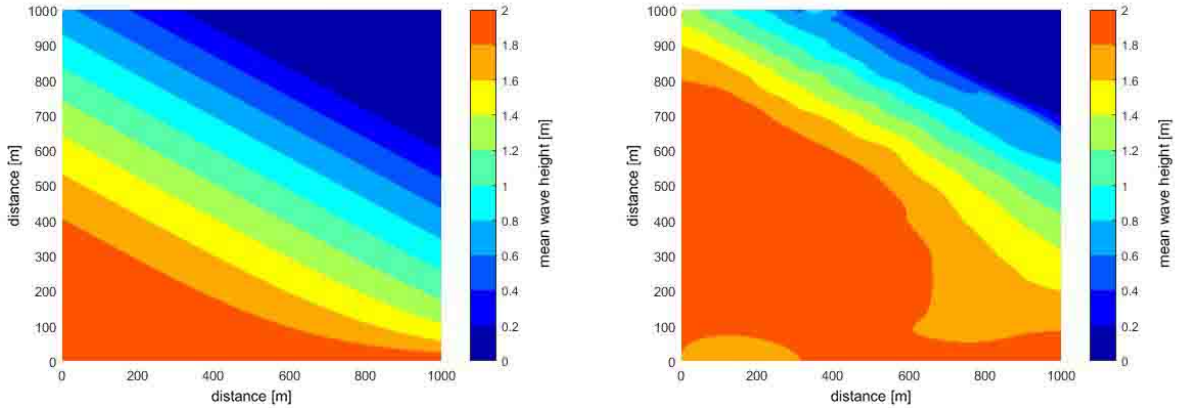

(a) Monochromatic obliquely incident waves in stationary mode

(b) Obliquely incident waves of spectrum in surfbeat mode

Figure C.11: Oblique incident waves in various XBeach modes

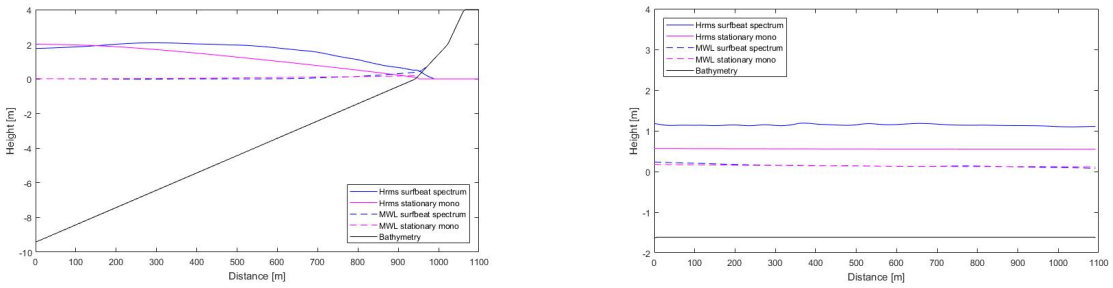

(a) Cross shore profile of mean wave height

(b) Alongshore profile of mean wave height

Figure C.12: Cross and along shore profiles of the mean wave height in case of oblique incident waves in stationary and surfbeat mode

The velocity results are shown in figures C.13 and C.15 for the normal and the oblique incident waves respectively. In figure C.13 it can be seen that the velocities in both modes are very similar. Only a band of higher velocities is visible along the coastline of the surfbeat mode. This is very clear visible in figure C.14.

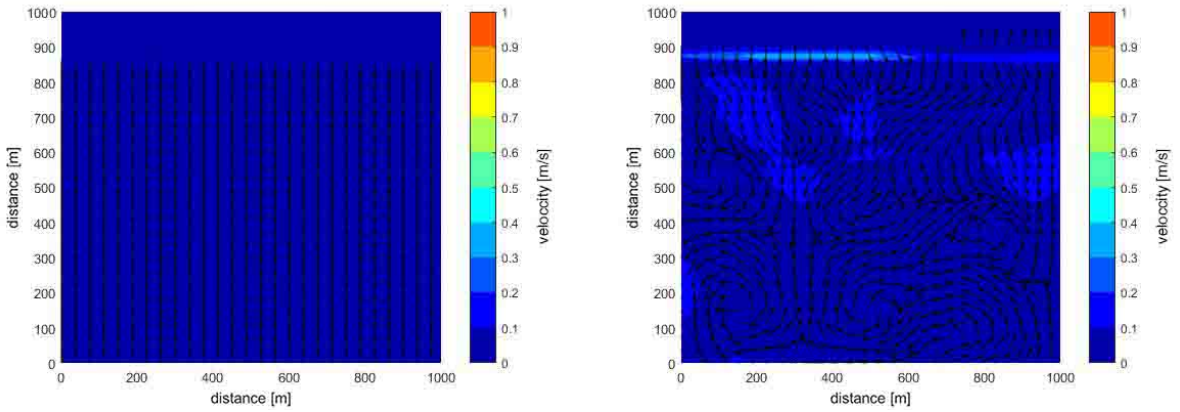

(a) Velocities on plain beach in case of normal incident waves in stationary mode

(b) Velocities on plain beach in case of normal incident waves in surfbeat

Figure C.13: Velocities on plain beach in case of normal incident waves in various modes of XBeach

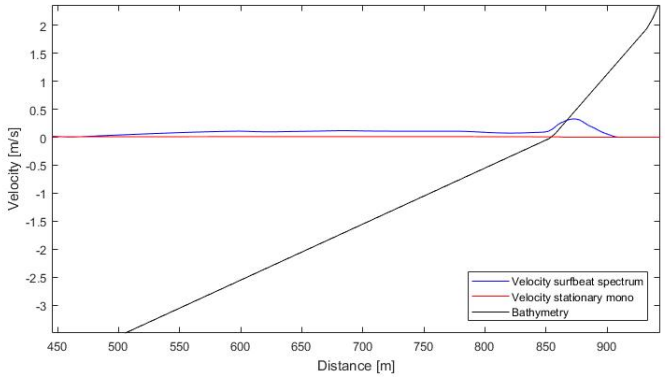

Figure C.14: Cross shore profile of the velocities in the stationary and surfbeat mode

The velocities in the oblique incident waves show more variation than the cases with normal incident waves. The directions are similar and in the expected alongshore direction however the magnitudes are much higher in the surfbeat mode. Since, some very high velocities are found at the boundaries of the model it is likely these boundary effects influence these velocity results along the coast. That these boundary effects play a role on plain beaches has already been described in appendix B.1.

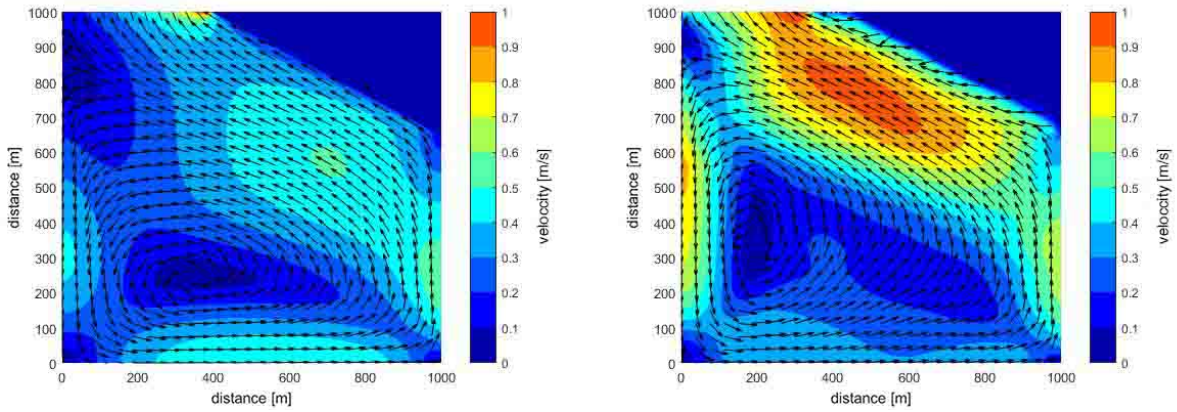

(a) Velocities on plain beach in stationary mode with monochromatic oblique incident waves

(b) Velocities on plain beach in surfbeat mode with oblique incident waves

Figure C.15: Velocities on plain beach with oblique incident waves

The sediment transport of the normal incident waves is very low in case the stationary mode is used (figure C.16a). Somewhat higher values can be found in case the surfbeat mode is used. The mean difference can be seen at and beyond the coastline (the red band in figure C.16b). In figure C.17 a cross shore profile at the shoreline is shown to see the differences in sediment transport. It can be seen that the amount of sediment transport in the surfbeat mode is slightly higher however, behind the shoreline the sediment transport increases in the surfbeat mode.

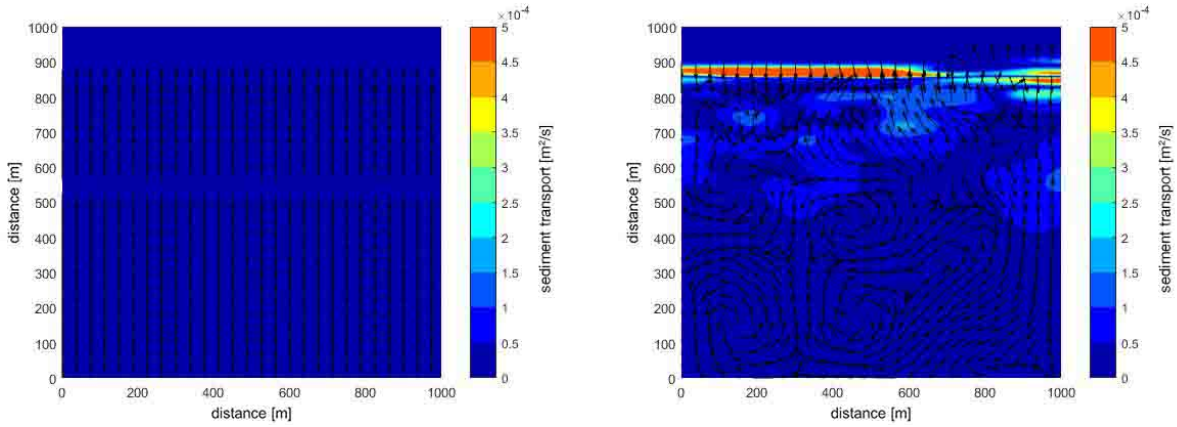

(a) Initial sediment transport in stationary mode

(b) Initial sediment transport in surfbeat

Figure C.16: Initial sediment transport under normal incident waves

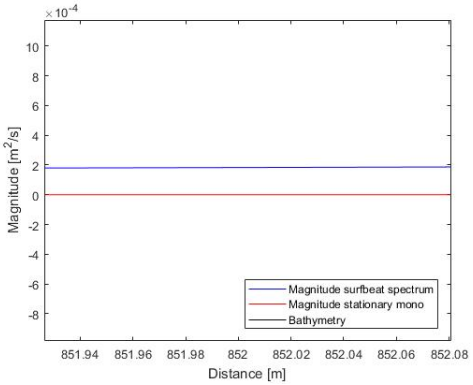

Figure C.17: Cross shore profile of the magnitudes of sediment transport in the stationary and surfbeat mode

In the case with oblique incident waves (figure C.18) magnitudes of sediment transport of the stationary mode are again quite low. Especially, when compared to the results of the surfbeat mode. This can be explained by the velocities in the surfbeat mode, which were also high and the influence of boundary effects.

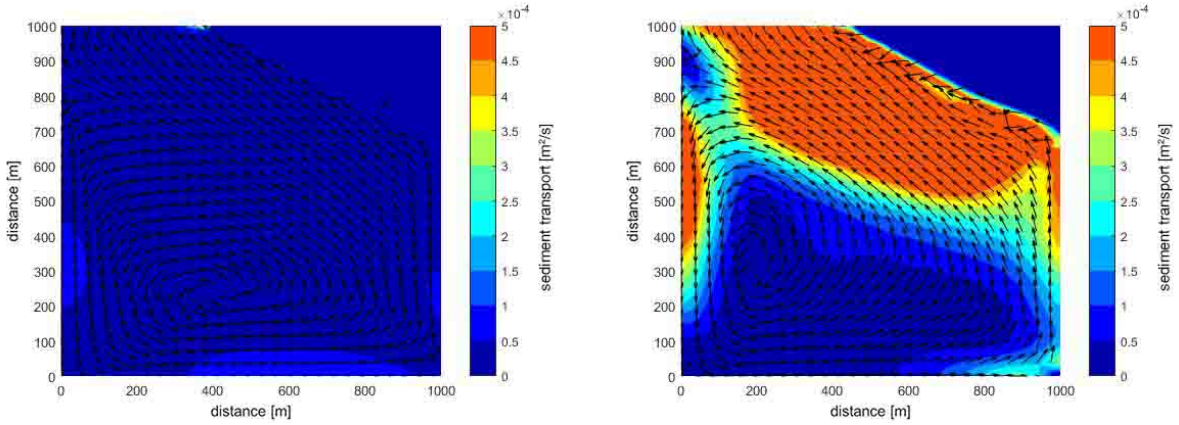

(a) Initial sediment transport in stationary mode

(b) Initial sediment transport in surfbeat mode

Figure C.18: Initial sediment transport under oblique incident waves

C.3. Short Wave Diffraction including Long Waves

In this section the same kind of figures are shown as in sections C.1 but in these cases a wave spectrum has been imposed instead of monochromatic waves. Rather than the stationary mode, now the surfbeat mode has been used next to the non hydrostatic mode. First a plain beach with normal incident waves is shown and thereafter a plain beach with oblique incident waves. Figure C.19 shows the mean wave height. In the surfbeat mode the water level variation contains the long waves and the short waves are simulated separately, like in the stationary mode. In figure C.20 the cross and alongshore profile of the wave heights based on the variance of the water level are shown. In these wave heights the long and short waves are included. The wave height is almost the same till a cross shore distance of 550 metres. Thereafter, both wave heights decrease towards the shoreline but the wave height in the non hydrostatic mode decreases faster. In figure C.20b a difference of about 25 centimeters can be seen at a distance of 700 metres in cross shore direction. At the shoreline and just before, the mean water level of the surfbeat simulation is a bit higher than the mean water level of the non hydrostatic simulation.

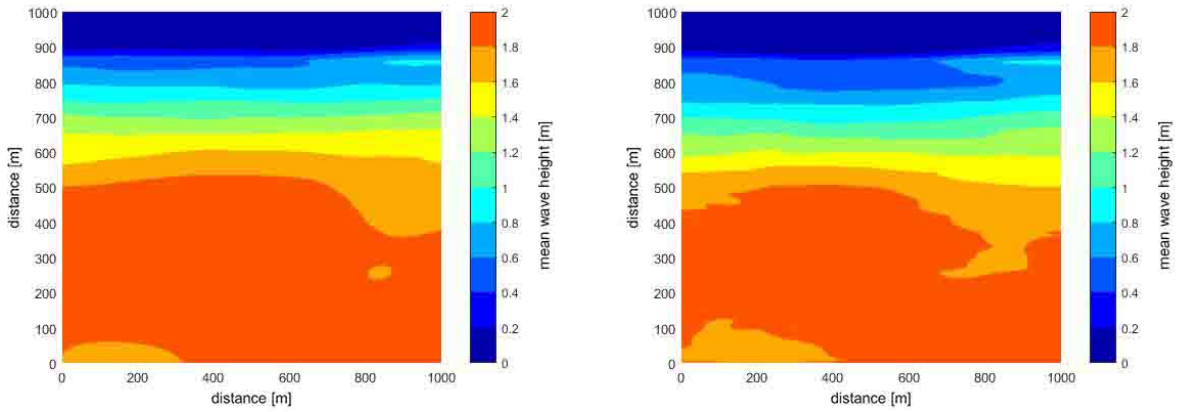

(a) Water level variations in surfbeat mode (b) Water level variations in non hydrostatic mode

Figure C.19: Water level variations under normal incident waves

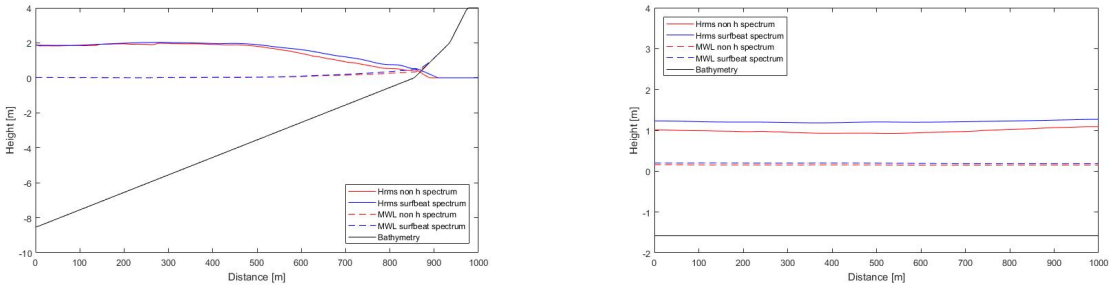

(a) Cross shore profile (b) Alongshore profile

Figure C.20: Cross and along shore profiles of long waves normal incident on beach

In figure C.21 the mean wave height in case of oblique incident waves can be seen. Due to the variation depth from left to right the wave height varies from left to right. In the deeper part the waves are longer high than in the shallower part. The surfbeat and non hydrostatic results look very similar.

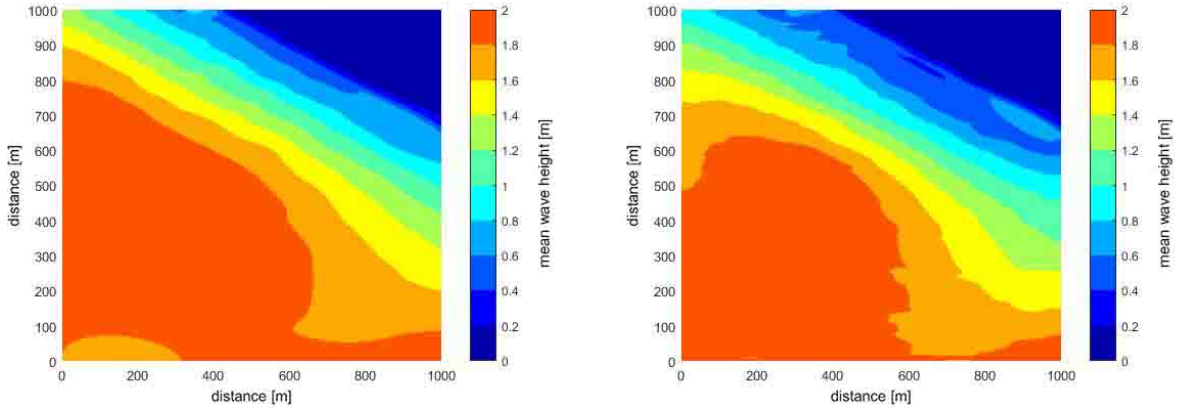

(a) Mean wave height in surfbeat mode (b) Mean wave height in non hydrostatic mode

Figure C.21: Mean wave height under oblique incident waves

The velocities are shown in figures C.22 and C.23. In the cases with normal incident waves the non hydrostatic mode shows a bit higher velocities while in the cases with oblique incident waves the surfbeat mode shows higher velocities. Furthermore, in both situations the velocities at the coastline are relatively larger in the

surfbeat mode. This is probably caused by the higher set up and wave height which could be seen in figure C.20a.

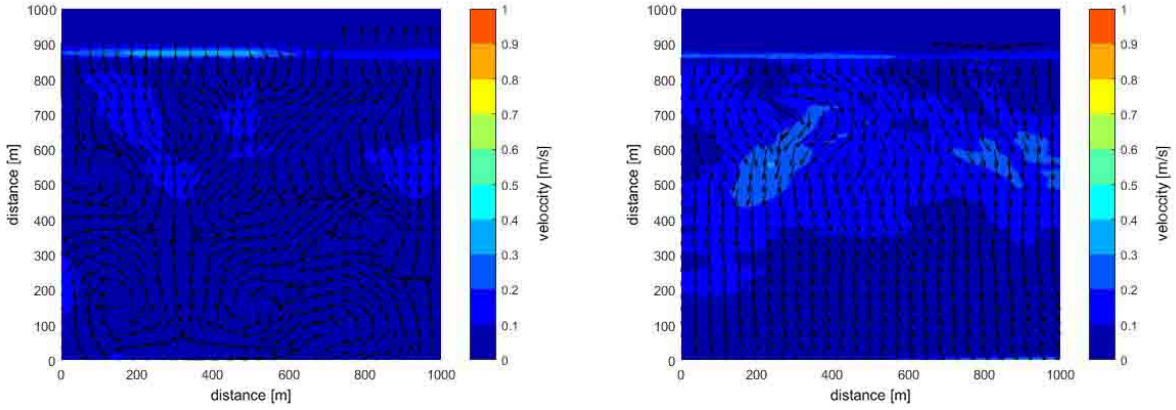

(a) Mean velocities in surfbeat mode

(b) Mean velocities in non hydrostatic mode

Figure C.22: Mean velocities under normal incident waves

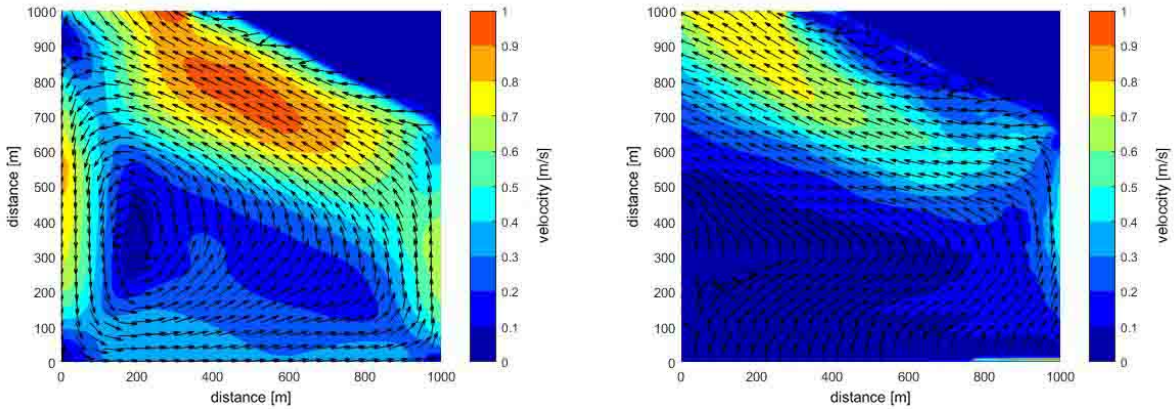

(a) Velocities in surfbeat mode

(b) Velocities in non hydrostatic mode

Figure C.23: Velocities under oblique incident waves

In figure C.24 the sediment transport magnitudes in case of normal incident waves in the surfbeat and non hydrostatic mode are shown. These figures are very similar. Both show closer to the coast some more sediment transport and the highest values are found close to the shoreline. The magnitudes along the shoreline are relatively higher in the surfbeat mode.

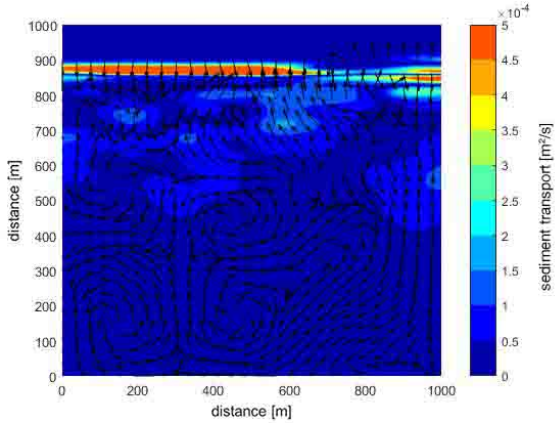

(a) Initial sediment transport in surfbeat mode

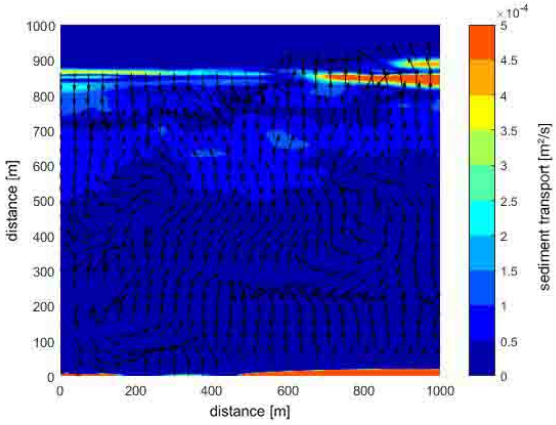

(b) Initial sediment transport in non hydrostatic mode

Figure C.24: Initial sediment transport under normal incident waves

The sediment transport patterns in case of oblique indicent waves show the same direction however, the magnitudes in the surfbeat simulation are higher than in the non hydrostatic simulation. Which is similar to the findings of the velocity results.

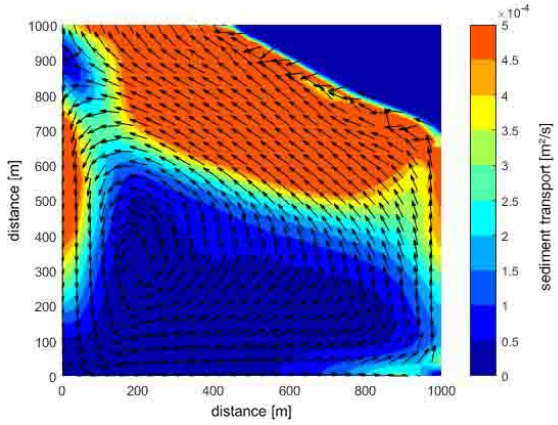

(a) Initial sediment transport in surfbeat mode (different scale)

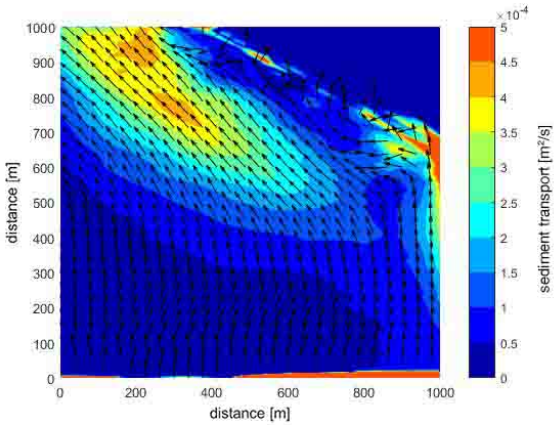

(b) Initial sediment transport in non hydrostatic mode

Figure C.25: Initial sediment transport under oblique incident waves

D

Wave Height Ratio

Diffraction diagrams in literature indicate the ratio of the local wave height to the incoming wave height. These diagrams are created for constant deep water depths. The ratio of local wave height to incoming wave height can be seen in the figures below. Due to the increasing depth the diagrams are hard to recognize, however, within the non hydrostatic mode diffraction patterns can be seen especially in the offshore parts of the shadow zones. Closer to the shore other processes become dominant such as wave breaking.

D.1. Simplified Pocket Beach

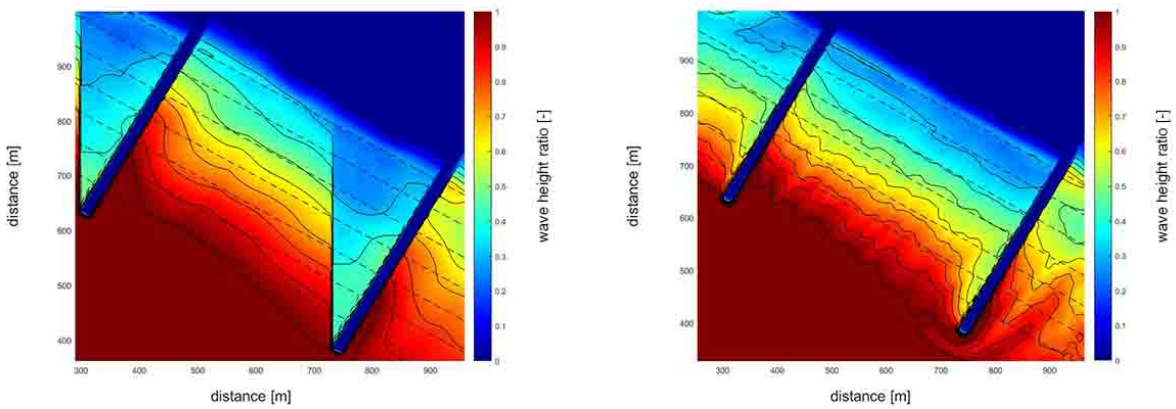

(a) Ratio of local wave height to the incoming wave height in the surfbeat mode

(b) Ratio of local wave height to the incoming wave height in the non hydrostatic mode

Figure D.1: Ratio of local wave height to the incoming wave height for the simplified pocket beach. Simulated in the surfbeat and non hydrostatic mode, both imposed with a wave spectrum

D.2. Case Study Constanta

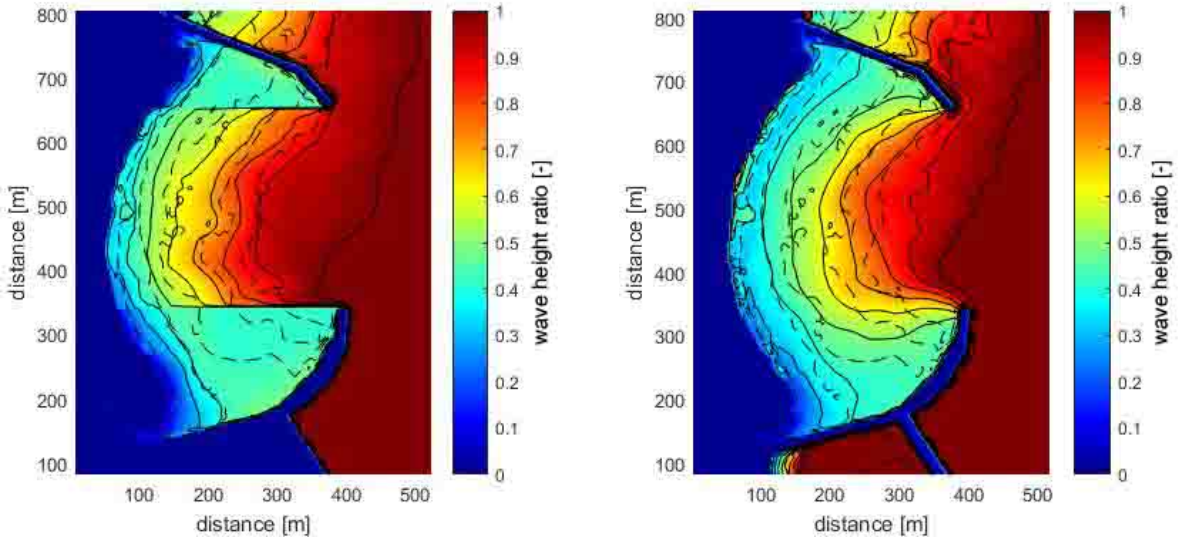

(a) Ratio of local wave height to the incoming wave height in the surfbeat mode

(b) Ratio of local wave height to the incoming wave height in the non hydrostatic mode

Figure D.2: Ratio of local wave height to the incoming wave height for the case study beach (Tomis South). Simulated in the surfbeat and non hydrostatic mode, both imposed with a wave spectrum

E

Sediment Transport Factor

The sediment transport formulations in the non hydrostatic mode of XBeach is not completely correct and not validated extinsively. To be able to compare the surfbeat mode and the non hydrostatic mode concerning sediment transport and morphologoly as much as possible a factor has been determined. Based on the the initial sediment transport caused by normal incident waves on a pocket beach in the two modes of XBeach a factor has been calculated from the mean initial sediment tranport in comparable areas. In figure E.1 the pocket beach with initial sediment transport in two modes can be seen. The pink square shows the compared area. In figure E.2 this compared are is shown in more detail. The mean of al the data points in these areas is compared and gives a factor of about 1.5. This means the sediment transport in the non hydrostatic mode should be multiplied with this factor to get comparable results as far as this is possible.

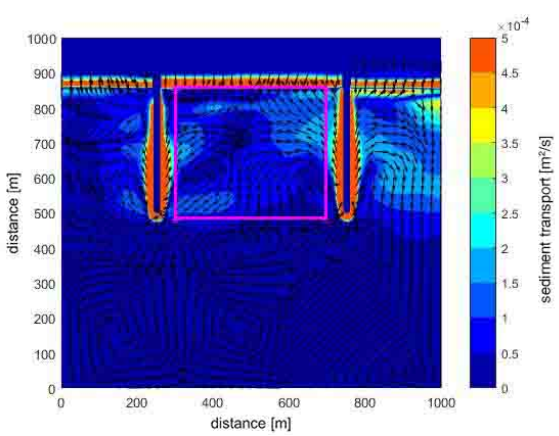

(a) Initial sediment transport in the surfbeat mode

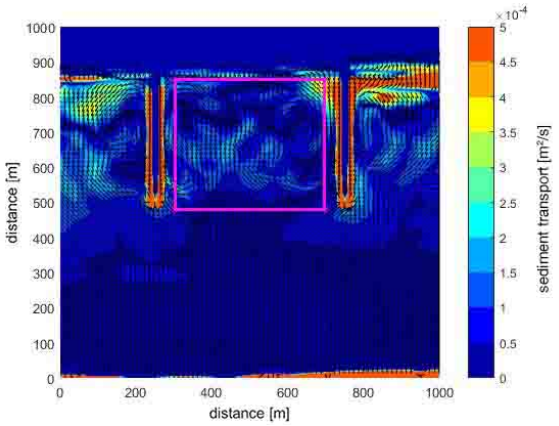

(b) Initial sediment transport in the non hydrostatic mode

Figure E.1: Area for sediment transport comparison (pink lines)

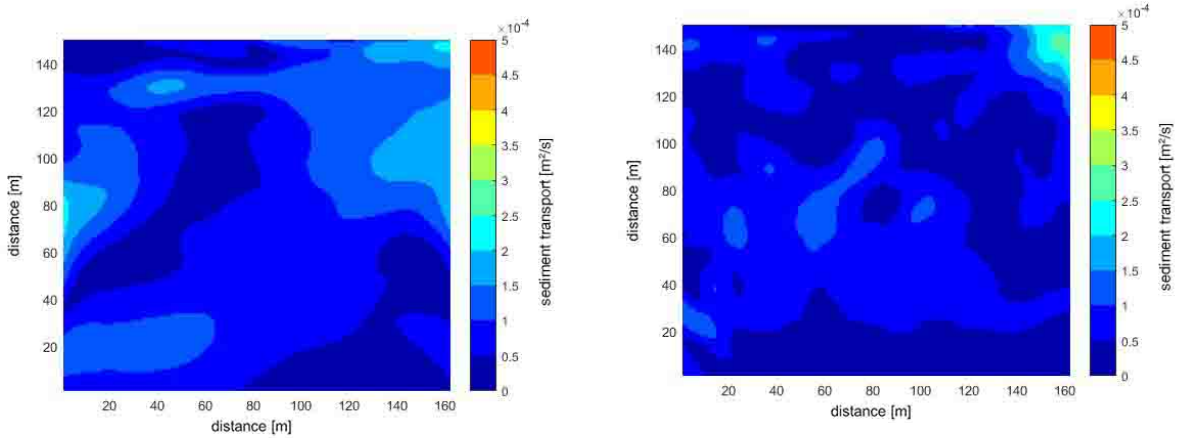

(a) Initial sediment transport in the surfbeat mode

(b) Initial sediment transport in the non hydrostatic mode

Figure E.2: Area for sediment transport comparison zoom in on the pink area of figure E.1

F

Volume Calculation

The losses of material out of the pocket beach are based on the areas created. The offshore line boundary of these areas is based on the depth related to the breaking depth. The ratio 4/3 for depth over wave height gives a depth of about 2.5 metres for the simplified and a depth of 4 metres for the case study beach. However, for the case study beach this depth is outside the groynes and therefore a depth of 3 metres is used. Outside the groynes the material is assumed to be lost from the system, for example it can be moved away by alongshore transport.

F.1. Simplified Pocket Beach

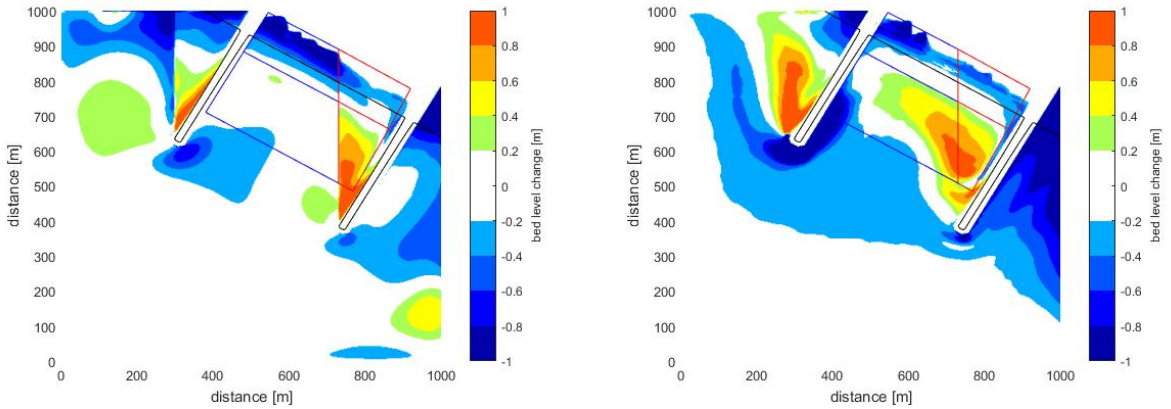

(a) Overview calculation areas simplified pocket beach projected on surfbeat results

(b) Overview calculation areas simplified pocket beach projected on non hydrostatic results

Figure F.1: Overview calculation areas simplified pocket beach projected on surfbeat and non hydrostatic results results (red = shadow zone areas, blue = exposed zone areas)

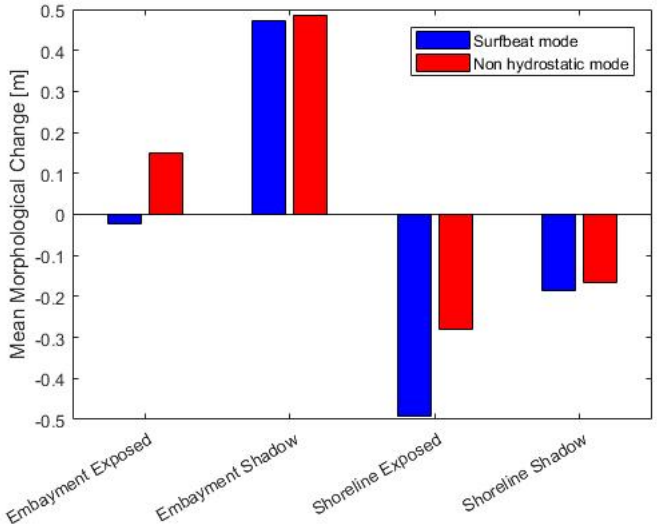

Figure F.2: Mean bed level change in surfbeat and non hydrostatic simulation

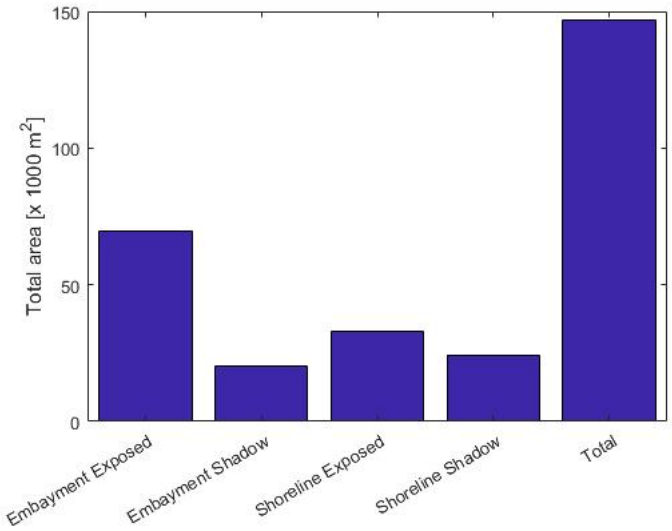

Figure F.3: Surface area of the simplified pocket beach

F.2. Case Study Constanta

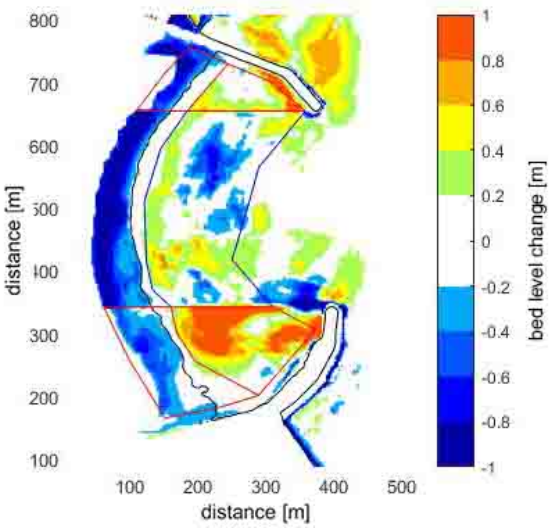

(a) Overview calculation areas simplified pocket beach projected on surfbeat results

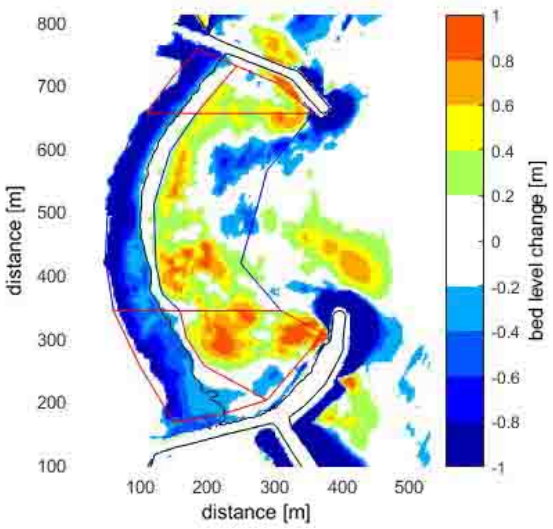

(b) Overview calculation areas simplified pocket beach projected on non hydrostatic results

Figure F.4: Overview calculation areas simplified pocket beach projected on surfbeat and non hydrostatic results results (red = shadow zone areas, blue = exposed zone areas)

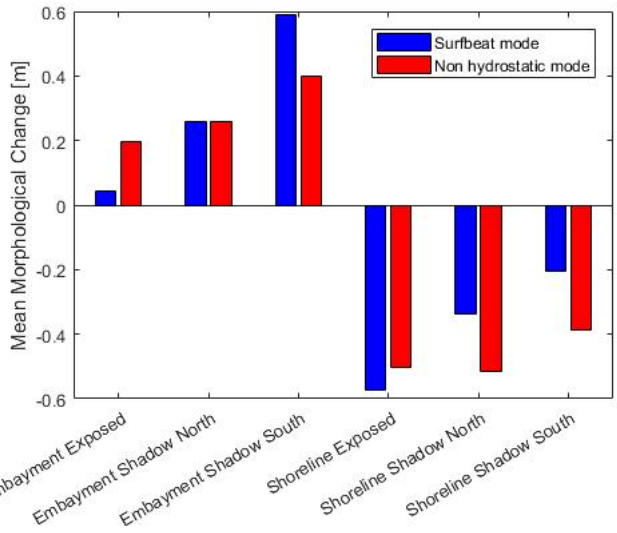

Figure F.5: Mean bed level change in surfbeat and non hydrostatic simulation

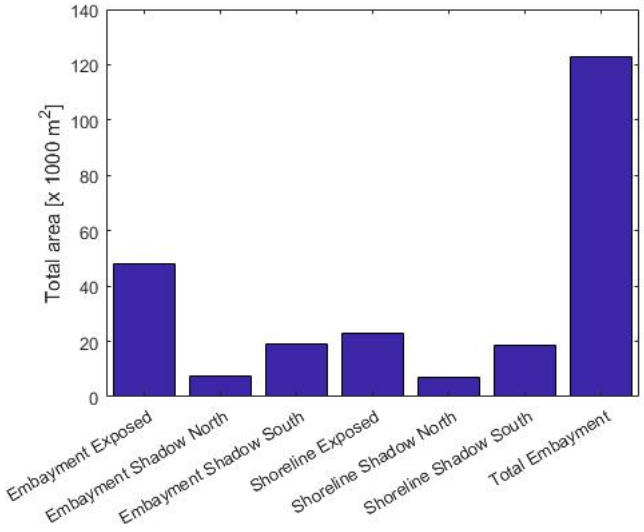

Figure F.6: Surface area of the case study beach